# *Potentiometric Titration of Thorium and Cerium Nitrates with Glass Electrode*

By Kuan PAN and Tong Ming HSEU

(Received July 14, 1954)

The complicating effects of hydrolysis and polymerization, together with the colloidal behavior and complex properties of thorium and cerium salts in aqueous solution cause great difficulties in the analytical procedures for the separation of thorium from cerium and other rare earths, especially, in the physico-chemical study of their electrolytic properties. The present paper reports the experimental results of potentiometric titration of thorium and cerous nitrates with glass electrode. Its purpose is two-fold: first to study the complex formation of thorium with oxalate ions; second, to determine thorium and cerium in the presence of one another with sodium hydroxide solution and to find the pH range at which thorium can be separated from cerous ions. The study of the stability of thorium complexes will be reported in a subsequent paper of this series.

## Experimental

**A) Experimental Procedures.**—The change in pH during the titration was followed by means of vacuum tube potentiometer constructed in our laboratory. The titration was carried out in an oil thermostat controlled to 25°C. Approximately ten-minute intervals were allowed for the attainment of equilibrium between the addition of increments of the titrant.

The point at which the solution began to become opaque was found with the aid of a beam of light conducted to the cell vertical to the line of vision of the observer. The reproducibility of these points was of the order of 0.05 pH unit for the solution of high concentration and approximately 0.1 pH unit at the stoichiometric point.

**B) Materials.** — Conductivity water with a specific conductivity of 1.6 to 2.4 $10^{-6}$ mho was used throughout this experiment.

Thorium nitrate of C.P. grade was purified as described in the previous paper[1].

Cerium nitrate of C.P. grade was treated with hydrogen peroxide in dilute nitric acid solution to reduce any ceric to cerous ion. An acid solution was used as the stock solution in order to prevent the hydrolysis of the salt. The concentration of the stock solution prepared above was determined by the gravimetric method. The stock solution was diluted to a desired concentration with conductivity water before each run.

Carbonate-free sodium hydroxide solution was prepared by diluting a saturated solution of pure sodium hydroxide with carbon dioxide-free water, and standardized against a standard solution of constant-boiling hydrochloric acid.

Sodium oxalate and ammonium oxalate of C.P. grade were purified by recrystallization from conductivity water.

## Experimental Results and Discussion

**A) Potentiometric Titration of Thorium Nitrate with Oxalates by Using Glass Electrode as an Indicator Electrode.** — Thorium nitrate is titrated potentiometrically with sodium or ammonium oxalate by using a glass electrode as an indicator electrode. Since the activity of the free oxalate, or the non-complex oxalate, $a_{c_2o_4}{}^{2-}$ is a function of the hydronium ion activity, $a_H$, the following equation is obtained:

$$a_{c_2o_4}{}^{2-} = \frac{K_1K_2c}{a_H^2 + \frac{K_1}{r_1}a_H + \frac{K_1K_2}{r_2}},$$

where $C$ is the total molar concentration of the non-complex oxalate ion, $K_1$ and $K_2$ are the primary and secondary ionization constants of oxalic acid, and $r_1$ and $r_2$ are the activity coefficients of bioxalate and oxalate ions.

The fact that thorium oxalate is soluble in a solution of ammonium or sodium oxalate was first pointed out by Bahr[2] and later used by Bunsen[3] to separate thorium from the rare earths. Brauner[4], Cleve[5] and Rosenheim, Samter and Davise[6] attributed this increased solubility to the formation of a definite ammonium and sodium or potassium thoroxalate isolated in crystalline form, such as $(NH_4)_4Th(C_2O_4)_4\cdot 7H_2O$, $Na_4Th(C_2O_4)_4\cdot 7H_2O$ and $2Th(C_2O_4)_2(NH_4)_2C_2O_4\cdot 7H_2O$, etc., from the results of solubility measurements. Britton

1) K. Pan and T. M. Hseu, This Bulletin, 28, 162 (1955).

2) T. Bahr, *Annalen*, 132, 231 (1864).
3) R. Bunsen, *Pogg. Ann.*, 155, 375 (1875).
4) B. Brauner, *J. Chem. Soc.*, 73, 951 (1898).
5) P. T. Cleve, *Bull. soc. chem.*, 21, 116 (1874).
6) A. Rosenheim, Samter and Davisohn, *Z. anorg. Chem.*, 35, 424, (1903).

CHEMISTRY HALL LIBRARY

and Maurice[7] reported the complex formation of thorium oxalate from the standpoint of the phase rule. In the present investigation the existence of these complex ions in dilute aqueous solution at 25°C was confirmed by means of potentiometric titration with glass electrode. It is found that the precipitation of thorium dioxalate is completed at pH 4.3 and the precipitate is then dissolved gradually with the addition of oxalate.

The pH value increases with the addition of oxalate after one type of complex formation is completely in equilibrium with the other, and it is kept constant when another type of complex begins to be formed. The milky suspension was dissolved gradually and a clear solution was obtained when the mole ratio exceeded 6:1.

It is evident, therefore, that when an excess precipitant is added, and when the pH value exceeds 4.5, the precipitate of thorium oxalate will be partially redissolved. Consquently a negative error will be found in the analytical result from the standpoint of analytical chemistry.

As shown in Fig. 1, in titrating a dilute solution of thorium nitrate with sodium or ammonium oxalate solution, four inflections are found in each titration curve of the thorium-oxalate system. The first sharp inflection, corresponding to the complete precipitation of thorium oxalate which is expected to have the mole ratio of oxalate ion to thorium ion, viz., the "$R$" value in brief, of 2 is found at the $R$ value of 1.9, and at pH ranging from 4.24 to 4.31 in each curve. The second, the third and the fourth inflections, which correspond to the formation of thoroxatale complexes, are found stepwisely in each curve at the approximate $R$ values of 3, 4 and 6 respectively.

In Fig. 1, curves (A) and (B) indicate the potentiometric titrations of 50 ml. of 0.001 M $Th(NO_3)_4$ with 0.01 M $Na_2C_2O_4$ and with 0.01 M $(NH_4)_2C_2O_4$ in pure aqueous solutions, and curve (C) and (D) indicate the corresponding titrations in 0.5 M $NaClO_4$ solutions, respectively. The $R$ value and pH observed at each point of inflection in these titration curves are summarized in Table I.

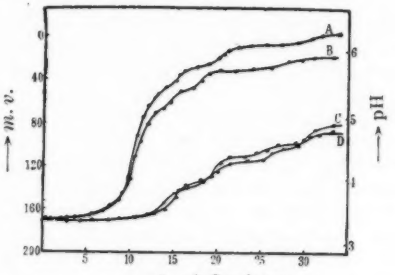


→ ml of Oxalates

Fig. 1. Potentiometric titration of thorium nitrate with oxalates.

**B) Potentiometric Titration of Thorium and Cerium Nitrates with Sodium Hydroxide Solution.**—The difference between the basicities of thorium and cerium ions or between those of ceric and cerous ions has been used in the separation of the former from the latter by several investigators[8]. Britton and Maurice[9] and Bowles and Partrige[10] reported the potentiometric titration of thorium and

7) H. T. S. Britton and Maurice, *J. Chem. Soc.*, 1936, 1419.

8) Therald Moeller, George K. Schweitzer and Donald D. Star, *Chem. Rev.*, 42, 64 (1938).

9) H. T. S. Britton, *J. Chem. Soc.*, 127, 2142 (1925).

10) T. A. C. Bowles and H. M. Partridge, *Ind. Eng. Chem. Anal. Ed.*, 9, 124 (1937).

TABLE I

THE MOLE RATIO AND pH AT EACH MAXIMUM INFLECTION IN THE TITRATION CURVES OF THORIUM-OXALATE SYSTEM

| Curve | Thorium Nitrate | Oxalate (M) | | Inflect found at I | II | III | IV | V |
|---|---|---|---|---|---|---|---|---|
| (A) | 0.001 M ($f$=1.070) in pure water | 0.01 ($f$=1.009) $Na_2C_2O_4$ | $R$ value | 1.89 | 2.89 | 3.87 | | 5.85 |
| | | | pH | 4.24 | 5.56 | 5.92 | | 6.19 |
| (B) | ,, | 0.01 M ($f$=1.003) $(NH_4)_2C_2O_4$ | $R$ value | 1.91 | 2.72 | 3.38 | | 5.53 |
| | | | pH | 4.31 | 5.22 | 5.56 | | 5.86 |
| (C) | 0.001 M ($f$=1.070) in 0.5 M $NaClO_4$ | 0.01 M ($f$=1.009) $Na_2C_2O_4$ | $R$ value | | 2.89 | 3.68 | 4.91 | 5.66 |
| | | | pH | | 3.76 | 4.14 | 4.39 | 4.66 |
| (D) | ,, | 0.01 M ($f$=1.003) $(NH_4)_2C_2O_4$ | $R$ value | | 2.63 | 3.67 | 4.69 | 5.72 |
| | | | pH | | 3.64 | 4.17 | 4.44 | 4.66 |

TABLE II

POTENTIOMETRIC TITRATION OF THORIUM AND CEROUS NITRATES WITH SODIUM HYDROXIDE SOLUTION

| Curve | Initial concentration $Th(NO_3)_4$ $Ce(NO_3)$ or the mixture | pH at which the solution becomes opaque | | Maximum inflection occurs at pH | mole ratio |
|---|---|---|---|---|---|
| (A) | 0.001 M $Th(NO_3)_4$ in aq. solution | 4.34 | 6.71 | 3.69 | : 1 |
| (B) | 0.001 M $Th(NO_3)_4$ in 0.5 M $NaClO_4$ | 4.78 | 6.61 | 3.94 | : 1 |
| (C) | 0.001 M $Ce(NO_3)_3$ in 0.0005 M $HNO_3$ | 7.32 | 8.39 | 2.92 | : 1 |
| (D) | 0.001 M $Ce(NO_3)_3$ in 0.0005 M $HNO_3$ and 0.5 M $NaClO_4$ | 6.51 | 7.73 | 2.97 | : 1 |
| (E) | 0.001 M $Th(NO_3)_4$ and 0.001 M $Ce(NO_3)_3$ in 0.0005 M $HNO_3$ | 7.62 | 5.59 and 8.76 | 3.70 and 2.92 | : 1 |
| (F) | 0.001 M $Th(NO_3)_4$ and 0.001 M $Ce(NO_3)_3$ in 0.0005 M $HNO_3$ and 0.5 M $NaClO_4$ | 5.86 | 5.08 and 8.22 | 3.60 and 2.97 | : 1 |

some rare earth ions to find the pH at ranges at which these hydroxides began to precipitate. In the present investigation, the potentiometric titration was extended to extreme dilute solutions having the final concentration of 0.001 molar with respect to cerous or thorium ions. Furthermore, by reducing ceric to cerous ions in a dilute solution containing thorium ion and titrating the resulting solution with sodium hydroxide solution, thorium and cerous ions could be determined in the presence of each other.

On account of the complicating effects of polymerization and the colloidal adsorption of these hydrous oxides in the basic solution, the coagulation points that are in coincidence with the maximum inflections of the titration curve occur before the attainment of the stoichiometric points which have the $R$ values of 4 for thorium and 3 for cerous hydroxide.

Inasmuch as the acid solution of cerous nitrate is used in the present investigation, the first inflection in the titration curve is attributed to the neutralization of the free acid and is subtracted from the total amount of the base added. The steep inflections are found at the $R$ values of 3.7 and 2.9 and at pH 6.7 and 8.4 in the titration curves for thorium and cerous salts respectively. The presence of sodium perchlorate represses the complicating effects of polymerization and colloidal adsorption of these hydrous oxides and draws the $R$ values in close proximity to the stoichiometric points at the $R$ values of 4 and 3, respectively.

In titration of a mixture of thorium and cerous nitrates with sodium hydroxide solution, the pH value at the coagulation point of cerous hydroxide is little influenced by the presence of thorium hydroxide, but that of the latter is remarkably lowered by the presence of the former. This fact facilitates the separation of the one from the other and the determination of the one in the presence of the other. In applying the above method to the determination of thorium and cerous ions individually or in the presence of another one however, the experimental results obtained

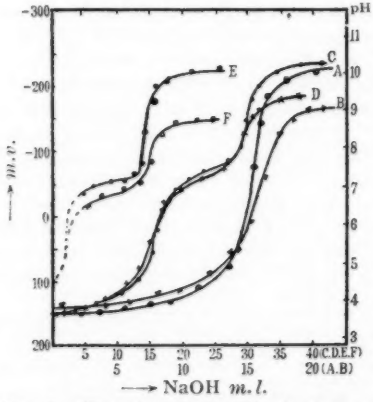


Fig. 2. Titration curves of thorium and cerous nitrates with sodium hydroxide.

from the potentiometric titration must be multiplied by experimental factors which are both greater than unity for correction, that is, 4.0/3.7 for the former and 3.0/2.9 for the latter.

**Summary**

1) Thorium nitrate was potentiometrically titrated with sodium and ammonium oxalates by using glass electrode as an indicator electode. Four inflections were found in the titration curves of the thorium-oxalate system. The first steep inflection, corresponding to the precipitation of thorium dioxide, was found at the mole ratio of $C_2O_4^{2-}$ to $Th^{4+}$, viz., the "$R$" value, 1.9 and at pH 4.3. The second the third and the fourth inflections, corresponding to the formation of thoroxalate complexes were found at the approximate $R$ value of 3.4, and 6, and at pH values ranging from 5.4 to 6.3.

2) Thorium and cerium nitrates were potentiometrically titrated by sodium hydroxide in dilute solutions with glass electrode. By reducing ceric to cerous ions in a solution containing thorium ion, and by titrating the resulting solution with sodium hydroxide solution, two steps of inflection, corresponding to the precipitation of thorium and cerous hydroxides, were found respectively, in the titration curve. In applying this method to the determination of thorium and cerous ions in the presence of one another, however, the experimental results obtained from the titration curve must be multiplied by the experimental factors which are both greater than unity for accuracy.

*Department of Chemistry, College of Science, National Taiwan University, Taiwan*

# *Determination of Dielectric Constant and Loss Factor by Free Wave Method. III. Measurement on Aliphatic Alcohols at the Wavelength of 1.38 cm.*

By Hideo OKABAYASHI

(Received January 19, 1955)

The theory of determining the dielectric constant and the loss factor of liquids by the free wave method has been developed by M. Yasumi.[1] The dielectric properties of various liquids have been investigated in the microwave region (wavelength=9.8, 4.5 and 3.24 cm.) in our laboratory[2,3,4], and several interesting results have been obtained.

Debye was the first who succeeded to explain theoretically the anomalous dispersion and the absorption of electric wave by polar substances[5]. The basic idea for the assumption of the internal field seems not to be entirely satisfactory. Nevertheless the assumption of the single relaxation time seems to be valid from the experimental point of view[4,7-10]. The validity of this assumption is being kept under consideration in our laboratory and is justified when we adopt a suitable internal field[11,12]. Assuming the single relaxation time, the following equations are shown to be valid irrespective of the relaxation mechanism.

$$\varepsilon' = \varepsilon_\infty + \frac{\varepsilon_0 - \varepsilon_\infty}{1+x^2}, \qquad (1)$$

$$\varepsilon'' = \frac{(\varepsilon_0 - \varepsilon_\infty)}{1+x^2} x, \qquad (2)$$

$$x = \omega\tau, \qquad (3)$$

1) M. Yasumi, This Bulletin, 24, 53 (1951).
2) M. Yasumi, K. Nukazawa and S. Mizushima, This Bulletin, 24, 60 (1951).
3) M. Yasumi, H. Okabayashi, M. Shirai and S. Mizushima, *J. Chem. Phys.*, 19, 978 (1951).
4) M. Yasumi, M. Shirai and S. Mizushima, This Bulletin, 25, 133 (1952).
5) P. Debye, "Polare Molekeln", Leipzig: Hirzel (1929).
6) A. Schallachmach, *Trans. Faraday Soc.*, 42A, 180 (1946).
7) C. H. Collie, J. B. Hasted and D. M. Ritson, *Proc. Phys. Soc.*, (London), 60, 145 (1948).
8) J. B. Hasted, G. H. Haggis and P. Hutton, *Trans. Faraday Soc.*, 47, 577 (1951).
9) G. H. Haggis, J. B. Hasted and T. J. Buchanan, *J. Chem. Phys.*, 20, 1452 (1952).
10) J. A. Saxton, *Proc. Roy. Soc.*, A, 213, 473 (1952).
11) J. Wyman, *J. Am. Chem. Soc.*, 58, 1482 (1936).
12) M. Yasumi and H. Komooka (to be published).

where $\varepsilon'$ is the dielectric constant, $\varepsilon''$ the loss factor and $\omega$ the angular frequency. $\varepsilon_0$ and $\varepsilon_\infty$ are the values of the dielectric constant at $x=0$ and $x=\infty$ respectively. $\tau$ is called the relaxation time and is related to the characteristic frequency $\lambda_s$ as follows.

$$\lambda_s = 2\pi c\tau, \qquad (4)$$

where $c$ denotes the velocity of light.

Much of our interest is concerned with the values of $\varepsilon_\infty$ for the liquids. In the earlier works,[13] the value of $\varepsilon_\infty$ was assumed to be identical with the value of the square of the refractive index $(n_{opt})^2$ at optical regions. If the liquids show marked absorption spectra in infra-red region, the $(n_{opt})^2$ is not identical with $\varepsilon_\infty$. The origin of the difference is due partly to the infra-red-active interatomic vibrations in a molecule and partly to the intermolecular vibrations in the liquid structure.

In our preliminary work[1], the dielectric constant and the loss factor were measured at the wavelength of 3.24 cm., and the values of $\varepsilon_\infty$ were calculated, assuming the validity of Eqs. (1) and (2). It was concluded there that the atomic polarizations due to the liquid structure are almost constant for various aliphatic alcohols investigated. The obtained result was concerned, however, only with the data at the wavelength of 3.24 cm. The result must be confirmed for the other frequencies.

In the present work, the dielectric constant and the loss factor were measured at the wavelength of 1.38 cm. The method of determining the dielectric constant and the loss factor of the liquids was described by M. Yasumi.[1] The important points will be repeated here. The linearly polarized plane wave of the wavelength $\lambda$ is emitted vertically into the free space. When the wave comes to the mercury surface, the perfect standing-wave pattern may appear in the space above the mercury surface. If the liquid layer is placed on mercury, the amplitudes of the incident and reflected waves will be generally different. Also the crystal detector shows the imperfect standing-wave when the position of the detector is shifted vertically from the liquid surface to the free space. If the crystal detector obeys the square law, the ratio of the maximum-to the minimum-current induced in the detector, $I_M/I_m$, is expressed by the following equation,

$$I_M/I_m = (1+R)^2/(1-R)^2. \qquad (5)$$

where $R^2$ is the reflection coefficient of the system consisting of the liquid layer of the thickness $d$ and the mercury layer. Such measurements are made at different thicknesses of the liquid layer.

$$R^2 = \frac{\sin h^2\left(\frac{2\pi kd}{\lambda} + \frac{1}{2}\ln R_{12}\right) + \cos^2\left(\frac{2\pi nd}{\lambda} - \frac{\tau}{2}\right)}{\sin h^2\left(\frac{2\pi kd}{\lambda} - \frac{1}{2}\ln R_{12}\right) + \cos^2\left(\frac{2\pi nd}{\lambda} + \frac{\tau}{2}\right)}, \qquad (6)$$

The reflection coefficient $R^2$ is expressed as follows:
where $n$ and $k$ are the refractive index and the absorption coefficient of liquid respectively, and further $R_{12}$ and $\tau$ are expressed as

$$R_{12}^2 = \frac{(n-1)^2+k^2}{(n+1)^2+k^2}, \quad \tan\tau = \frac{2k}{n^2-1+k^2}. \qquad (7)$$

The real part $\varepsilon'$ and the imaginary part $\varepsilon''$ of the complex dielectric constant are related to $n$ and $k$ in the following manner,

$$\varepsilon' = n^2 - k^2, \quad \varepsilon'' = 2nk. \qquad (8)$$

It is more convenient to choose as parameters in Eq. (2) $n$ and $k$ than $\varepsilon'$ and $\varepsilon''$, as easily seen from Eqs. (6) and (7).

Given $n$ and $k$, we can use Eqs. (6) and (7) to calculate the reflection coefficient $R^2$ for the various thickness $d$ and draw the curve of $R$ *versus* $d$. Here, it is convenient to take $d/\lambda$ as the abscissa instead of $d$ because in Eq. (6) the thickness $d$ appears always in the form of $d/\lambda$.

The method of obtaining the value of $n$ and $k$ for the liquid concerned is as follows. First we obtain the values of $I_M/I_m$ for various thicknesses experimentally. Secondly we calculate the value of $R$ for each value of $d/\lambda$. Then we draw the curve of $R$ *versus* $d/\lambda$. This experimentally obtained curve is compared with those calculated by Eqs. (6) and (7) for various $n$ and $k$. The values of $n$ and $k$ assumed in the theoretical curve which fit most satisfactorily the experimental curve, will be taken as values for the liquid investigated. In practice, the interpolation method is used. To confirm whether the values of $n$ and $k$ thus determined are the fittest or not, we make the curve $R$ *versus* $d/\lambda$ for the values of $n$ and $k$ thus obtained, and compare it with the experimental curve.

13) S. Mizushima, *Sci. Papers Inst. Phys. Chem. Res.*, (Tokyo), **9**, 109 (1928).

## Apparatus

The apparatus constructed is shown as a block diagram in Fig. 1.

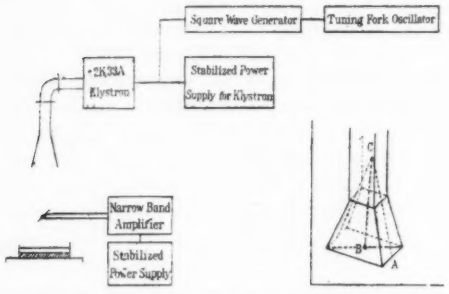


Fig. 1. The block diagram of our apparatus.

A type 2K33A reflex klystron is used as a source of the radiation. The high voltage power supply for the klystron must be highly stabilized by an electronic device because the output power and the frequency of the reflex klystron are extremely sensitive to the beam voltage and the reflector voltage. Our circuit diagram of the voltage stabilizer is shown in Fig. 2.

The electromagnetic horn is connected with the cavity of the klystron through an *E*-bend waveguide. In order that the wavefront at the aperture may approximate a plane, the difference between the distances from the point C to the center B and to the point A on the edge of the aperture (refer to Fig. 1) is designed to be smaller than $\lambda/8$. The dimension of the aperture is $7.5\times7.5\,cm^2$. The waveguide connected with the cavity of the klystron has a section of $1.07\times0.43\,cm^2$ and is operated in a mode $H_{01}$ when the wavelength is 1.38 cm. The electric field in the waveguide makes a right angle to its larger side. Therefore if the waveguide is enlarged gradually to the aperture of the horn, the electric field in the free space is kept in a fixed direction. Thus the radiated wave from the horn is linearly polarized.

The distance between the aperture of the horn and the surface of mercury is about 75 cm., so that the obtained radiation behaves like the plane wave near the liquid surface.

The vessel is made of wood and lacquered, and its dimension is $20\times20\,cm^2$. This area is sufficiently large to remove the effect of the edges The thickness of the liquid layer is determined from the volume of the liquid poured in.

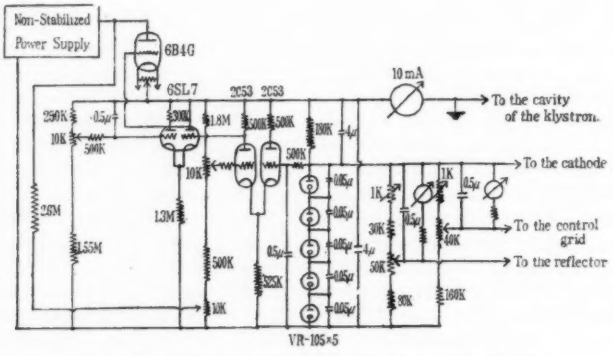


Fig. 2. The high voltage stabilizer for the klystron.

Modulation of the microwave source makes it possible to use a. c. amplification of the signal from the crystal detector and to shorten the time required for each measurement more than to use a galvanometer. For the standing-wave measurement, the percentage of the amplitude modulation should be large, but the frequency modulation must be avoided. Therefore, the "on-off" modulation, with a square modulation envelope, is preferred. Modulation is introduced in the reflector circuit by a square-wave voltage superposed on the steady-state reflector voltage. The square-wave generator is synchronized with the tuning fork oscillator of 1000 c/s., and is constructed so that on- and off-states have almost equal durations, and the rise- and fall-times are extremely short[14].

The crystal detector is made of a tungsten wire and a small pellet of silicon crystal picked out from a commercial crystal detector, 1N23B. Two leads of phosphor bronze which support the crystal and the wire are bound by a rubber ring to adjust the pressure of the tungsten wire against the silicon crystal. The crystal detector so constructed is stably fixed except in the case of a great mechanical shock. The detector system is arranged so that the direction from the tungsten wire to the crystal is parallel to the electric field of the linearly polarized wave. This

14) C. G. Montgomery, "Technique of Microwave Measurements", McGraw-Hill Book Company, Inc., New York and London (1947).

detector is shifted vertically to the liquid surface by the micrometer.

The signal of the square-wave from the crystal detector is amplified and introduced in an indicating ammeter of 1 m amp. Because some frequency modulation may occur during the rise- and fall-times of the modulating square-wave, the tuning amplifier is used in order to prevent a spurious signal. The frequency sensitivity of the amplifier is provided by a twin-T feedback network tuned in the 1000 c/s[14].

On adjusting the whole apparatus, the important points to be kept in mind are to determine the region in which the electric field may be measured by the crystal detector, and to construct a sufficiently small crystal detector, so that it might not disturb the radiation field except so slightly as to be negligible, and further to adjust the contact between the wire and the pellet of silicon crystal in order to give a high sensitivity to the microwave field.

Near the aperture of the horn, the radiation pattern is complicated, and far from the plane wave. Also because we cannot place a liquid layer in the infinite and empty space, we must choose the region near the liquid surface in order to avoid the effects of other bodies, for example, of the walls and of the supporter of the vessel, etc. On the other hand, the disturbance of the detector may be detected as a departure from the $(\text{sine})^2$ law for the standing-wave pattern which appears on the mercury layer.

By trial and error, we adjusted the whole system in order that it may be operated under the best conditions, changing the frequency of the radiation source slightly. As the result we knew that the detector may be shifted in the region near the height 6 cm. from the liquid layer. The dimension of the crystal detector which was used is shown in Fig. 3. The resulting standing-wave

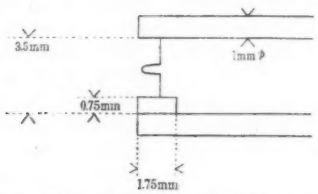


Fig. 3. The dimension of the crystal detector.

pattern on the mercury layer showed that near the above-mentioned height the maximum values of the induced current fluctuated within ±1 percent, and that the minimum values were recognized as zero as far as we used the ammeter of 1 m amp. as an indicating meter. The maximum point shifted about 0.15 mm from the middle point of two successive minimum points towards the radiation source. The induced currents showed the square law except in the region where the current was very small. We can determine the wavelength within the accuracy of ±0.2 percent from this perfect standing-wave pattern. In many cases the wavelength was 1.378 cm.

## Materials

Methyl alcohol: Commercial methyl alcohol is boiled with freshly burnt lime under reflux and distilled. Then the distillate is refluxed with silver nitrate and distilled. The distillate is dried over magnesium activated with iodine, b. p. 67.0–67.4°C.

Ethyl alcohol is purified by the same procedure as methyl alcohol, b. p. 77.8–78.3°C.

Purified *n*-butyl alcohol is obtained by means of the efficient fractionating column constructed by T. Tamura[15], b. p. 117.0–117.2°C.

Isobutyl alcohol is treated with freshly burnt lime, and then the distillate is dried over anhydrous copper sulphate, b. p. 107.5–108.2°C.

Tertiary butyl alcohol is dried over sodium hydroxide and then fractionated by means of the above-mentioned column, b. p. 83.5–83.8°C.

## Measurements

Each measurement is operated half an hour later, after the whole apparatus was switched on. At first we measure the standing-wave pattern when the vessel contains only mercury. The wavelength is determined from it. Thereafter a certain amount of liquid is poured in, and we measure the standing-wave ratio by shifting the crystal detector vertically to the liquid surface. These operations are repeated. Finally we can draw the curve $R$ *versus* $d/\lambda$ using the table of the standing-wave ratio *versus* the square root of the reflection coefficient, $R$.

For $n \gg k$, the maximum and minimum values of the square root of the reflection coefficient and the corresponding values of $d/\lambda$ are expressed approximately by simple equations derived from Eq. (2).[1] Therefore we can determine roughly $n$ and $k$ from the experimental curve, even if the condition $n \gg k$ is not satisfied. However, we have

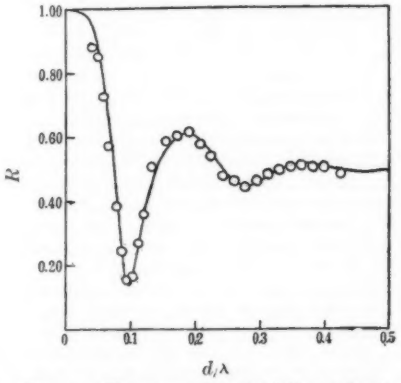


Fig. 4. The square root of the reflection coefficient of the methyl Alcohol layer of the thickness $d/\lambda$ measured at 9°C and the calculated curve corresponding to $n=2.72$ and $k=0.78$.

15) Cf. T. Tamura, *Reports of the Radiation Chemistry Research Institute* (Tokyo Univ; in Japanese), **5**, 49 (1950).

prepared many calculated curves for values of $n$ between 7.00 and 1.50 and of $k$ between 2.00 and 0.10, and we compared the experimental curve with the calculated ones. Two examples of the calculated curves are shown in Figs. 4 and 5.

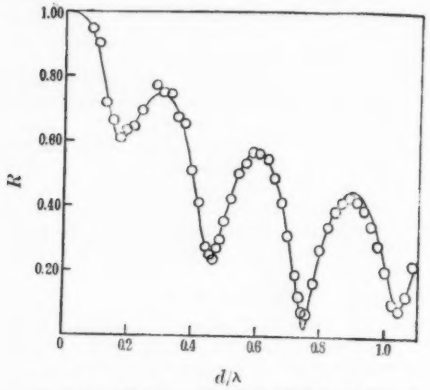


Fig. 5. The square root of the reflection coefficient of the *tert*-Butyl alcohol layer of the thickness $d/\lambda$ measured at 26°C and the calculated curve corresponding to $n=1.685$ and $k=0.135$.

But the number of such calculated curves are not sufficient to determine the values of $n$ and $k$ accurately. We can choose the two nearest curves among the calculated ones. Now we choose a more suitable set of values of $n$ and $k$, taking into account that the interval of $d/\lambda$ corresponding to the two neighboring minimum points depends mainly upon the value of $n$ and that the maximum and minimum values of $R$ depend mainly on the value of $k$. By means of the interpolation method, we can determine more accurately the values of $n$ and $k$ respectively. Then we draw a curve with this set of $n$ and $k$, and compare it once more with the experimental curve. If the experimental curve shows a deviation from the calculated one, we repeat the abovementioned procedure once more. Thus we can determine a more and more suitable set of $n$ and $k$, and therefore $\varepsilon'$ and $\varepsilon''$. In this experiment, we measured in many cases the standing-wave ratio until the thickness of the liquid layer became greater than the wavelength used. Therefore we could measure several maximum and minimum positions of $R$, as seen from Fig. 5.

Evaporation gives rise to an error in determining the thickness of liquid. To remove this effect, first we increase the volume of the liquid concerned in order to know the behaviour of the square root of the reflection coefficient, and then decreasing the thickness, we measure the standing-wave ratio very rapidly and accurately.

In a case when liquid shows the medium absorption in this microwave region as *tert*-butyl alcohol does, it is fairly easy to determine the maximum and minimum points of the square root of the reflection coefficient. Taking into account that the feature of the curve $R$ *versus* $d/\lambda$ depends markedly on a given set of $n$ and $k$, we can compare the experimental curve with the calculated ones and determine accurately the set of $n$ and $k$. The errors in determining the values

TABLE I

THE SQUARE ROOT OF THE REFLECTION COEFFICIENT $R_e$ OF THE ETHYL ALCOHOL LAYER OF THE THICKNESS $d/\lambda$ MEASURED AT 9°C AND THE CALCULATED ONE $R_c$ CORRESPONDING TO $n=2.09$ AND $k=0.34$.

| $d/\lambda$ | $R_e$ | $R_c$ | $d/\lambda$ | $R_e$ | $R_c$ |
|---|---|---|---|---|---|
| 0.088 | 0.773 | 0.722 | 0.288 | 0.536 | 0.557 |
| 0.099 | 0.623 | 0.583 | 0.310 | 0.433 | 0.451 |
| 0.110 | 0.448 | 0.429 | 0.332 | 0.307 | 0.311 |
| 0.122 | 0.324 | 0.296 | 0.343 | 0.206 | 0.241 |
| 0.133 | 0.246 | 0.257 | 0.354 | 0.159 | 0.188 |
| 0.144 | 0.287 | 0.299 | 0.365 | 0.164 | 0.170 |
| 0.155 | 0.366 | 0.372 | 0.377 | 0.179 | 0.195 |
| 0.177 | 0.506 | 0.499 | 0.388 | 0.232 | 0.241 |
| 0.199 | 0.594 | 0.582 | 0.399 | 0.285 | 0.290 |
| 0.221 | 0.634 | 0.627 | 0.421 | 0.375 | 0.377 |
| 0.243 | 0.635 | 0.640 | 0.443 | 0.429 | 0.435 |
| 0.266 | 0.617 | 0.618 | 0.465 | 0.473 | 0.466 |

TABLE II

THE SQUARE ROOT OF THE REFLECTION COEFFICIENT $R_e$ OF THE $n$ BUTYL ALCOHOL LAYER OF THE THICKNESS $d/\lambda$ MEASURED AT 18°C AND THE CALCULATED ONE $R_c$ CORRESPONDING TO $n=1.72$ AND $k=0.165$

| $d/\lambda$ | $R_e$ | $R_c$ | $d/\lambda$ | $R_e$ | $R_c$ |
|---|---|---|---|---|---|
| 0.077 | 0.932 | 0.943 | 0.612 | 0.514 | 0.508 |
| 0.099 | 0.862 | 0.863 | 0.634 | 0.468 | 0.467 |
| 0.121 | 0.735 | 0.738 | 0.656 | 0.402 | 0.401 |
| 0.143 | 0.610 | 0.604 | 0.678 | 0.311 | 0.308 |
| 0.155 | 0.554 | 0.554 | 0.690 | 0.252 | 0.250 |
| 0.166 | 0.550 | 0.536 | 0.701 | 0.195 | 0.192 |
| 0.188 | 0.582 | 0.555 | 0.712 | 0.136 | 0.134 |
| 0.210 | 0.621 | 0.605 | 0.723 | 0.091 | 0.082 |
| 0.233 | 0.648 | 0.654 | 0.734 | 0.057 | 0.056 |
| 0.255 | 0.693 | 0.689 | 0.745 | 0.078 | 0.084 |
| 0.277 | 0.735 | 0.708 | 0.756 | 0.122 | 0.132 |
| 0.299 | 0.736 | 0.711 | 0.768 | 0.170 | 0.185 |
| 0.322 | 0.721 | 0.695 | 0.779 | 0.218 | 0.228 |
| 0.344 | 0.667 | 0.650 | 0.790 | 0.264 | 0.271 |
| 0.366 | 0.594 | 0.578 | 0.812 | 0.330 | 0.337 |
| 0.389 | 0.464 | 0.460 | 0.834 | 0.374 | 0.383 |
| 0.411 | 0.328 | 0.316 | 0.857 | 0.403 | 0.409 |
| 0.422 | 0.248 | 0.240 | 0.879 | 0.419 | 0.415 |
| 0.433 | 0.179 | 0.176 | 0.901 | 0.409 | 0.403 |
| 0.444 | 0.157 | 0.142 | 0.924 | 0.382 | 0.371 |
| 0.456 | 0.162 | 0.159 | 0.946 | 0.334 | 0.324 |
| 0.467 | 0.220 | 0.208 | 0.968 | 0.274 | 0.265 |
| 0.478 | 0.267 | 0.263 | 0.990 | 0.220 | 0.205 |
| 0.500 | 0.369 | 0.364 | 1.013 | 0.166 | 0.161 |
| 0.522 | 0.450 | 0.435 | 1.035 | 0.168 | 0.167 |
| 0.545 | 0.499 | 0.493 | 1.057 | 0.199 | 0.201 |
| 0.567 | 0.523 | 0.520 | 1.080 | 0.257 | 0.252 |
| 0.589 | 0.533 | 0.525 | | | |

of $n$ and $k$ by comparison are 0.2 percent for $n$ and 2.0 percent for $k$. On the other hand, in a case when the liquid shows high absorption in this microwave region, as methyl alcohol does, the maximum and minimum points except for the first minimum point cannot be accurately recognized from the experimental curve and the large part of the curve is in the high reflection region as easily seen from Fig. 4. Further we must take into account that the standing-wave ratio measurement has the disadvantage of being unable to show the high reflection coefficient accurately. In this case the accuracy of determining the value of $n$ is one percent.

Taking into account the errors due to the determination of the liquid thickness and of the wavelength, the accuracy in $n$ is 0.8 percent for *n*-butyl- and isobutyl-alcohol. For methyl alcohol, ethyl alcohol and *tert*-butyl alcohol, showing the high vapour pressure, the accuracies may be 2.5, 1.6, and 1.6 percent, respectively.

The measured square roots of the reflection coefficients for various thicknesses of the liquid layer are plotted in Figs. 4 and 5 for methyl alcohol and *tert*-butyl alcohol, respectively. For ethyl, *n*-butyl and isobutyl alcohol, the experimental square roots of the reflection coefficients are listed in Table I, II, and III, together with the calculated ones for the experimentally determind values of $n$ and $k$.

TABLE III

THE SQUARE ROOT OF THE REFLECTION COEFFICIENT $R_e$ OF THE *iso*-BUTYL ALCOHOL LAYER OF THE THICKNESS $d/\lambda$ MEASURED AT 23°C AND THE CALCULATED ONE $R_c$ CORRESPONDING TO $n=1.70$ AND $k=0.160$.

| $d/\lambda$ | $R_e$ | $R_c$ | $d/\lambda$ | $R_e$ | $R_c$ |
|---|---|---|---|---|---|
| 0.072 | 0.930 | 0.959 | 0.585 | 0.524 | 0.527 |
| 0.095 | 0.880 | 0.889 | 0.608 | 0.515 | 0.522 |
| 0.117 | 0.797 | 0.776 | 0.630 | 0.494 | 0.493 |
| 0.139 | 0.613 | 0.641 | 0.652 | 0.438 | 0.440 |
| 0.162 | 0.570 | 0.552 | 0.675 | 0.351 | 0.357 |
| 0.173 | 0.550 | 0.543 | 0.697 | 0.256 | 0.256 |
| 0.184 | 0.554 | 0.551 | 0.719 | 0.144 | 0.139 |
| 0.195 | 0.585 | 0.570 | 0.730 | 0.093 | 0.083 |
| 0.217 | 0.635 | 0.619 | 0.741 | 0.064 | 0.045 |
| 0.240 | 0.685 | 0.665 | 0.753 | 0.074 | 0.072 |
| 0.262 | 0.696 | 0.692 | 0.764 | 0.123 | 0.122 |
| 0.284 | 0.686 | 0.711 | 0.775 | 0.167 | 0.173 |
| 0.307 | 0.705 | 0.711 | 0.797 | 0.245 | 0.261 |
| 0.329 | 0.678 | 0.691 | 0.820 | 0.308 | 0.333 |
| 0.351 | 0.631 | 0.647 | 0.842 | 0.357 | 0.380 |
| 0.373 | 0.543 | 0.570 | 0.864 | 0.389 | 0.407 |
| 0.396 | 0.451 | 0.451 | 0.886 | 0.404 | 0.416 |
| 0.418 | 0.310 | 0.309 | 0.909 | 0.408 | 0.406 |
| 0.429 | 0.233 | 0.238 | 0.931 | 0.359 | 0.380 |
| 0.440 | 0.181 | 0.180 | 0.953 | 0.340 | 0.333 |
| 0.452 | 0.148 | 0.154 | 0.976 | 0.248 | 0.272 |
| 0.463 | 0.176 | 0.175 | 0.998 | 0.188 | 0.209 |
| 0.474 | 0.209 | 0.221 | 1.020 | 0.147 | 0.158 |
| 0.496 | 0.317 | 0.330 | 1.043 | 0.145 | 0.150 |
| 0.518 | 0.405 | 0.410 | 1.065 | 0.185 | 0.185 |
| 0.541 | 0.462 | 0.474 | 1.087 | 0.220 | 0.234 |
| 0.563 | 0.501 | 0.511 | 1.110 | 0.277 | 0.283 |

The dielectric constant and the related quantities of some aliphatic alcohols are shown in Table IV.

TABLE IV

DIELECTRIC PROPERTIES OF SOME ALIPHATIC ALCOHOLS

| Substance | Temp. | $n$ | $k$ | $\varepsilon'$ | $\varepsilon''$ |
|---|---|---|---|---|---|
| Methyl alcohol | 9°C | 2.72 | 0.78 | 6.79 | 4.24 |
| Ethyl alcohol | 8°C | 2.09 | 0.34 | 4.25 | 1.42 |
| *n*-Butyl alcohol | 18°C | 1.72 | 0.165 | 2.93 | 0.57 |
| *iso*-Butyl alcohol | 23°C | 1.70 | 0.160 | 2.86 | 0.54 |
| *tert*-Butyl alcohol | 26°C | $1.68_5$ | 0.135 | 2.82 | 0.45 |

## Conclusions

The dielectric constant and the loss factor of some aliphatic alcohols were measured by means of the free wave method developed by M. Yasumi. For liquids showing high boiling points, such as n-butyl and isobutyl alcohol, the accuracies of $n$ and $k$ are 0.8 and 2.0 percent, respectively. We should like to improve further the apparatus in the following points.

1) The accuracy in determining the thickness of the liquid layer must be increased.

2) Because we place the liquid layer on mercury in the free space, we can control the temperature within a limited range. But in order to study the dielectric properties of liquids, we must extend the temperature range. Also if the accuracy of measurement is further increased, the slight fall of temperature due to evaporation is a source of error. In the case of hygroscopic liquids, this effect may give rise to serious error.

3) It is necessary to make the radiation pattern more like the plane wave. By doing so, the error in fitting the experimental curve in the calculated curves will be decreased.

According to the plan described above, we are now improving the apparatus in order to increase the accuracy of measurement. We will postpone the detailed discussion of experimental results till later.

In conclusion, thanks are especially due to Dr. Masasi Yasumi for his guidance and to Prof. San-ichiro Mizushima for his kind advice and encouragement. The author also wishes to thank Mr. Yoshio Tsubahara who assisted him in constructing the electronic part of this apparatus, and to Mr. Tsurahide Cho and Mr. Takaaki Tamura who prepared the samples used in these experiments. The present work has been supported partly by the Scientific Research Grant from the Ministry of Educations.

*The Institute of Science and Technology,*
*Tokyo University,*
*Tokyo*

# *Reaction Rate of Water-Gas Shift Reaction*[1]

By Shinjiro KODAMA, Akira MAZUME, Koso FUKUBA and Kenichi FUKUI

(Received February 2, 1955)

The rate equation plays the most fundamental role in the industrial application of gas phase catalytic processes. It gives us the information which is necessary for the design of the catalytic reactor as well as for the operation of the plant. For example, the optimum temperature distribution in a catalyst layer can be calculated for a given inlet gas composition and a given space velocity when the rate constants and the equilibrium constants of the reaction are known at every temperature[2]. Other sorts of useful knowledge, such as the temperature distribution in an adiabatic type reactor[3] and in a self-heat-exchanger-type reactor[4] and the optimum space velocity which gives the maximum space time yield in an adiabatic reactor[5], may also be predicted from the rate equation.

Water-gas shift reaction is one of the most important methods for producing hydrogen on an industrial scale. Therefore, the kinetical study of the water-gas shift reaction is very significant.

Padovani and Lotteri[6] and also Laupichler[7] presented the following as a rate equation:

$$-\frac{dP_{CO}}{dt}=k_1\{P_{CO}P_{H_2O}-K_pP_{CO_2}P_{H_2}\} \quad (1)$$

In the process of an industrial-scale production of hydrogen, in which a large excess of water vapor is added to dry gas, the change in concentration of water vapor can be neglected during the course of reaction. Based on this fact, Laupichler derived the following equation as an approximation for Eq. (1).

$$-\frac{dP_{CO}}{dt}=k_1\{P_{CO}-P_{CO}^{\infty}\} \quad (2)$$

Kal'kova and Temkin[8] gave a different equation

$$-\frac{dP_{CO}}{dt}=k_1\left\{P_{CO}\left(\frac{P_{H_2O}}{P_{H_2}}\right)^{\beta}-K_pP_{CO_2}\left(\frac{P_{H_2}}{P_{H_2O}}\right)^{1-\beta}\right\} \quad (3)$$

where $\beta=0.45\sim0.55$.

This equation reproduces, according to the authors, the results of their experiments, which were made at relatively short contact times.

Reaction rates over a coprecipitated $Fe_2O_3-Cr_2O_3$ catalyst were followed in our laboratory[9] at also relatively short contact times and expressed by an equation different from Eq. (3), i.e.,

$$-\frac{dP_{CO}}{dt}=k_1\frac{P_{CO}P_{H_2O}-K_pP_{CO_2}P_{H_2}}{P_{CO_2}+KP_{H_2O}} \quad (4)$$

All of the above mentioned studies[3,7,8,9] are unsatisfactory for industrial purposes in the following points. First, in all of the experiments stated above the inlet gas compositions were limited in very narrow ranges. And, in the studies of Kal'kova and Temkin[8] and in our laboratory[9], the contact times were far shorter than those used in industrial reactors. Moreover, the experimental verifications of these equations have been tried for only a very limited range of initial gas composition and space velocity.

The kinetics of reverse shift reaction is also one of the most interesting problems not only from an academic viewpoint, but also because of its industrial importance. As the reverse shift reaction occurs during the gasification of coal in industry, kinetical studies at high temperatures have been made by many investigators. On the other hand at relatively low temperatures reaction proceeds so slowly that very little has been known concerning the rate of reaction. Recently Barkley, Corrigan, Wainwright and Sands[10] followed the reaction rate by passing 1:4 to 4:1 mixtures of $CO_2$ and $H_2$ at 1000°F over

1) Part of this paper was presented at the 7th Annual Meeting of the Chemical Society of Japan, April 2, 1954.

2) S. Kodama, K. Fukui, H. Tanaka and A. Mazume, *Chem. Eng.* (Japan), **15**, 85 (1951); P.H. Calderbank, *Chem. Eng. Progress*, **49**, 585 (1953); D. Annable, *Chem. Eng. Sci.*, **1**, 145 (1952).

3) S. Kodama and K. Fukui, *Chem. Eng.* (Japan), **15**, 145 (1951).

4) S. Kodama, K. Fukui and H. Tanaka, *J. Chem. Soc. Japan* (*Ind. Chem. Sec.*), **54**, 303 (1951); C. van Heerden, *Ind. Eng. Chem.*, **45**, 1242 (1953).

5) S. Kodama, K. Fukui and A. Mazume, *Ind. Eng. Chem.*, **45**, 1644 (1953).

6) C. Padovani and A. Lotteri, *J. Soc. Chem. Ind.*, **56**, 391T (1937).

7) F.G. Laupichler *Ind. Eng. Chem.*, **30**, 578 (1938).

8) N. B. Kal'kova and M. I. Temkin, *Zhur. Fiz. Khim.*, **23**, 695 (1949); *Chem. Abstr.*, **43**, 7308 (1949).

9) S. Kodama, K. Fukui, T. Tame and M. Kinoshita, *Catalyst* (Japan), **8**, 50 (1952).

10) L. W. Barkley, T. E. Corrigan, H. W. Wainwright and A. E. Sands, *Ind. Eng. Chem.*, **44**, 1066 (1952).

$Fe_2O_3$—CuO catalyst at different flow rates and derived the following rate equation,

$$\frac{dP_{CO}}{dt}=k_2\frac{P_{CO_2}P_{H_2}-\frac{1}{K_p}P_{CO}P_{H_2O}}{1+KP_{CO}+K'P_{CO_2}} \quad (5)$$

But they did not make sure if this equation holds also in the water-gas shift reaction.

Under the circumstances mentioned above, it may be significant to obtain a rate equation of water-gas shift reaction which would be at least both accurate and practically useful for designing reactors. At the same time, it is of interest to ascertain that the rate expression obtained for the water-gas shift reaction would also be fit for the reverse shift reaction with the opposite sign, as it should be theoretically. Both the reactions were kinetically studied over a wide range of space velocity and inlet gas composition.

## Experimental

Experiments were made by flow method at atmospheric pressure. Schematic flow diagrams of the apparatuses for the forward and the reverse reaction are shown in Figs. 1 and 2, respectively.

Carbon dioxide and hydrogen were taken from cylinders. Carbon monoxide was generated by dehydration of formic acid. These gases were purified by the usual methods.

The industrial catalyst used was of the composition shown below:

| | | | |
|---|---|---|---|
| $Fe_2O_3$ | 72.25 (wt. %) | MgO | 4.69 (wt. %) |
| $Al_2O_3$ | 12.55 ( „ ) | $K_2O$ | 1.53 ( „ ) |
| $Cr_2O_3$ | 7.46 ( „ ) | | |

The particle size of the catalyst was ranging in diameter from 10 to 20 Tyler mesh.

Flow rates of carbon monoxide and hydrogen were measured by a wet-type gas meter and that of carbon dioxide by an orifice-type flowmeter.

For water-gas shift reaction, inlet gas composition was determined from the analysis of dry gas and the saturation temperature with steam. For reverse shift reaction, inlet gas composition was calculated from the flow rates of carbon dioxide and hydrogen.

In the case of water-gas shift reaction dry gas was saturated with steam in a two-stage packed column kept at constant temperature. In order to prevent unsaturation, flow rates of dry gas were carefully kept at constant. The comple-

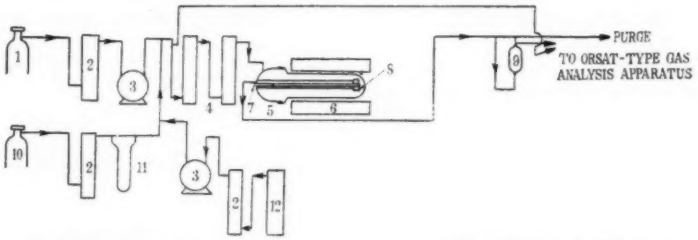


1. CYLINDER HYDROGEN
2. PURIFICATION TRAIN
3. WET-TYPE GAS METER
4. WATER SATURATOR (TWO-STAGE PACKED COLUMN)
5. SELF-HEAT-EXCHANGER-TYPE PYREX REACTOR
6. ELECTRIC FURNACE
7. THERMOCOUPLE WELL
8. CATALYST PACKED LAYER
9. GAS BURETTE
10. CYLINDER CARBON DIOXIDE
11. ORIFICE-TYPE FLOWMETER
12. CARBON MONOXIDE GENERATING APPARATUS

Fig. 1. Schematic flow diagram of the apparatus used for forward Reaction.

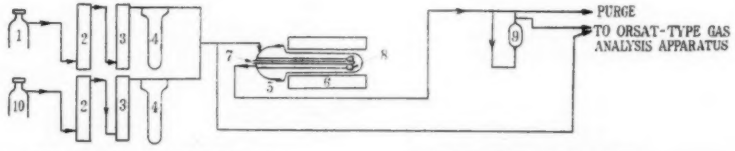


1. CYLINDER HYDROGEN
2. PURIFICATION TRAIN
3. DEHYDRATING TOWER
4. ORIFICE-TYPE FLOWMETER
5. SELF-HEAT-EXCHANGER-TYPE PYREX REACTOR
6. ELECTRIC FURNACE
7. THERMOCOUPLE WELL
8. CATALYST PACKED LAYER
9. GAS BURETTE
10. CYLINDER CARBON DIOXIDE

Fig. 2. Schematic flow diagram of the apparatus used for the reverse reaction.

teness of saturation was confirmed by preliminary experiments at each temperature.

In order to avoid the non-uniformity in the temperature distribution of the catalyst layer, a two-path-counter-current-type pyrex reactor[11] was used. Several reactors of different diameters were used for the experiments of different catalyst volumes, so that the packed length did not exceed 25 mm. and practically uniform temperature distribution was secured. The temperature of the catalyst layer was measured with a calibrated chromel-alumel thermocouple which was inserted in the bed.

Samples of both inlet and exit gas were analyzed with an Orsat-type gas analyzer. Most of the samples were analyzed for carbon dioxide, carbon monoxide and hydrogen.

## Experimental Results

In Figs. 3, 4, 5, 6, 7, and 8 are shown the results for the water-gas shift reaction, plotted as the fractional conversions of carbon monoxide ($Z$) against contact times ($t$) for each investigated temperature and inlet gas composition. Fig. 9 shows the results of the reverse shift reaction by the plot of the

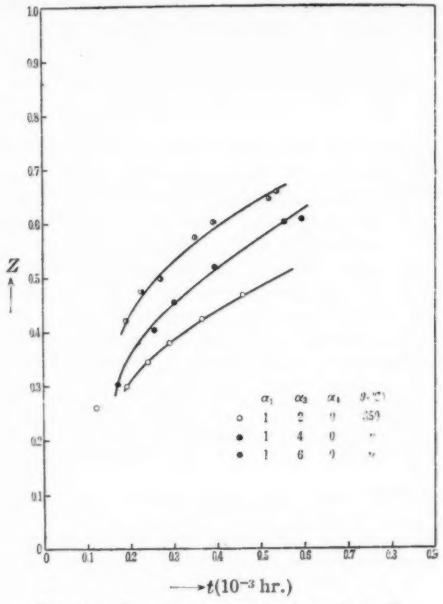


Fig. 4. Fractional conversion of carbon monoxide ($Z$) vs. contact time ($t$).

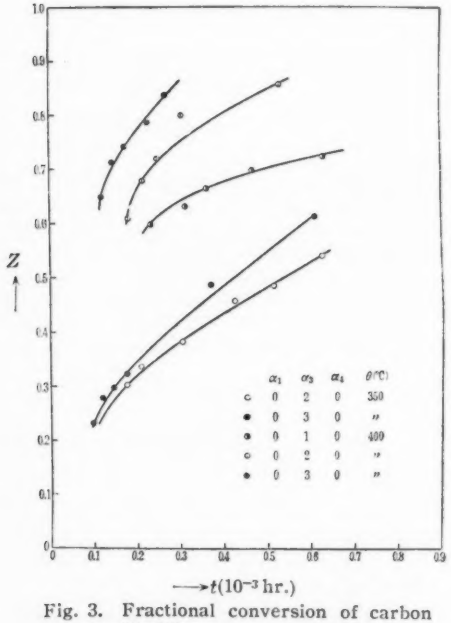


Fig. 3. Fractional conversion of carbon monoxide ($Z$) vs. contact time ($t$).

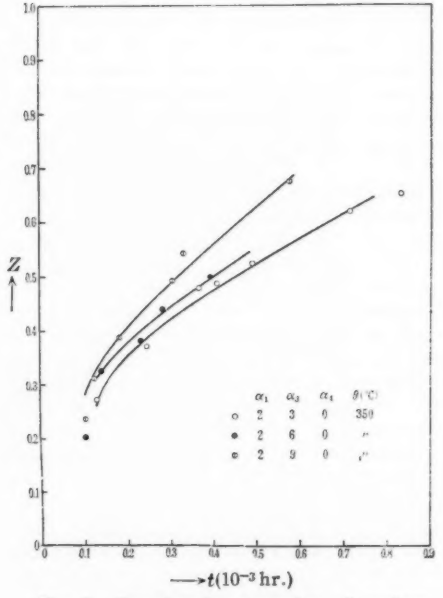


Fig. 5. Fractional conversion of carbon monoxide ($Z$) vs. contact time ($t$).

11) A. F. Farkas and H. W. Melville, "Experimental methods in gas reactions," Mac Millan and Co. Ltd., London, (1939) p. 305.

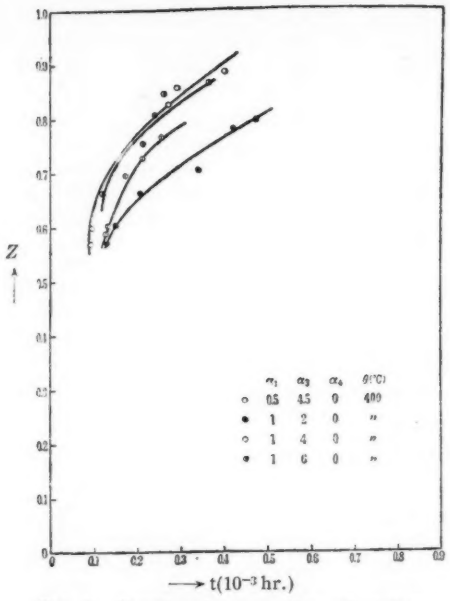


Fig. 6. Fractional conversion of carbon monoxide ($Z$) vs. contact time ($t$).

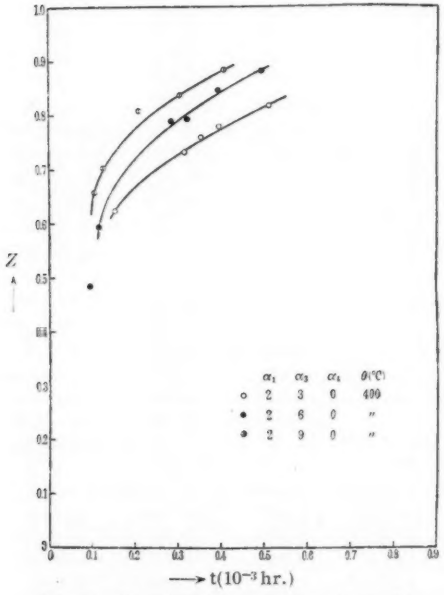


Fig. 7. Fractional conversion of carbon monoxide ($Z$) vs. contact time (t).

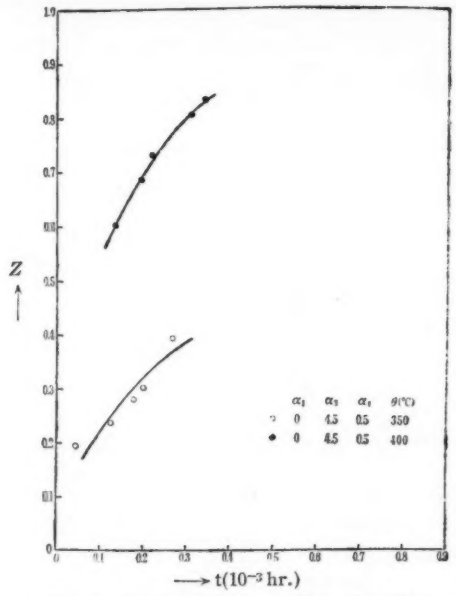


Fig. 8. Fractional conversion of carbon monoxide ($Z$) vs. contact time ($t$).

fractional conversions of carbon dioxide ($Z'$) vs. contact times ($t$). The values of $Z$ and $Z'$ were calculated from the carbon dioxide content in the exit gas and the inlet gas composition, neglecting the side reaction, and $t$ was calculated by the follwing equation.

$$t = \frac{\text{packed volume of catalyst (c.c.)}}{\text{total flow rate at each reaction temperature (c.c./hr.)}}$$

**a) Water-Gas Shift Reaction.**—In order to find the rate equation for the water-gas shift reaction which can reproduce the present results, many equations were put to the test, among which the following was proved to be most satisfactory.

$$-\frac{dP_{CO}}{dt} = k_1 \frac{P_{CO}P_{H_2O} - K_p P_{CO_2} P_{H_2}}{1 + KP_{CO} + K'P_{H_2O} + K''P_{H_2} + K'''P_{CO_2}} \quad (6)$$

The partial pressure of the component $i$, $P_i$ can be written in terms of fractional conversion and inlet gas composition, as

$$P_i = \frac{\alpha_i - \nu_i Z}{\sum_r \alpha_r}$$

where

$$\alpha_i = \frac{P^\circ_i}{P^\circ_{CO}} \quad (7)$$

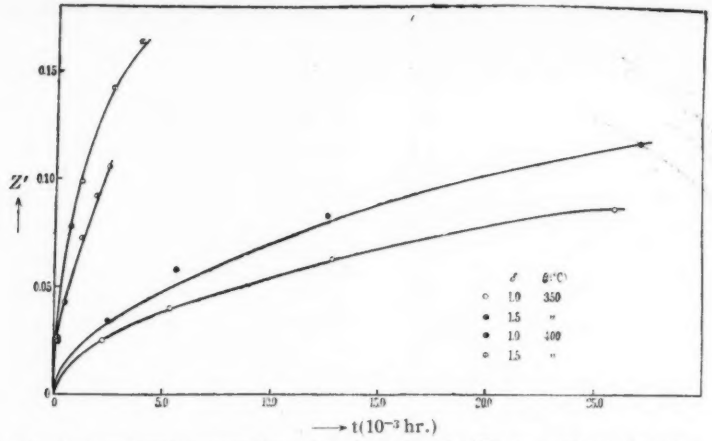


Fig. 9. Fractional conversion of carbon dioxide ($Z'$) vs. contact time ($t$).

and $\nu_i$ represents the stoichiometric ratio of the component $i$ in the forward reaction[8], i.e.,

$$\nu_{CO}=\nu_{H_2O}=1, \quad \nu_{CO_2}=\nu_{H_2}=-1$$

Using Eq. (7) the rate expression is represented as a function of $Z$ and $t$. On integrating Eq. (6), the relation of $Z$ and $t$ is derived as follows:

$$P\frac{k_1 t}{2.303}=\frac{1}{\beta-\gamma}\Big[\{1+KP+\alpha_3(1+K'P)+\alpha_1(1+K''P)+\alpha_4(1+K'''P)+(K'''+K''-K'-K)P\beta\}\times\log\frac{\beta-Z}{\beta}-\{1+KP+\alpha_3(1+K'P)+\alpha_1(1+K''P)+\alpha_4(1+K'''P)+(K'''+K''-K'-K)P\gamma\}\times\log\frac{\gamma-Z}{\gamma}\Big] \tag{8}$$

where $\beta$ and $\gamma$ are the positive and negative roots of the following equation, respectively.

$$(1-K_p)Z^2-\{K_p(\alpha_1+\alpha_4)+(\alpha_3+1)\}Z+(\alpha_3-K_p\alpha_1\alpha_4)=0 \tag{9}$$

Table I shows the values of $k_1$ calculated

TABLE I

VALUES FOR $k_1$ (atm.$^{-1}$ hr.$^{-1}$ Unit)

(I) $\theta=350$, $K=0.3$ (atm.$^{-1}$), $K'=1.5$ (atm.$^{-1}$), $K''=4$ (atm.$^{-1}$), $K'''=20$ (atm.$^{-1}$)

| $\alpha_1=0$, $\alpha_3=2$, $\alpha_4=0$ | | $\alpha_1=0$, $\alpha_3=3$, $\alpha_4=0$ | |
|---|---|---|---|
| $t$(10$^{-3}$ hr.) | $k_1$(10$^4$) | $t$(10$^{-3}$ hr.) | $k_1$(10$^4$) |
| 0.176 | 1.048 | 0.0982 | 1.016 |
| 0.207 | 0.890 | 0.113 | 1.039 |
| 0.308 | 0.970 | 0.144 | 1.036 |
| 0.424 | 0.949 | 0.175 | 1.022 |
| 0.515 | 0.881 | 0.373 | 0.936 |
| 0.626 | 0.972 | 0.611 | 0.974 |

| $\alpha_1=1$, $\alpha_3=2$, $\alpha_4=0$ | | $\alpha_1=1$, $\alpha_3=4$, $\alpha_4=0$ | |
|---|---|---|---|
| $t$(10$^{-3}$ hr.) | $k_1$(10$^4$) | $t$(10$^{-3}$ hr.) | $k_1$(10$^4$) |
| 0.145 | 1.745 | 0.171 | 1.050 |
| 0.191 | 1.679 | 0.258 | 1.078 |
| 0.239 | 1.673 | 0.300 | 1.135 |
| 0.289 | 1.441 | 0.395 | 1.091 |
| 0.365 | 1.649 | 0.555 | 1.070 |
| 0.457 | 1.516 | 0.595 | 0.977 |
| $\alpha_1=1$, $\alpha_3=6$, $\alpha_4=0$ | | $\alpha_1=2$, $\alpha_3=3$, $\alpha_4=0$ | |
| $t$(10$^{-3}$ hr.) | $k_1$(10$^4$) | $t$(10$^{-3}$ hr.) | $k_1$(10$^4$) |
| 0.189 | 1.191 | 0.130 | 0.972 |
| 0.226 | 1.186 | 0.246 | 1.391 |
| 0.269 | 1.062 | 0.364 | 1.530 |
| 0.348 | 1.062 | 0.407 | 1.404 |
| 0.389 | 1.011 | 0.491 | 1.366 |
| 0.520 | 0.909 | 0.713 | 1.355 |
| 0.537 | 0.914 | 0.831 | 1.294 |
| $\alpha_1=2$, $\alpha_3=6$, $\alpha_4=0$ | | $\alpha_1=2$, $\alpha_3=9$, $\alpha_4=0$ | |
| $t$(10$^{-3}$ hr.) | $k_1$(10$^4$) | $t$(10$^{-3}$ hr.) | $k_1$(10$^4$) |
| 0.105 | 0.920 | 0.106 | 1.025 |
| 0.140 | 1.224 | 0.151 | 1.049 |
| 0.228 | 0.959 | 0.183 | 1.159 |
| 0.282 | 0.909 | 0.308 | 0.996 |
| 0.392 | 0.864 | 0.331 | 1.080 |
| | | 0.574 | 0.985 |

| $\alpha_1=0$, $\alpha_3=4.5$, $\alpha_4=0.5$ | |
|---|---|
| $t$(10$^{-3}$ hr.) | $k_1$(10$^4$) |
| 0.044 | 1.149 |
| 0.126 | 1.220 |
| 0.178 | 1.079 |
| 0.200 | 1.065 |
| 0.268 | 1.168 |

(II) $\theta=400$, $K=0.1$ (atm.$^{-1}$), $K'=0.5$ (atm.$^{-1}$), $K''=2$ (atm.$^{-1}$), $K'''=10$ (atm.$^{-1}$)

| $\alpha_1=0$, $\alpha_3=1$, $\alpha_4=0$ | | $\alpha_1=0$, $\alpha_3=2$, $\alpha_4=0$ | |
|---|---|---|---|
| $t$(10$^{-3}$ hr.) | $k_1$(10$^4$) | $t$(10$^{-3}$ hr.) | $k_1$(10$^4$) |
| 0.233 | 4.450 | 0.181 | 4.132 |
| 0.311 | 4.258 | 0.215 | 4.187 |
| 0.360 | 4.453 | 0.249 | 3.713 |
| 0.466 | 4.442 | 0.305 | 4.432 |
| 0.630 | 3.635 | 0.527 | 3.358 |

| $\alpha_1=0$, $\alpha_3=3$, $\alpha_4=0$ | | $\alpha_1=0.5$, $\alpha_2=4.5$, $\alpha_4=0$ | |
|---|---|---|---|
| $t(10^{-3}$ hr.) | $k_1(10^4)$ | $t(10^{-3}$ hr.) | $k_1(10^4)$ |
| 0.120 | 3.162 | 0.0884 | 2.802 |
| 0.145 | 3.276 | 0.0921 | 2.932 |
| 0.172 | 3.126 | 0.272 | 2.471 |
| 0.224 | 3.002 | 0.290 | 2.551 |
| 0.313 | 2.788 | 0.400 | 2.217 |
| $\alpha_1=1$, $\alpha_3=2$, $\alpha_4=0$ | | $\alpha_1=1$, $\alpha_3=4$, $\alpha_4=0$ | |
| $t(10^{-3}$ hr.) | $k_1(10^4)$ | $t(10^{-3}$ hr.) | $k_1(10^4)$ |
| 0.130 | 4.000 | 0.125 | 2.552 |
| 0.149 | 4.215 | 0.131 | 2.578 |
| 0.205 | 4.028 | 0.173 | 2.583 |
| 0.342 | 2.907 | 0.209 | 2.590 |
| 0.414 | 3.622 | 0.255 | 2.358 |
| 0.470 | 4.132 | | |
| $\alpha_1=1$, $\alpha_3=6$, $\alpha_4=0$ | | $\alpha_1=2$, $\alpha_3=3$, $\alpha_4=0$ | |
| $t(10^{-3}$ hr.) | $k_1(10^4)$ | $t(10^{-3}$ hr.) | $k_1(10^4)$ |
| 0.117 | 2.702 | 0.150 | 2.780 |
| 0.216 | 1.966 | 0.315 | 3.045 |
| 0.239 | 2.342 | 0.353 | 3.080 |
| 0.259 | 2.553 | 0.394 | 3.062 |
| 0.368 | 2.000 | 0.510 | 2.976 |
| $\alpha_1=2$, $\alpha_3=6$, $\alpha_4=0$ | | $\alpha_1=2$, $\alpha_3=9$, $\alpha_4=0$ | |
| $t(10^{-3}$ hr.) | $k_1(10^4)$ | $t(10^{-3}$ hr.) | $k_1(10^4)$ |
| 0.095 | 2.156 | 0.107 | 2.323 |
| 0.116 | 2.480 | 0.126 | 2.758 |
| 0.284 | 1.970 | 0.211 | 2.614 |
| 0.319 | 1.924 | 0.304 | 1.860 |
| 0.392 | 1.970 | 0.407 | 1.740 |
| 0.496 | 2.047 | | |

| $\alpha_1=0$, $\alpha_3=4.5$, $\alpha_4=0.5$ | |
|---|---|
| $t(10^{-3}$ hr.) | $k_1(10^4)$ |
| 0.135 | 2.618 |
| 0.195 | 2.379 |
| 0.220 | 2.456 |
| 0.313 | 2.412 |
| 0.344 | 2.468 |

by Eq. (8). The numerical values of $K_p$ used were taken from Lewis and Randall's work[12] and $K$, $K'$, $K''$, and $K'''$ were chosen so that the value of $k_1$ becomes most satisfactorily constant at a given temperature.

Experiments were also made at 450°C for a wide range of inlet gas composition and contact time. But in this case Eq. (6) failed to reproduce the experimental results.

**b) Reverse Shift Reaction.**—If Eq. (6) reproduces the results of the water-gas shift reaction, the reaction rate of the reverse shift reaction must be given as:

$$\frac{dP_{CO}}{dt} = k_2 \frac{P_{CO_2} P_{H_2} - \frac{1}{K_p} P_{CO} P_{H_2O}}{1+KP_{CO}+K'P_{H_2O}+K''P_{H_2}+K'''P_{CO_2}} \quad (10)$$

12) G. N. Lewis, and M. Randall, "Thermodynamics and free energy of chemical substances," Mc Graw Hill Book Co., New York, (1923) p. 574.

As in the case of the forward reaction, also, the relation of $Z'$ and $t$ is derived for the reverse shift reaction from Eq. (10), as

$$P\frac{k_2 t}{2.303} = \frac{1}{-\beta'+\gamma'}\left\{[1+K'''P+\delta(1+K''P) +(K+K'-K''-K''')\beta' P]\log\frac{\beta'-Z'}{\beta'} -[1+K'''P+\delta(1+K''P) +(K+K'-K''-K''')\gamma' P]\log\frac{\gamma'-Z'}{\gamma'}\right\} \quad (11)$$

where $\delta$ represents the mole ratio of hydrogen to carbon dioxide at inlet, and $\beta'$ and $\gamma'$ are the positive and negative roots of the following equation, respectively.

$$(1-Z')(\delta-Z')-\frac{1}{K_p}Z'^2=0 \quad (12)$$

Calculated values of $k_2$ for all the experimental conditions are tabulated in Table II. The values of $K$, $K'$, $K''$, $K'''$ and $K_p$ used for computing are the same as those used in the calculation for $k_1$.

TABLE II

VALUES FOR $k_2$ (in atm.$^{-1}$ hr.$^{-1}$ Unit)

(I) $\theta=350$, $K=0.3$ (atm.$^{-1}$), $K'=1.5$ (atm.$^{-1}$) $K''=4$ (atm.$^{-1}$) $K'''=20$ (atm.$^{-1}$)

| $\delta=1.0$ | | $\delta=1.5$ | |
|---|---|---|---|
| $t(10^{-3}$ hr.) | $k_2(10^2)$ | $t(10^{-3}$ hr.) | $k_2(10^2)$ |
| 2.23 | 5.381 | 2.505 | 5.164 |
| 5.35 | 5.056 | 5.680 | 5.482 |
| 12.86 | 5.170 | 12.65 | 5.241 |
| 25.97 | 5.203 | 27.22 | 5.129 |

(II) $\theta=400$, $K=0.1$ (atm.$^{-1}$), $K'=0.5$ (atm.$^{-1}$), $K''=2$ (atm.$^{-1}$), $K'''=10$ (atm.$^{-1}$)

| $\delta=1.0$ | | $\delta=1.5$ | |
|---|---|---|---|
| $t(10^{-3}$ hr.) | $k_2(10^3)$ | $t(10^{-3}$ hr.) | $k_2(10^3)$ |
| 0.175 | 2.067 | 0.128 | 1.925 |
| 0.403 | 2.078 | 0.749 | 2.097 |
| 1.242 | 1.915 | 1.224 | 1.966 |
| 1.890 | 1.943 | 2.660 | 1.956 |
| 2.534 | 1.985 | 3.924 | 1.890 |

## Discussion

As seen from Tables I and II, the constancy of $k_1$ and $k_2$ is fairly good, which reveals the fact that the rate equations (6) as well as (10) are sufficiently accurate at least for the practical purpose.

Namely, the values of $k_1$ given in Table I are sufficiently constant over the contact time range $0.1$–$0.8\times10^{-3}$ hr. and various inlet gas compositions at 350°C. At 400°C, $k_1$ varies somewhat with $P°_{CO}$. This change in $k_1$ may reasonably be attributed to the occurrence of the catalytic decomposition of carbon monoxide. However, at relatively small

$P^{\circ}_{CO}$, as in the case of industrial reactors, the dependence of $k_1$ upon $P^{\circ}_{CO}$ is negligibly small, so that Eq. (6) may be useful for the reactor design.

Eqs. (1), (2), and (4) may be derived through some simplifications from Eq. (6), but Kalkova and Temkin's equation may not. Eq. (6) is similar to that of Horiuchi[13], derived theoretically.

Within the range of experimental error, no systematic deviation of the rate constants $k_2$ can be found from Table II. As is seen from these data, it is evident that Eq. (10) reproduces the rate data well.

Equilibrium constants $K_p$ at 350°C and 400°C are calculated from $k_1$ and $k_2$. These values of $K_p$ are shown in Table III together

TABLE III

VALUES FOR $K_p$

| $\theta$(°c) | $K_p$ | |
|---|---|---|
| 350 | 0.041 | Neumann and Kōhler[14] |
| | 0.0471 | Lewis and Randall[12] |
| | 0.0474 | Kodama, Mazume, Fukuba and Fukui |
| 400 | 0.0734 | Engels[a] |
| | 0.080 | Neumann and Köhler[14] |
| | 0.0824 | Lewis and Randall[12] |
| | 0.0796 | Kodama, Mazume, Fukuba and Fukui |

a) Engels, Dissertation, (1911) Karlsuhe (Cited in Reference 14).

with those previously presented. The values of $k_1$ at 400°C used in calculating $K_p$ are the average of $k_1$'s obtained at relatively small $P^{\circ}_{CO}$. The present values of $K_p$ are in good agreement with previous publications, especially with values obtained by the direct method[14]. Eq. (6) may suggest something to us concerning the reaction mechanism, but no direct evidence for it has been given. It may rather be stressed that Eq. (6) serves as an empirical equation which is useful for industrial purposes.

## Conclusion

The conclusion is as follows:

A rate equation for the water-gas shift reaction as well as for the reverse shift reaction which can reproduce the experimental results at 350°C and 400°C for various inlet gas compositions and contact times is obtained.

The equation seems to be sufficiently accurate at least for industrial purposes.

The assistance of Mr. T. Okada and Mr. M. Okazaki are gratefully acknowledged. Also the authors are indebted to The Befu Chemical Co. Ltd., for liquefied carbon dioxide.

*Faculty of Engineering, Kyoto University, Kyoto*

13) J. Horiuti, *Catalyst* (Japan) 8, 58 (1952).

14) B. Neumann and G. Köhler, *Z. Elektrochem.*, **34**, 218 (1928).

$k_1$, $k_2$, $K$, $K'$, $K''$, $K'''$=constants in the rate equation, which are function of temperature only.

$K_p$=equilibrium constant of the water-gas reaction

$$= \frac{P^{\infty}_{CO}\ P^{\infty}_{H_2O}}{P^{\infty}_{H_2}\ P^{\infty}_{CO_2}}$$

$P_i$=partial pressure of component i, atmospheres.

$P$=total pressure atmospheres.

$t$=contact time measured at reaction temperature, hours.

$Z$=fractional conversion of carbon monoxide for the forward reaction.

$Z'$=fractional conversion of carbon dioxide for the reverse reaction.

$\alpha_i$=mole ratio of component i to carbon monoxide in feed of the forward reaction ($\alpha_2$=1).

$\delta$=mole ratio of hydrogen to carbon dioxide in feed of the reverse reaction.

$\theta$=temperature, °C.

Subscripts 1, 2, 3 and 4 designate hydrogen, carbon monoxide, water and carbon dioxide, respectively.

Superscript $\infty$ designates equilibrium conditions.

Superscript 0 designates inlet conditions.

# *Polymorphic Phase Transition of Beryllium Oxyacetate* $Be_4O(CH_3CO_2)_6$*

By Masanobu MOMOTANI,** Syûzô SEKI, Hideaki CHIHARA and Hiroshi SUGA

(Received February, 16, 1955)

## Introduction

In 1943, by Preston and Trotter[1] as well as by Beevers[2] it was found that the symmetry of Laue photograph of the cubic modification of this crystal changes from $T_h$-m3 to $O_h$-m3m in the temperature interval of 30°~50°C. Beevers explained this phase transition as due to the change in the parameter values of the carboxyl oxygen atom from (−0.17, −0.06, −0.04) to (−0.17, −0.05, −0.05) when the temperature rises and passes the transition range, thus bringing all the oxygen atoms exactly onto (110) planes. On the other hand, in 1947, Jaffray[3] measured the specific heat of this crystal below and above the transition region and found that at 40.5±0.5°C there is an anomaly of typical λ-type in the heat capacity curve.

In 1949, Watanabé and Saito[4] observed that this crystal became waxy when it was heated above 160°C, though it melted very sharply at about 285°C. They studied the crystal structure of this high temperature modification as well as the above-mentioned phase transition at about 40°C by the X-ray method and in order to explain the results they put forward a mechanism of the order-disorder type. They also investigated the so-called γ-form of this crystal which was obtained by sublimation at ordinary pressure.

We have undertaken to study these phase transitions as a part of our thermochemical investigation on the nature of the so-called plastic crystals.

## Experimental

**a) Sample.**—Beryllium oxide was dissolved in acetic acid and by evaporating the excess acid in the evaporating dish we obtained the crude specimen. This was then recrystallized three times from chloroform and finally subjected to fractional sublimation under high vacuum ($10^{-5}$ mmHg), m.p. 286.7°C.

**b) Apparatas and Procedures.**—The apparata used for the differential thermal analysis,[5] dilatometry[6], vapor pressure measurement[7] and the conduction calorimetry[8] were all the same as those that have been used hitherto in our laboratory, so that their description may be omitted here.

## Experimental Results

**i) Differential thermal analysis.**—As mentioned above, by the observation of the change of appearance of the crystal above 160°C by Watanabé and Saito, it was strongly inferred that this crystal would undergo a phase transition around this temperature. To determine the accurate temperatures of transition and melting, we carried out the differential thermal analysis. One of the typical curves is given in Fig. 1. From

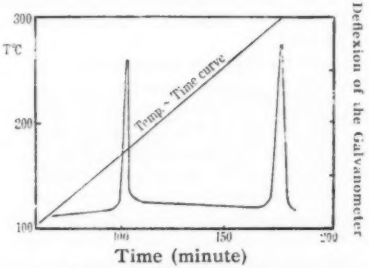


Fig. 1. Curves of differential thermal analysis of $Be_4O(CH_3CO_2)_6$.

this curve, it was found that the magnitude of the heat effects accompanying these two phase changes are comparable with each other. To examine the nature of the polymorphic phase transition further in detail, we then performed a series of thermal analyses under various conditions. All the experimental curves of the deflection of the galvanometer for measuring the temperature head are shown in Fig. 2.* We may enumerate some features of these curves as follows:

* A part of this research was already published in *Nature*, **163**, 226 (1949).

** Present address: Momotani Juntenkan Co., Ltd., Osaka.

1) G. D. Preston and T. Trotter, *Nature*, **151** 166 (1943).

2) C.A. Beevers, *Nature*, **152**, 447 (1943).

3) J. Jaffray, *Compt. rend.*, **225**, 106 (1947).

4) T. Watanabé and Y. Saito, *Nature*, **163**, 225 (1949). T. Watanabé, Y. Saito and H. Koyama, ibid., **164**, 1056 (1949).

5) H. Chihara and S. Seki, This Bulletin, **26**, 88 (1953).

6) I. Nitta, S. Seki and M. Momotani, *Proc. Japan Acad.*, **26**, (10) 11, (1950).

7) I. Nitta, S. Seki, M. Momotani and K. Sato, *J. Chem. Soc. Japan*, **71**, 378 (1950).

8) S. Seki, M. Momotani, K. Nakatsu and T. Oshima, This Bulletin, (in press).

* The figure attached at the highest temperature side of each curve means the temperature at which the heating was stopped.

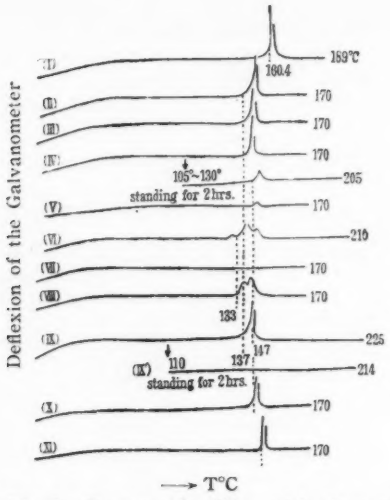


Fig. 2. Curves of differential thermal analyses of $Be_4O(CH_3CO_2)_6$ at various conditions.

(a) Curve (i) represents the result of the sample which has been stored for about half a year in a desiccator over calcium chloride. As shown in the figure this sample shows the highest transition point of 160.4°C (heating velocity is about 2~2.5°C/min.).

(b) When the sample was not heated above around 210°C, it always shows the transition point at about 140°~147°C (curves (ii), (iii), (iv)).

(c) If the sample was cooled down below 110°C, standing it at this temperature for about two hours and then heated again, it showed a small hump at about 147°C. However, if it was not cooled down below 110°C, no transition phenomenon could be observed.

(d) If the sample was heated above 210°C and then left to natural cooling down to the room temperature, there appeared no transition phenomenon in the heating curve which was measured again, even on the following day (two sets of curves (vi) and (vii), and (ix) and (ix)'). However, if the supercooled sample which showed no phase change was ground in an agate mortar at room temperature, it exhibited phase change of a rather complex nature (curves (vi) and (viii)).

(e) Freshly prepared sample by sublimation shows normal phase change at about 147°C (see Fig. 1 and curve (x)). But, when such sample was thoroughly ground to very fine powders, it showed a little higher temperature of phase change (curve (xi)).

A possible explanation of the somewhat complex characteristics of these curves may be given after the following description on the dilatometric investigation.

**ii) Dilatometric investigation.**—Since the method of differential thermal analysis was not sensitive enough to detect a phase change with small heat effect, we then measured the volume change very carefully using the freshly prepared specimen in order to find out some clues to explain the complex nature just mentioned above. As the results, we could find out that the expansion coefficient changes at four temperatures, namely, 32±0.5°C, 42±0.4°C, 77±0.4°C, and 124.5±0.5°C, and further that the volume itself increases abruptly at 148°C by a great amount which corresponds to about 5.6% of the volume at 25°C. Of these temperatures, the secound one, 42±0.4°C,

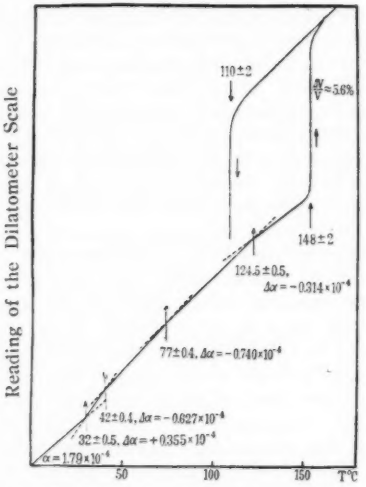


Fig. 3. Volume vs. temperature curve of $Be_4O(CH_3CO_2)_6$.

coincides with that determined by Jaffray, while the third and the fourth were discovered first by the present experiment. Moreover, it was revealed that the transition at 148°C shows a hysteresis phenomenon covering over a wide range of temperatures, the volume change in the cooling curve taking place at 110±2°C, far below the transition point observed in heating direction. Among these changes of expansion coefficient at four temperatures only the first one has the plus sign. It is to be added that after these results were published,** Jaffray[9] recently confirmed our experimental results.

**iii) Heat capacity measurement.**—As mentioned above, the transition at about 42°C seems to be of particular interest, since the crystal structures on each side of the transition temperature have been already known. Although Jaffray has measured the heat capacities at these temperatures, the temperature range was not wide enough to determine the heat of transition, so we measured anew the heat capacities extending our measurements over a much wider temperature range both in heating and cooling directions. Our

** See footnote (*) in page 325.

9) J. Jaffray, Compt. rend. de la deuxième Réunion Annuelle tenue en Commun avec la Commission de Thermodynamique de l'Union Internationale de Physique Changements de Phases. p. 267. (1952).

data are given in Table I and the heat capacity curves are shown in Fig. 4. In the figure, we can

TABLE I

HEAT CAPACITY OF $Be_4O(CH_3CO_2)_6$

| Heating direction | | Cooling direction | |
|---|---|---|---|
| $t$°C | $C_p$ cal./mole | $t$°C | $C_p$ cal./mole |
| 0.00 | 116.5 | 85.22 | 138.1 |
| 13.02 | 118.7 | 79.60 | 136.0 |
| 19.4 | 120.93 | 76.84 | 135.5 |
| 25.7 | 123.0 | 75.20 | 138.7 |
| 31.48 | 127.9 | 73.81 | 131.9 |
| 38.15 | 133.7 | 73.15 | 130.7 |
| 41.78 | 136.3 | 71.78 | 138.4 |
| 43.05 | 129.6 | 70.58 | 132.4 |
| 44.20 | 126.6 | 69.20 | 131.5 |
| 50.21 | 126.9 | 62.20 | 129.0 |
| 62.20 | 129.0 | 56.25 | 126.8 |
| 66.87 | 129.9 | 50.21 | 124.7 |
| 69.20 | 130.9 | 47.82 | 124.1 |
| 71.52 | 134.1 | 45.41 | 124.7 |
| 72.68 | 131.8 | 43.05 | 127.7 |
| 73.81 | 132.1 | 40.60 | 135.0 |
| 74.99 | 132.9 | 40.08 | 134.4 |
| 76.13 | 135.9 | 38.15 | 132.2 |
| 76.84 | 134.9 | 35.66 | 130.8 |
| 78.46 | 134.8 | 30.72 | 126.1 |
| 80.73 | 135.9 | 25.70 | 122.8 |
| 83.00 | 136.6 | | |
| 85.22 | 137.8 | | |
| 97.48 | 139.1 | | |

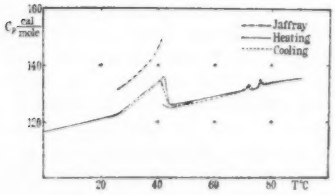


Fig. 4. Heat capacity vs. temperature curves of $Be_4O(CH_3CO_2)_6$.

realize that the heating curve almost completely coincides with the cooling one, showing no hysteresis. By this measurement, it was made clear that the temperature (32°C) where the expansion coefficient increases sharply, corresponds to the temperature where the heat capacity curve begins to increase.

**iv) Vapor pressure measurement.**—This material sublimes slowly even at room temperatures, so we attempted to measure the sublimation pressures below and above the transition point to determine the heat of sublimation as well as the heat of transition. The results are all given in Table II. The heat and entropy of fusion were estimated to be 6.5 kcal./mole and

TABLE II

VAPOR PRESSURES OF $Be_4O(CH_3CO_2)_6$

| $t$°C | $P$ mm Hg $\times 10^3$ | $t$°C | $P$ mm Hg $\times 10^3$ |
|---|---|---|---|
| 120.7 | 2.828 | 152.6 | 52.22 |
| 124.9 | 4.081 | 156.3 | 65.33 |
| 126.5 | 4.539 | 160.0 | 92.92 |
| 134.4 | 9.508 | 164.6 | 124.8 |
| 135.1 | 11.30 | 168.3 | 164.1 |
| 139.9 | 15.93 | 172.8 | 213.6 |
| 145.6 | 29.60 | | |
| 145.7 | 30.43 | | |
| 148.6 | 39.98 | | |

$$\log P = 15.029_9 - 6934.8/T$$
(below the transition point)
$$\log P = 12.626_9 - 5922.8/T$$
(above the transition point)

| | $\Delta H$ kcal./mole | $\Delta F$ cal./mole | $\Delta S$ e.u. |
|---|---|---|---|
| Sublimation (low-temp. phase) | 31.7 | $31734 - 60.170T$ | 60.2 |
| Sublimation (high-temp. phase) | 27.1 | $27102 - 44.598T$ | 44.6 |
| Transition | 4.6 | — | 15.6 |

11.6 e.u., respectively by comparison of the corresponding areas of the two peaks obtained by the thermal analysis (see Fig. 1).

## Discussion of Results

As pointed out by Watanabé and Saito, the fact that the melting point of this material is abnormally higher than those of other compounds of homologous series and also that the soft waxy appearance above the transition temperature of 148°C suggests that the high-temperature modification will belong to the so-called plastic crystal. By our measurements of the entropy changes at the transition and melting points, we can confirm the fact that their prediction is correct. They further investigated the X-ray diffraction effects of the high temperature modification at various temperatures of 160°, 170°, 220°, 270° and 280°C. According to them, the crystal structure gradually changes with the rise of temperature and approaches the final structure which belongs to a rhombohedral lattice with the cell dimensions of $a = 9.72$ kX and $\alpha_r = 54°20'$, containing one molecule in it.[10] They noticed, however, that the crystal structure just above the transition temperature may be of a little lower symmetry than the final rhombohedral lattice structure which is reached gradually between 220° and 280°C. In our thermal analysis study, we have noticed the curious fact that the sample which was

10) Y. Saito, *X-rays*, **7**, 1 (1952).

previously heated above about 210°C did not exhibit the transition phenomenon in the repeated heating experiments carried out on the following day. This phenomenon and the above-mentioned results of the X-ray investigation seem to imply that the crystal structure in the temperature region between the transition point and about 210°~220°C will retain some characteristic feature of the structure below the transition point rather than that of the high temperature form above 220°C.

The transition at 148°C is of a typical 1-st order type, judging from the discontinuities of vapor pressure curves and of volume change. This transition point is, however, sensitive to the history of the crystal lattice and is displaced to higher temperatures when the crystal was stored for a long time after the preparation (see curve (i) in Fig. 2) or ground mechanically (curve (xi) in Fig. 2). The curves of the differerential thermal analysis sometimes show more or less complex structures which are observed in the temperature region about 130°~147°C (see curve (vi) and (viii) in Fig. 2). This process may also be explained as due to the relative degree of metastability of the phases which exist between 124°C and 148°C and of the high temperature phase above the transition point.[11] This result also reminds us of the fact that $Pb(C_2H_5)_4$ and $Sn(C_2H_5)_4$[12] show several melting points depending on the heating or cooling rate as well as on the previous histories. These phenomena suggest that for the molecular crystals composed of molecules which have methyl groups at their periphery, it is rather difficult to establish the real equilibrium state on account of the meshing-gear-like interaction between methyl groups belonging to one and the same molecule as well as to the neighbouring other molecules.

Now, we proceed to the discussion of the phase transition at about 40°C. As shown in Fig. 4, the heat capacity curve is of typical λ-type and the heat of transition is very small compared with that at 147°C. Nonexistence of the hysteresis phenomenon is in agreement with the prediction by Staveley from the stand point that the lattice strain energy is very small in the case of higher-order phase transition[13]. Thus, these facts reasonably indicate the higher order type of this transition.

As already mentioned, the crystal structures above and below this transition point are already investigated in detail by several authors. According to their results, it may be said that there may exist two kinds of molecules of *d*- and *l*- types, so to speak, below the transition temperature in reference to the two equivalent potential minima for the orientation of the oxygen pair of the carboxyl group.* Confining our study to the intramolecular interaction, no difference can exist between these two kinds of molecules. However, if we consider the intermolecular interaction, the interaction energy between two different types of molecule will be different from that between two of the same type of molecule and the former is probably larger than the latter. As a result, it may be assumed that the *d*- (or *l*-) type molecule is the more stable the larger the number of the neighbouring *l*- (or *d*-) type molecules. As the temperature rises, the rotational vibration of the carboxyl group about C–C axis becomes more and more violent and the distinction between these two types of molecule will disappear when two oxygen atoms of the carboxyl group surmount the potential barrier between the two potential minima. The difference of intermolecular energies between a pair of the same kind of molecules and a pair of different kinds just mentioned above also disappears at the same time. In such a way, we may understand this phase transition as a kind of order-disorder type. In the case of the ordinary order-disorder transition of an alloy system, the interchange of the atomic position between different kinds of atoms takes place, while in the present case only the transition of atoms from unequivalent potential minima to equivalent ones occurs within one and the same molecule. Thus, it may be said that this case is somewhat similar to the so-called Ising model designed for the ferromagnetic transition, etc.

Finally, we should like to propose a tentative theory on the rotational transition of the molecular crystal of this sort, although it may be of qualitative nature.

Following the theory of Fowler on the rotational phase transition[14], we assume all the libration and rotation to be classical. Then the total energy in Hamiltonian form is

$$H=T+V, \qquad \text{with } V=-\frac{W}{2}\cos\theta,$$

where $T$ is the kinetic energy of rotation of the rigid rotator with axial symmetry, $V$

11) A.R. Ubbelohde, *Nature*, **169**, 832 (1952).
12) D.G. Thomas and L.A.K. Staveley, *J. Chem. Soc.*, (1951) 2572.
13) L.A.K. Staveley et al. *J. Chem. Soc.*, (1950) 2290.

* As to the possibility of two forms of this molecule, see reference 11).
14) Fowler: *Statistical Mechanics* (1936), p. 810.

the potential energy due to the surrounding field of force, $W$ the height of the hindering potential of the rotator, and $\theta$ the displacement of the axis of figure from a single preferred direction of equilibrium. The probability $P(\theta)d\theta$ of finding the rotator between $\theta$ and $\theta+d\theta$, is

$$P(\ )d\theta=\int_0^{2\pi}\int_{-\infty}^{+\infty}\int_{-\infty}^{+\infty}e^{-H/kT}dP_\theta dP_\varphi d\varphi d\theta$$

The partition function $f$ is then given by

$$f=\frac{2\pi IkT}{h^2}\cdot 2\pi\cdot\int_0^\pi e^{-V/kT}\sin\theta d\theta$$

$$=\frac{8\pi^2IkT}{h^2}\cdot\frac{kT}{W}\sin hW/kT \qquad (3)$$

where $I$ is the moment of inertia of the rotationg group of the molecule. As is well known, Fowler defined the degree of nonrotation $S$ by the next equation:

$$S=f_0/f$$

where

$$f_0=\int\int_{H<\beta V}e^{-H/kT}dP_\theta d\theta \qquad (4)$$

Here, the parameter $\beta$ is the measure of nonrotation in the sense that the molecule having less energy than $\beta V$ can not rotate anyhow. However, the physical meaning of $\beta$ is not very obvious, and this ambiguity may be removed in a slightly improved way by defining the order parameter by the following quantity,

$$S=\int_0^\pi P(\theta)(-\cos\theta)d\theta/f$$

$$=\int_0^\pi e^{-W/2kT\cos\theta}(-\cos\theta)\sin\theta d\theta$$

$$=\coth W/2kT-2kT/W \qquad (5)$$

At 0°K, $S=1$ and as temperature rises $S$ decreases gradually from 1. According to the Bragg-Williams approximation, we then assume

$$W=W_0S+W_0^\circ. \qquad (6)$$

In this equation, $W_0^\circ$ is the part of $W$ which does not depend on $S$. In other words, this means that even above the transition temperature the molecules are not necessarily to be looked upon as free rotators. $W_0^\circ$ is, therefore, a measure of hindering potential which is not affected by the long range cooperation. Thus, if the ratio of $W_0^\circ/W$ is not zero, the straight line representing the above equation does not start from the origin in the plot of $S$ against $\alpha$ $(=W/2kT)$ (see Fig. 5).

Now, on the assumption, in the case of the present substance, that for the potential energy $V$ for the rotation of carboxyl radical,

$$V=\frac{W}{2}\cos 2\theta,$$

the order parameter $S$ mentioned above becomes

$$S=I_1/I_0,$$

where $I_1$ and $I_0$ are the 1-st and 0-th order modified Bessel functions, respectively. The relation between $S$ and $\alpha$ is shown in Fig. 5,

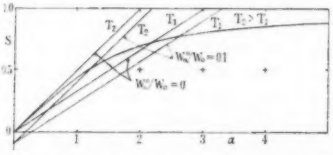

Fig. 5. Dependence of order parameter $S$ upon $\alpha$.

and that between $S$ and $T/T_c$ is given in Fig. 6. In these figures two cases of $W_0^\circ/W_0$

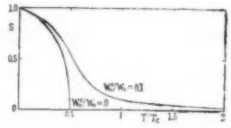

Fig. 6. Relation between order parameter $S$ and $T/T_c$.

$=0$ and $=0.1$ are represented. By the ordinary method we can then calculate the energy as a function of temperature as illustrated in Fig. 7. By differentiation we can finally

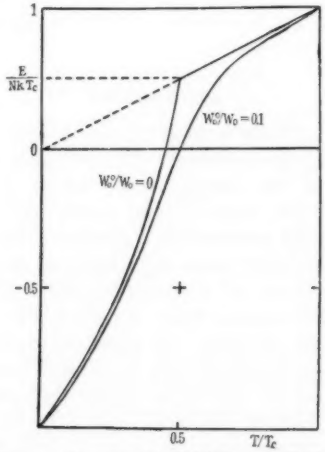

Fig. 7. Curves of $E/NkT_c$ vs. $T/T_c$.

find the heat capacity curve as shown in Fig. 8.

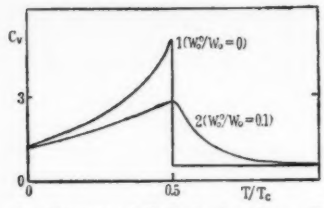


Fig. 8. Curves of $C_v$ (calculated) vs. $T/T_c$.

From the results of these curves, we can find out that when the ratio $W_0'/W_0$ is not zero, there occurs no phenomenon of the latent heat. The heat capacity curve (1) in Fig. 8 is similar in shape to the actual behavior found in this material at about 40°C. In this case the value of $W_0$ is calculated to be about 2.5 kcal./mole which seems to be not so unreasonable an order of magnitude for a molecular crystal like the present material.

Although these results are only of qualitative nature, it may be of some significance to understand the rotational phase transition in such a simple way.

In conclusion, the authors should like to express their hearty appreciation to Professor Nitta for his gracious interest during this work and to Dr. Y. Saito of Osaka City University and Dr. K. Motojima of Kyoto Ritsumeikan University for kindly giving the samples used. The cost of this research was defrayed from the funds of Taniguchi Kôgyô Shôreikai as well as from the Scientific Research Expenditure Grant from the Ministry of Education, to which the thanks of the present authors are due.

*Department of Chemistry, Faculty of Science, Osaka University, Osaka*

Note added in Proof: K.N. Semenenko, Yu.P. Simanov and A.V. Novoselova have recently raised an objection about the reality of the transition at 148°C. (Vestnik Moskov Univ., 9, No. 2, Ser. Fiz-Mat. i Est. Nauk No. 1, 61 (1954)). They, however, dealt only with the monoclinic γ-modification, even though prepared by three different methods, and did nothing with the cubic modification. Because they carried out neither the thermal analysis nor the dilatometric investigations of the cubic modification, it is quite natural that they did not observe the transition at 148°C. The determination as to which of the monoclinic or the rhombohedral modification is more stable at high temperatures requires measurements of the vapor pressures of the monoclinic form in addition to those of the rhombohedral form described in the present paper.

# *Internal Rotation in n-Propyl Chloride and Bromide*

By Chizuko KOMAKI, Isao ICHISHIMA, Kenji KURATANI, Tatsuo MIYAZAWA, Takehiko SHIMANOUCHI, and San-ichiro MIZUSHIMA

(Received February 19, 1955)

## Introduction

In a previous paper it was shown by the Raman measurement that *n*-propyl halides exist in two forms in the liquid state and in only one form in the crystalline state.[1] The same conclusion was drawn by Brown and Sheppard[2] from their infrared absorption measurement of *n*-propyl bromide. Goubeau and Pajenkamp have reported the energy difference between the rotational isomers of *n*-propyl chloride and *n*-propyl bromide[3]. However, as the stable molecular forms have not yet been determined, we have made further spectroscopic studies of these substances. The results will be reported in the present paper.

## Vibrational Spectra

The sample used in the measurement was prepared from *n*-propyl alcohol and phosphorous trihalide and purified by distillation under ordinary pressure using a column having 30 theoretical plates. The materials used were center fraction boiling over a range of ±0.1°C. Raman spectra were measured with the spectrograph of our own construction[4] and the infrared absorptions with the Baird spectrophotometer with the NaCl and KBr prisms. The results are listed in Tables I and II. In these tables are also shown

1) S. Mizushima, Y. Morino and S. Nakamura, *Sci. Pap. Inst. Phys. Chem. Res. Tokyo*, 37, 205 (1940).

2) J. K. Brown and N. Sheppard, *Disc. Faraday Soc.*, 9, 144 (1950).

3) J. Goubeau and H. Pajenkamp, *Acta Physica Austriaca*, 3, 283 (1949).

4) S. Mizushima, "Structure of Molecules and Interna Rotation," Academic Press, New York (1954).

TABLE I

RAMAN AND INFRARED FREQUENCIES OF $CH_3CH_2CH_2Cl$

| Observed | | | | | | Calculated | | | |
|---|---|---|---|---|---|---|---|---|---|
| Gas | | Liquid | | Solid | | | | | |
| I.R. | | I.R. | R. | I.R. | R.[1] | *trans* | *gauche* | Type of Vibration | |
| | | | 144 (2b) | | | | | | |
| | | | 220 (0b) | | | | | | |
| | | | 249 (2b) | | 229 (1) | 252 | | δ | *trans* |
| | | | 292 (3) | | —— | | 267 | δ | *gauche* |
| | | | 368 (6) | | 363 (5) | 334 | | δ | *trans* |
| | | 426 (m) | 426 (4) | | —— | | 429 | δ | *gauche* |
| 660 | (s) | 648 (s) | 651 (8) | —— | —— | | 708 | ν (C-Cl) | *gauche* |
| | | | | 700 (w) | | | | | |
| 743 | (s) | 729 (s) | 728 (6b) | 717, 725 (s) | 716 (7) | 744 | | ν (C-Cl) | *trans* |
| | | 749 (m) | —— | 749 (s) | | | | $CH_2$ *rocking* | *trans* |
| 787, 793, 800 | (s) | 789 (s) | 788 (6) | —— | —— | | | $CH_2$ *rocking* | *gauche* |
| 852, 858, 864 | (s) | 856 (s) | 856 (4) | 863 (m) | | | | | |
| 894, 903 | (s) | 897 (s) | 896 (3) | 898 (s) | | | | | |
| 1038 | (m) | 1034 (s) | 1026 (6) | 1030 (m) | 1029 (5) | | | | |
| 1050 | (m) | 1067 (m) | 1064 (1) | 1065 (w) | | | | | |
| 1067 | (w) | 1081 (w) | 1088 (0) | 1083 (m) | | | | | |
| 1097 | (w) | 1094 (w) | | | | | | | |
| | | 1104 (w) | 1108 (1) | 1103 (w) | | | | | |
| | | 1158 (w) | | 1155 (vw) | | | | | |
| | | 1213 (w) | 1211 (1) | 1218 (vw) | | | | | |
| 1253, 1261 | (s) | 1258 (s) | 1255 (2) | 1257 (s) | | | | | |
| 1300, 1309 | (s) | 1304 (s) | 1297 (1) | 1287 (vw) | | | | | |
| 1331 | (m) | 1338 (m) | 1341 (3) | 1332 (m) | | | | | |
| 1390 | (m) | 1385 (s) | 1381 (0) | 1370 (m) | | | | | |
| 1456 | (s) | 1447 (s), 1460 (s) | 1441 (5), 1462 (2b) | 1460 (s) | 1441 (2) | | | | |
| | | | 2743 (4) | | | | | | |
| | | | 2854 (2) | | 2829 (0) | | | | |
| 2870 | (s) | | 2876 (6) | | 2870 (5) | | | | |
| | | 2900 (s) | 2900 (3b) | | 2894 (2) | | | | |
| | | | 2915 (3b) | | 2908 (2) | | | | |
| | | | 2936 (6) | | 2941 (6) | | | | |
| 2950 | (s) | 2960 (s) | 2957 (6) | | | | | | |
| | | | 2979 (3) | | 2975 (0) | | | | |
| | | | 3003 (3) | | 2997 (0) | | | | |

1. Frequencies reported in reference 1).

the infrared absorption spectra in the crystalline state observed in the frequency range 600 to 800 $cm.^{-1}$ with the use of a spectrophotometer of our own construction[4].

## Rotational Isomers

As has been shown in many of our previous papers on internal rotation, the absence of some of the liquid spectral lines in the solid state (Tables I and II) shows the presence of rotational isomers in the liquid state[1]. In the solid state, however, the presence of only one isomer is sufficient to account for the number of the observed lines.

TABLE II

INFRARED FREQUENCIES OF $CH_3CH_2CH_2Br$

| Gas | Liquid | Solid | Type of Vibration |
|---|---|---|---|
| | 406 | | |
| 561 (s) | 564 (s) | | $\nu$(C-Br) *gauche* |
| 658 (s) | 646 (s) | 638 (s) | $\nu$(C-Br) *trans* |
| 742 (w) | 741 (m) | 737 (s) | $CH_2$ *rocking trans* |
| 775<br>780 (s)<br>785 | 777 (s) | —— | $CH_2$ *rocking gauche* |
| 837 (s) | 838 (s) | 849 (w) | |
| 892 (s) | 887<br>893 (s) | 892 (s) | |
| 1033 (s) | 1030 (s) | 1025 (m) | |
| 1085 (m) | 1079 (m) | 1038 (s) | |
| | 1094 (w) | 1099 (m) | |
| | 1196 (m) | | |
| 1232 (s) | 1225 (s) | 1218 (s) | |
| 1290 (s) | 1284 (s) | —— | |
| 1339<br>1351 (m) | 1326<br>1340 (m) | 1321 (s) | |
| 1391 (s) | 1381 (s) | 1364 (s) | |
| 1456 (s) | 1437<br>1460 (s) | 1445 (s) | |
| 2900 (s) | 2890 (s) | | |
| 2960 (s) | 2960 (s) | | |

We are now interested in determining the molecular configurations of the rotational isomers. The symmetry considerations cannot be applied conveniently for this molecule. However, from the nature of the hindering potential discussed in a previous paper[5], the stable configurations of this molecule can be considered to be the *trans* and *gauche* forms shown in Fig. 1. Accordingly the normal vibration calculation of the skeleton $(CH_3)\cdot(CH_2)\cdot(CH_2)\cdot Cl$ has been made for the *trans* and *gauche* forms according to the method described in a previous paper[6]. The force constants used in this calculation are those which yielded the computed frequency values in good agreement with those observed for other molecules with similar structure.

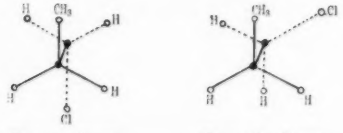

*Trans* form *Gauche* form

Fig. 1. Stable molecular configurations of *n*-propyl chloride.

The computed skeletal frequencies of *n*-propyl chloride are shown in Table I. Those for the *trans* form are close to the frequencies observed in the solid state. Accordingly we conclude the stable configuration in the solid state to be the *trans* form, in which the $CH_3$ group and the Cl atom are farthest apart. The fact that all the solid frequencies are also observed in the liquid state shows that the *trans* form is one of the stable configurations in this state. The other stable configuration can be considered to be the *gauche* form, since the Raman lines observed only in the liquid state have frequencies close to those calculated for the *gauche* form.

In order to confirm this conclusion, we have calculated the dependence of the skeletal deformation frequency on the azimuthal angle $\theta$ of internal rotation, because this frequency is very sensitive to the change of this angle[6] and accordingly we can determine fairly accurately the azimuthal angle from the observed frequency value. The result of this calculation is shown in Fig. 2, from which we see that the observed frequencies are close to those calculated for the *trans* ($\theta=180°$) and the *gauche* ($\theta=60°$) forms, respectively.

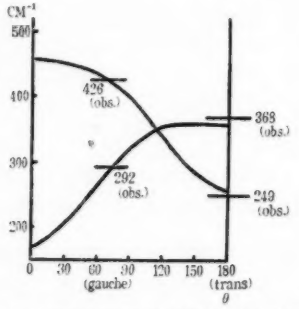


Fig. 2. Dependence of skeletal deformation frequencies on azimuthal angle.

The conclusion was also checked by the product rule derived in our previous paper[3]. If we denote the kinetic energy matrices for the *trans* and *gauche* forms by $G_t$ and $G_g$, respectively, we have

$$(|G_g|/|G_t|)^{\frac{1}{2}}=\Pi\nu_g/\Pi\nu_t \qquad (1)$$

where $\nu_t$ and $\nu_g$ are the normal frequencies of the *trans* and the *gauche* molecules. The ratio on the left-hand side of this equation has been calculated as the function of $\theta$ as shown in Fig. 3, putting $\theta$ of the *trans* form as 180°. The experimental value $\Pi\nu_g/\Pi\nu_t$ is close to that calculated for the *gauche* form ($\theta=60°$).

5) S. Mizushima, Y. Morino and T. Shimanouchi, *J. Phys. Chem.*, **56**, 324 (1952).
6) S. Mizushima, T. Shimanouchi, I. Nakagawa and A. Miyake, *J. Chem. Phys.*, **21**, 215 (1953).

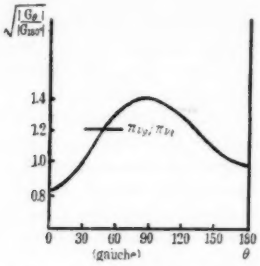


Fig. 3. The calculated values of $(|G_\theta / G_{180^\circ}|)^{1/2}$ and the observed value of $\Pi\nu_g/\Pi\nu_t$.

In addition to the confirmations made by these calculations we have an experimental evidence in support of the assignment of lines made above. *n*-Propyl chloride has a chain structure similar to that of ethylene chlorhydrin so that the skeletal frequencies of these two molecules will not be very different from each other. Actually these two substances show similar low frequency lines in the liquid and the gaseous states. However, there is a great difference between the spectra of these two substances in the solid state. Namely, the lines 292, 426, 651 cm.$^{-1}$ of liquid *n*-propyl chloride disappear on solidification, whereas the corresponding lines of ethylene chlorhydrin persist in the solid state. From this we can conclude that the configuration of *n*-propyl chloride in the solid state must be different from that of the crystalline ethylene chlorhydrin. Now that our previous measurement[7] has shown the *gauche* form to be present in the crystalline state of ethylene chlorhydrin, we can conclude that the molecule of *n*-propyl chloride in the solid state is the *trans* form in conformity with the conclusion drawn from the normal vibration calculation.

## Energy Difference between the Rotational Isomers

The energy difference between the rotational isomers has been determined by the measurement of the ratio of optical densities $D$ of the two infrared absorption bands, one assigned to the *trans* form and the other to the *gauche* form:

$$D_t/D_g = \frac{\kappa_t}{2\kappa_g} e^{-\frac{\Delta S}{R}} e^{\frac{\Delta E}{RT}},$$

where $\Delta S = S_g - S_t$ and $\Delta E = E_g - E_t$ denote the differences in entropy and energy, $\kappa$ the molecular absorption coefficient and suffices $t$ and $g$ refer to the *trans* and *gauche* molecules, respectively. In a narrow range of temperature $\Delta S$ and $\Delta E$ can be considered to be constant and accordingly the value of $\Delta E$ can be determined by measuring the temperature dependence of the ratio $D_t/D_g$ of the two bands. As these bands we have chosen one at 793 cm.$^{-1}$ or 660 cm.$^{-1}$ assigned to the *gauche* form and the other at 743 cm.$^{-1}$ assigned to the *trans* form.* From the measurement in the gaseous state made in the temperature range from 20°C to 150°C, the energy difference has been obtained as:

$$\Delta E = -0.05 \pm 0.15 \text{ kcal./mol.}$$

For the measurement in the liquid state in the temperature range from 10° to −60°C we have chosen two bands at 789 cm.$^{-1}$ (*gauche*) and at 729 cm.$^{-1}$ (*trans*). The energy difference has been found to be

$$\Delta E = +0.05 \pm 0.06 \text{ kcal./mol.}$$

This is in agreement with the value obtained by Goubeau and Pajenkamp from their Raman measurement[3], provided that the assignment of lines is made as referred to above.

It is to be noted that the energy difference found in the gaseous state is nearly equal to that in the liquid state. This is compatible with our explanation of the interaction of molecules in the liquid state[8]. It is seen that the *trans* and the *gauche* forms of *n*-propyl chloride will have almost the same value of the dipole moment which will result in the same change of energy in the liquid state. In other words, the energy difference between the *trans* and *gauche* molecules will have almost the same value in the liquid state as in the gaseous state.

The intensity measurement made for *n*-propyl bromide by use of two bands at 780 cm.$^{-1}$ (*gauche*) and 658 cm.$^{-1}$ (*trans*) in the temperature range from 20° to 150°C gave the value of enery difference $-0.1 \pm 0.2$ kcal./mol. in the gaseous state.

In our previous papers[4,5,7] we have discussed the energy difference between the *trans* and *gauche* forms of many disubstituted ethanes. The very small value of $\Delta E$

7) S. Mizushima, T. Shimanouchi, T. Miyazawa, K. Abe and M. Yasumi, *J. Chem. Phys.*, **19**, 1477 (1951).

* We are sure that no *trans* band (strong enough to disturb the energy difference measurement) overlaps the 793 and 660 cm.$^{-1}$ *gauche* bands, because these two bands disappear in the solid state. Nor is the 743 cm.$^{-1}$ *trans* band considered to be overlapped by any *gauche* band, because the only *gauche* frequency expected to appear in this range is the $CH_2$-rocking frequency assigned to the 793 cm.$^{-1}$ band. This assignment is made from comparisons with the spectra of *n*-propyl bromide, dichloroethane, etc. See I. Nakagawa and S. Mizushima, *J. Chem. Phys.*, **21**, 2195 (1953).

8) I. Watanabe, S. Mizushima and Y. Mashiko, *Sci. Pap. Inst. Phys. Chem. Res. Tokyo*, **40**, 425 (1942). See also reference 4).

obtatined for *n*-propyl chloride and bromide is very interesting as compared with the large values found in the cases of 1,2-dichloro and 1,2-dibromoethane. This fact provides us data useful for the further development of our view[5] concerning the nature of the hindering potential to internal rotation**.

**Summary**

Infrared spectra of *n*-propyl chloride and bromide have been measured in the gaseous, liquid and solid states. The Raman measurement was also made in the liquid state. From the normal vibration calculation and by comparison with the spectra of ethylene chlorhydrin it has been concluded that in the liquid state both the *trans* and *gauche* forms are present and of these only the *trans* form persists in the solid state. The energy difference between the *trans* and the *gauche* forms has been determined by the absorption intensity measurement.

*Chemical Laboratory, Faculty of Science, Tokyo University, Tokyo*

** After our manuscript was finished, a paper by J. K. Brown and N. Sheppard, *Trans, Faraday. Soc.*, 50, 1164 (1954), became available to us. They reported a detailed infrared measurement of *n*-propyl halides in the solid state, the result of which supports our assignment of the bands used for the determination of the energy difference. Other conclusions reported in this paper are also in good agreement with ours.

# *Phototropy of New Photosensitive Complexes between a Fluorescent Pigment and SH-Compounds*

By Eiji FUJIMORI

(Received February 21, 1955)

## Introduction

Recently it has been recognized that the SH-group plays an important role not only in coenzyme-A and many enzymes, but also in the synthesis of the hormone and its activity, the coagulation of blood, the penetration of cellular membrane, the contraction of muscles, and cellular mitosis. It would be specially significant also in the reversibility of light energy conversion in vision and photosynthesis. On the other hand, there are many biological fluorescent pigments in the organism, such as porphyrin, carotenoids, flavin, and pteridine, which exhibit their physiological functions in close association with other biological substances such as protein and suitable oxidizing or reducing agents.

During the course of the investigation on the synthesis and preparation of organic fluorescent and photosensitive substances, their spectral structures, their abilities of emission, and their photosensitized and other photochemical reactions, the author noticed that the combination and interaction of these fluorescent pigments with some foreign substances possessing the SH-group responsible for the migration of excitation energy by molecular complex formation and electron transfer might be significant for their photosensitivity as light-sensitive substances. In confirmation of this point of view, it has been found in this laboratory that the complexes between a fluorescent pigment and SH-compounds selected as the reaction partner for the above mentioned reasons exhibit a specific photosensitivity.

It is well known that there are several photosensitive pigment-protein complexes in the retina of the eye[1]. One of them, visual purple or rhodopsin has the light absorption maximum at about 500 m$\mu$. The absorption of light by this rhodopsin activates the pigment molecules and stimulates rod vision. Rhodopsin is bleached by light to retinene, and protein opsin, and is then regenerated from them in the dark. Recently, the liberation of SH-groups in the photobleaching of rhodopsin has been discovered by Wald and Brown[2], who ascertained the important role of SH-groups in the synthesis and bleaching of rhodopsin. As the author succeeded in fitting a fluorescent pigment into the SH-group of SH-protein or other SH-compounds

1) G. Wald, *J. Opt. Soc. Am.*, **41**, 949 (1951); *Federation Proc.*, **12**, 606 (1953); *Ann. Rev. Biochem.*, **22** 497 (1953).

2) G. Wald and P. K. Brown, *J. Gen. Physiol.*, **35**, 797 (1952); **37**, 189 (1953).

and since these pigment-SH compound complexes showed a phototropy analogous to this rhodopsin, the experimental results are described in this paper.

## Experimental Methods

**Materials.**—The fluorescent pigment (I) used in this experiment was derived from fluorescein by the same method as described in the previous paper[3]. This yellow pigment showed a stable yellow fluorescence in a neutral aqueous solution. Hoffmann-La Roche reagent grade glutathione and Wako reagent grade egg albumin, cysteine, and thioglycolic acid were used.

On addition of this pigment solution to the alkaline solution of SH-compounds such as egg albumin, glutathione, cysteine, and thioglycolic acid, the yellow color disappeared with a slow appearance of an absorption in the longer wave length range, and its yellow fluorescence was partly quenched at the moment of the addition and then gradually deactivated as the reaction proceeded. These pigment-SH compound complexes were bleached by light and regenerated thermally in the dark. Since the experimental results were different in each complex, each case will be described separately below.

**Measurements.**—For the photobleaching reaction, the white light of a 1-KW projection lamp was allowed to fall upon a reaction cell of 2.5 cm. ×2.5 cm. ×3 cm. at a distance of 20 cm. from the light source. The variation of green light absorption during the formation reaction and regeneration reaction of the complexes was photoelectrically measured by the use of a 6-volt headlight lamp filtered through the Mazda glass filter V-G1 (maximum transmission at about 520 mμ) as a light source, at right angles to the irradiation source for photobleaching, and would be represented by the ratio of the initial value at the beginning of the reaction, $I_i$, to the respective measured value, I. The absorption spectra were measured by the Beckman spectrophotometer.

## Experimental Results

(1) **Egg Albumin.**—When $2.5\times10^{-4}$ M pigment (I) reacted with 1–7.5% egg albumin in 0.1–3 N NaOH solution, its yellow color disappeared and a red color of the reaction product appeared gradually as shown in Fig. 1. Fig. 2 shows the absorption spectra of

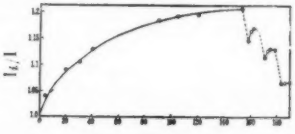


Fig. 1. Formation and phototropy of pigment-SH-protein complex. Dotted lines indicate bleaching during the illumination by light. $2.5\times10^{-4}$ M pigment and 7.5 % egg albumin in 3 N NaOH.

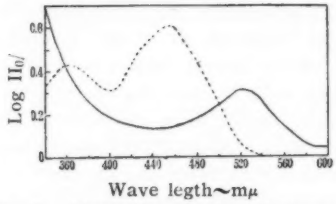


Fig. 2. Absorption spectra of pigment (I) and its complex with egg albumin:..... $10^{-4}$ M pigment in phosphate buffer solution at pH 7.0;—, $10^{-4}$ M pigment and 1 % egg albumin in 3 N NaOH.

this pigment and the reaction complex. The absorption maximum of the yellow pigment at 453 mμ shifted to the longer wave length of 520 mμ, together with the deactivation of its fluorescence, which occurred instantaneously at the beginning of the reaction and continued to complete disappearance as the reaction proceeded.

This non-fluorescent red pigment-protein complex was bleached by light and regenerated rapidly within about two minutes at room temperature in darkness (Fig. 1). In this case, the more often the photobleaching was repeated, the lower the degree of regeneration became. The average initial regeneration degree was about 30, 15, and 8 %, respectively, to 7.5, 5 and 2.5 % of protein concentration; thus the regeneration degree was parallel to the protein concentration.

The addition of cysteine to this protein complex altered the color from red to orange. This fact seems to suggest the reversible formation of an orange pigment-cysteine complex; i, e., the exchange reaction of the SH-compound.

(2) **Glutathione.**—The absorption maximum of a complex produced by the reaction of glutathione with the pigment was at the same 520 mμ as in the csae of protein. In light this complex showed a deep color, in-

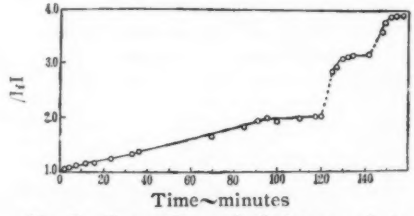


Fig. 3. Formation and phototropy of pigment-glutathione complex. $2.5\times10^{-4}$ M pigment and 0.05 M glutathione in 3 N NaOH.

3) E. Fujimori, *J. Chem. Soc. Japan (Pure Chem. Sect.)*, 75, 24 (1954); *J. Am. Chem. Soc.*, in the press.

stead of bleaching, which changed towards regeneration in darkness (Fig. 3). This strange regeneration reaction was completed within about ten minutes at room temperature. Such a photochemical change to a deep color took place even in the case of cysteine and thioglycolic acid, but on account of its slowness the ordinary photobleaching and regeneration were observed on short irradiation, as will be mentioned below. The light absorption maximum before and after irradiation was at the same wave length, namely 520 mμ (Fig. 4).

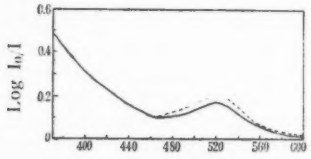


Fig. 4. Absorption spectra of pigment-glutathione complex:—, before irradiation of light;....., after irradiation and regeneration. $2.5 \times 10^{-4}$ M pigment and 0.02 M glutathione in 1.2 N NaOH.

(3) **Cysteine.**—The reaction between the pigment and cysteine of high concentration in alkaline solution produced an orange complex whose absorption maximum was at 505 mμ (Fig. 6). It was found that the phototropy is repeated many times as shown in Fig. 5. As long as the irradiation time was short, the bleached product showed a pale yellow color which returned to the original orange color in the dark, but on repeating the illumination many times or irradiating it for a long time it changed to a pale red and in the dark converted into a deep red color whose absorption maximum gradually approached 520 mμ (Fig. 6). In both cases the regeneration degree was almost 100%. The initial orange complex fluoresced more weakly than the original pigment, while the red complex produced photochemically showed the almost complete disappearance of fluorescence as in protein complex. This color and phototropy remained unchanged by neutralization with hydrochloric acid.

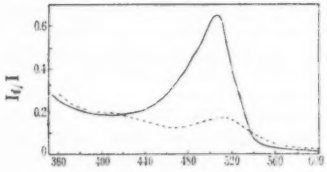


Fig. 6. Absorption spectra of pigment-cysteine complex:—, before irradiation of light;....., after irradiation and regeneration. $10^{-4}$ M pigment and 0.4 M cysteine-HCl in 1.2 N NaOH.

(4) **Thioglycolic Acid.**—Thioglycolic acid behaved in a manner analogous to that of

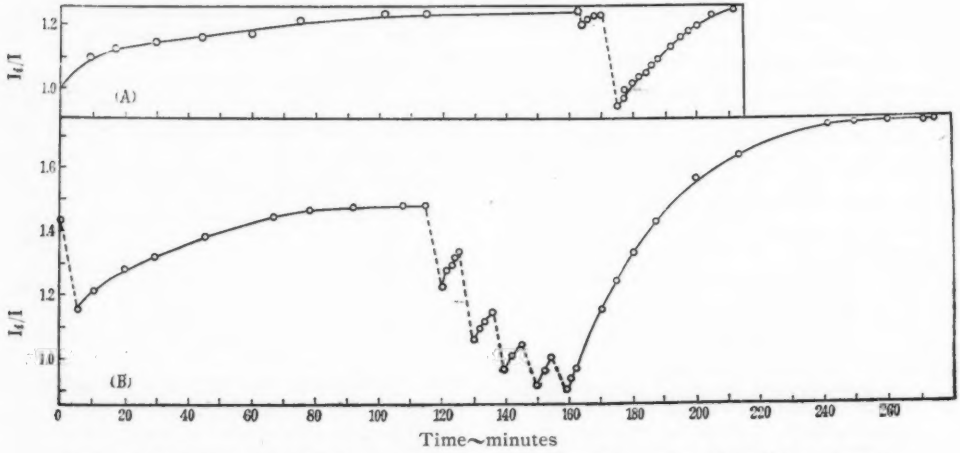


Fig. 5 (A) Formation and phototropy of pigment-cysteine complex. $2.5 \times 10^{-4}$ M pigment and 1 M cysteine-HCl in 3 N NaOH.
(B) Phototropy followed after standing for about 15 hours from the terminal of Fig. 5A.

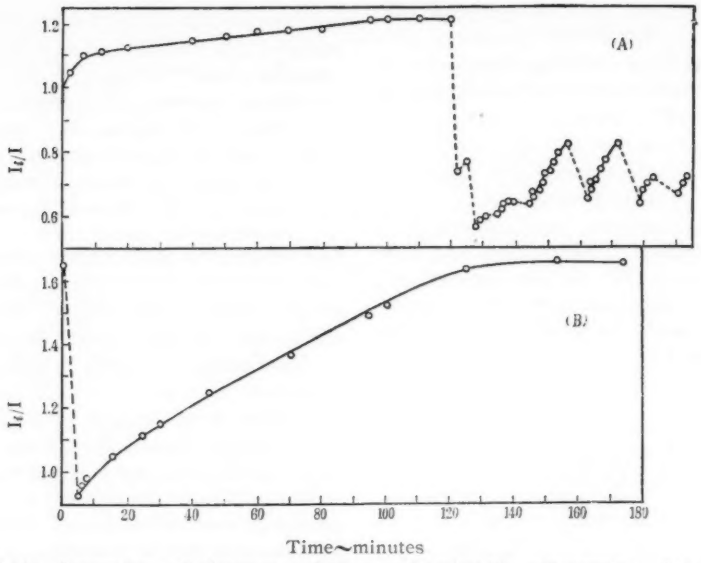


Fig. 7 (A) Formation and phototropy of pigment-thioglycollic acid complex. $2.5 \times 10^{-4}$ M pigment and 1.5 M thioglycolic acid in 3 N NaOH.
(B) Phototropy followed after standing for about 15 hours from the terminal of Fig. 7A.

cysteine. The absorption maxima of pigment-thioglycollic acid complex were initially at 470 and 495 mμ, but later changed to 520 mμ on illumination (Fig. 8). Since this spectral shift to 520 mμ due to some photochemical reaction took place more easily than that of cysteine-complex, the same change to a deep color as in the case of glutathione was observed in the third irradiation of Fig. 7A. The phototropy was observed in both complexes of different spectra. The regeneration degree was 100% and the regeneration time about two hours at room temperature, which was longer by about one hour than in the case of cysteine.

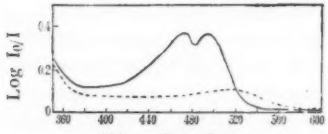


Fig. 8. Absorption spectra of pigment-thioglycolic acid complex:—, before irradiation of light;....., after irradiation and regeneration. $10^{-4}$ M pigment and 0.6 M thioglycolic acid in 1.2 N NaOH.

It was found, moreover, that this dark regeneration is generally a thermal reaction accelerated by heat. The relation between temperature and regeneration time in the case of thioglycolic acid is shown in Table I. Since the initial absorption maximum, the degree of regeneration, and the time required for regeneration are very different with each SH-compound, the summary of these experimental results is shown in Table II.

TABLE I
RELATION BETWEEN TEMPERATURE AND REGENERATION TIME AFTER IRRADIATION FOR FIVE MINUTES

| Temp. (°C) | Reg. time (min.) |
|---|---|
| 15 | 120 |
| 30 | 85 |
| 50 | 60 |

TABLE II
VARIOUS PROPERTIES OF PIGMENT-SH COMPOUND COMPLEXES

| SH-compound / Properties | Absorp. Max. (mμ) | Reg. Deg. (%) | Reg. time* (min.) |
|---|---|---|---|
| Egg albumin | 520 | 30–8 | about 2 |
| Glutathione | 520 | — | 10 |
| Cysteine | 505→520 | 100 | 60 |
| Thioglycolic acid | 470. 495→520 | 100 | 120 |

* Regeneration time at room temperature after irradiation for five minutes.

## Discussion

The evidence that oxonium hydroxide of the pigment (I) reacts with SH-group in these reactions is obvious from the experimental facts that sodium sulfide also reacted to produce the non-fluorescent red compound (II) with the absorption maximum at 520 mμ and that such a reaction could not occur at all in the reduction product (III) and OH-transition product (IV) of the pigment (I). It is certain, therefore, that the reaction with protein should be represented by the following schema:

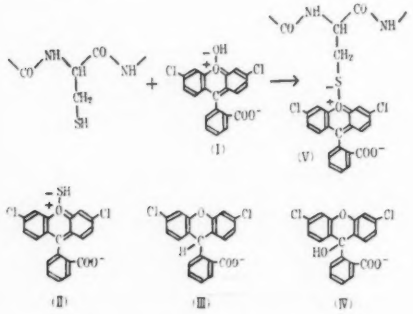

The reaction products with glutathione, cysteine, and thioglycolic acid would be (VI), (VII), and (VIII), respectively.

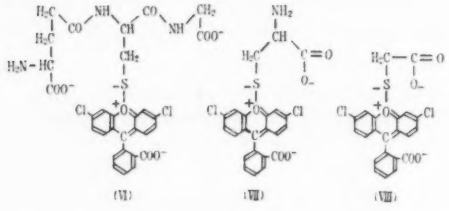

In egg albumin and glutathione, both of which are polypeptides, the absorption maximum is at 520 mμ from the beginning, while in cysteine and thioglycolic acid with free carboxyl group adjacent to the SH-group it is at a shorter wave length than 520 mμ and shifts to 520 mμ by light absorption. This fact seems to suggest some photochemical change of intramolecular orientation, namely photochemical isomerization, in these complexes and some effect of the adjacent free carboxyl ion upon this.

Since these red complicated complexes show the same absorption maximum at 520 mμ and non-fluorescence as in the more simple SH-pigment (II), the discussion described in the previous paper[3] will be true for the present complexes between a fluorescent pigment and complicated SH-compounds; thus the ionic combination of oxonium oxygen of the pigment (I) with SH-group, resulting in the formation of $-S^{-}-{}^{+}O=$ bond, would bring the remarkable deactivation of fluorescence and the shift of absorption spectrum into a longer wave length range. Moreover, the mechanism of this remarkable deactivation of fluorescence in these complexes will be analogous to that, in the SH-pigment (II), considered in connection with the instantaneous quenching of OH-pigment (I) fluorescence by SH-compounds; i. e., it may probably be due to the electron-transfer based on the reducing power of SH-group. Such a remarkable deactivation of fluorescence and a shift of absorption spectrum is likely to be observed in a static molecular complex formed in the ground state. In such a case, the transfer of excitation energy may sometimes bring about a specific photosensitivity. The present series of complexes seems to belong to this category.

Although (II) shows neither fluorescence nor photochemical change under irradiation, the pigment-SH compound complex is bleached in light, stays in some bleaching metastable state with the lifetime made longer by the specific effect of combined $^{-}$S-R, and is regenerated slowly to the original state in the dark as shown in the experiments. As such a bleaching state, a diradical and especially a semiquinone radical with an ·S-R free thiol radical may be of significance. If so, this phototropy of oxidizing oxonium pigment-reducing SH-compound complexes will be regarded as a sort of photo-reversible oxidation-reduction reaction where intramolecular electron transfer takes place through the diradical and semiquinone radical with the formation of ·S-R radical by light absorption.

The dark and light reactions of the pigment ant pigment-SH-compound complexes discussed above, including the previous results on the bleaching reaction of the pigment itself, will presumably be summarized by the following various model equations according to the above assumption:

| | | |
|---|---|---|
| 1 | $D—OH+h\nu_a \rightarrow D^*—OH$ | Light absorption of the pigment |
| 2 | $D^*—OH \rightarrow D—OH+h\nu_f$ | Fluorescence of the pigment |
| 3 | $D—OH \rightarrow HO—D$ | Dark bleaching reaction of the pigment |
| 4 | $D^*—OH \rightarrow HO—D$ | Light bleaching reaction of the pigment |
| 5 | $D^*—OH+{}^-S-R \rightarrow (\cdot D \cdot —OH+{}^-S-R) \rightarrow \cdot D^-—OH+\cdot S-R$ | Quenching of the fluorescence |
| 6 | $\cdot D^-—OH+\cdot S-R \rightarrow D—OH+{}^-S-R$ | Reverse reaction |
| 7 | $D—OH+{}^-S-R \rightarrow D—S—R_I+OH^-$ | Formation of the complex |
| 8 | $D—S—R_I+h\nu_a' \rightarrow D^*—S—R_I$ | Light absorption of the complex |
| 9 | $D^*—S—R_I \rightarrow \cdot D \cdot —S—R_I \rightarrow \cdot D^- \cdot S—R_I$ | Bleaching reaction of the complex |
| 10 | $\cdot D^- \cdot S—R_I \rightarrow \cdot D \cdot —S—R_I \rightarrow D—S—R_I$ | Regeneration reaction of the complex |
| 11 | $D^*—S—R_I \rightarrow D—S—R_{II}$ | Photo-isomerization |
| 12 | $D—S—R_{II}+h\nu_a'' \rightarrow D^*—S—R_{II}$ | Light absorption of the isomer |
| 13 | $D^*—S—R_{II} \rightarrow \cdot D \cdot —S—R_{II} \rightarrow \cdot D^- \cdot S—R_{II}$ | Bleaching reaction of the isomer |
| 14 | $\cdot D^- \cdot S—R_{II} \rightarrow \cdot D \cdot —S—R_{II} \rightarrow D—S—R_{II}$ | Regeneration reaction of the isomer |
| 15 | $D—S—R_I+{}^-S—R_{III} \rightarrow D—S—R_{III}+{}^-S—R_I$ | Exchange reaction of SH-compound |

where D-OH is the pigment (I); D*-OH, the normal excited state (singlet); HO-D, the colorless OH-transition product (IV); $^-$S-R, the negative ion of SH-compound; D-S-$R_I$, the initial complex; D-S-$R_{II}$, an isomer produced by light; $\cdot D \cdot$, a diradical (tiplet state); $\cdot D^-$, a semiquinone radical; and ·S-R, also a free radical. The complex between $\cdot D^-$ and ·S-R, $\cdot D^- \cdot$S-R, will be regarded especially as a complex diradical responsible for the bleaching metastable state with a longer lifetime and seems to be closely related to the diradical, $\cdot D \cdot$-S-R, so as to stabilize it and the diradical by forming a resonance complex.

Thus this phototropy seems to be based on the photochemical formation of pigment free radicals and ·S-R free radical, especially $\cdot D^- \cdot$S-R complex through $\cdot D \cdot$-S-R. Although the formation of ·S-R free thiol-radical was assumed by Waters[4] or Barron[5] in the function of SH-enzymes, e. g., FAD- or DPN-SH protein enzyme, and ascertained by Crawshaw and Speakman[6] in the photolysis of disulfides, there are several studies on pigment free radicals in the field of photochemistry. In 1940, the phototropy due to the formation of a semiquinone radical was studied by Rabinowitch[7] in thionine-ferrous ion system. Schenck[8] suggested the possibility of a diradical in vision, and Livingston[9),10] showed that the formation of a diradical and a semiquinone free radical in the illuminated solution of chlorophyll is the cause of its phototropy.

4) W. A. Waters, "The chemistry of free radicals", Clarendon Press, Oxford, (1946), P. 257–283.
5) E. S. G. Barron, *Advances in Enzymol.*, **11**, 201. (1951).
6) G. H. Crawshaw and J. B. Speakman, *J. Soc. Dyers and Colourists*, **70**, 81 (1954).
7) E. Rabinowitch, *J. Chem. Phys.*, **8**, 551, 560 (1940).
8) G. O. Schenck, *Naturw.* **40**, 212 (1953); *Z. Elektrochem.*, **57**, 675 (1953).
9) R. Livingston and V. A. Ryan, *J. Am. Chem. Soc.*, **75**, 2176 (1953).
10) R. Livingston, G. Porter and M. Windsor, *Nature*, **173**, 485 (1954).

## Summary

The absorption maximum of all pigment-SH compound complexes shifted to a longer wave length range than that of the pigment itself. Although in protein and glutathione the absorption maximum was at 520 mμ from the beginning, in cysteine and thioglycolic acid it was in a shorter wave length range than 520 mμ and shifted to 520 mμ after some photochemical reaction. These complexes with their absorption maxima in a shorter wave length range than 520 mμ fluoresced more weakly than the original pigment, while those at 520 mμ showed the almost complete disappearance of fluorescence. Before these SH-compounds combined with the pigment, its fluorescence was partly instantaneously quenched by them. Both complexes of different spectra showed a phototropy; i. e., bleaching in light and regeneration in darkness. The regeneration reaction was thermal: its velocity was parallel to the molecular weight of the SH-compound in these SH-compounds used in the present experiment. The degree of regeneration was low in protein but about 100 % in cysteine and thioglycolic acid. The concentration of protein influenced the degree of regeneration but not the velocity of regeneration. This phototropy was discussed from the point of view of an ·S-R free radical and pigment radicals.

*Department of Chemistry and Metallurgy,*
*Institute of Industrial Science,*
*University of Tokyo, Chiba*

# *The Effect of Concentration and Valency of Added Salts on the Critical Micelle Concentration of Sodium and Calcium Dodecyl Sulfates*

By Kōzō SHINODA

(Received February 21, 1955)

## Introduction

In the preceding report[1], the theoretical equation for the critical micelle concentration (CMC) was derived, and it has been shown that the electrical charges of micelle forming ions play an important role in the process of micellization. In order to criticize this equation the following experiments are needed: to investigate (1) the effect of added salts on the CMC[2-5], (2) the effect of added alcohols on the CMC[3-8], (3) the CMC of soap mixtures[9-11], (4) the CMC of the surfactants which possess two or three dissociable groups at one end of their hydrocarbon chains[12], etc. As for the investigation (1), a number of papers have been published on the effect of uni-valent counterions on the CMC, and the effect of bi- or tri-valent counterions has been measured by H. Lange[3], but, so far as we know, no quantitative explanation has been published.

The present investigation was undertaken to derive the theoretical formula for the CMC values as a function of the concentration and valency of added salts and to compare it with the experimental results given by Lange[3,13].

## Electrical Potential at the Charged Surface of the Micelle

If it is assumed that the surface of a micelle is plane (or at least the double layer thickness is small in comparison with the radius of curvature of micelle surface) and the charge layer on the micelle surface is homogeneous, the counterions distribute homogeneously and parallel to the micelle surface, and the electrical potential is only a function of the normal coordinate. Now the Poisson-Boltzmann equation is applied for the micelle of a plane uniformly charged surface in contact with a solution of strong electrolytes, and the following equation is obtained:

$$\Delta\phi=\frac{\mathrm{d}^2\phi}{\mathrm{d}x^2}=-\frac{4\pi}{D}\sum' z_i n_i \mathrm{e}\exp(-z_i\mathrm{e}\phi/kT), \quad (1)$$

where $\phi$ is the electrical potential, $x$ the coordinate normal to the surface, $D$ the dielectric constant of the medium, e the elementary charge, $z_i$ the valencies of the positive and negative ions, $n_i$ the numbers of respective ions per cc. in the bulk of the solution ($n_i=C_iN/1000$, $C_i$ mole number of ions per liter, N Avogadro number), $k$ the Boltzmann constant and $T$ the absolute temperature.

Considering the boundary conditions, $\phi=0$ and $\frac{\mathrm{d}\phi}{\mathrm{d}x}=0$ for $x=\infty$, we obtain;

$$\frac{1}{2}\left(\frac{\mathrm{d}\phi}{\mathrm{d}x}\right)^2=\frac{4\pi kT}{D}\sum' n_i\{\exp(-z_i\mathrm{e}\phi/kT)-1\}, \quad (2.1)$$

and therefore,

$$\frac{1}{2}\left(\frac{\mathrm{d}\phi}{\mathrm{d}x}\right)_{x=0}^2=\frac{4\pi kT}{D}\sum' n_i\{\exp(-z_i\mathrm{e}\phi_0/kT)-1\}. \quad (2.2)$$

The surface charge density, $\sigma$, may be obtained directly from the potential function. To this end we make use of the general equation[14],

$$\sigma=-\int_0^\infty \rho\mathrm{d}x=\frac{D}{4\pi}\int_0^\infty \frac{\mathrm{d}^2\phi}{\mathrm{d}x^2}\mathrm{d}x=-\frac{D}{4\pi}\left(\frac{\mathrm{d}\phi}{\mathrm{d}x}\right)_{x=0}. \quad (3)$$

The latter quantity may be read from equation (2.2)

$$\left(-\frac{4\pi\sigma}{D}\right)^2=\left(\frac{\mathrm{d}\phi}{\mathrm{d}x}\right)_{x=0}^2=\frac{8\pi kT}{D}\sum' n_i \{\exp(-z_i\mathrm{e}\phi_0/kT)-1\}. \quad (4)$$

1) K. Shinoda, *Bull. Chem. Soc. Japan*, **26**, 101 (1953).
2) M. L. Corrin and W. D. Harkins, *J. Am. Chem. Soc.*, **69**, 683 (1947).
3) H. Lange, *Kolloid-Z.*, **121**, 66 (1951).
4) E. D. Goddard, O. Harva and T. G. Jones, *Trans. Faraday Soc.*, **49**, 980 (1953).
5) H. B. Klevens, *J. Phys. Chem.*, **52**, 130 (1948).
6) M. L. Corrin and W. D. Harkins, *J. Chem. Phys.*, **14**, 640 (1946).
7) S. H. Herzfeld, M. L. Corrin and W. D. Harkins, *J. Phys. Chem.*, **54**, 271 (1950).
8) K. Shinoda, *J. Phys. Chem.*, **58**, 1136 (1954).
9) H. B. Klevens, *J. Chem. Phys.*, **14**, 742 (1946).
10) H. Lange, *Kolloid-Z.*, **131**, 96 (1953).
11) K. Shinoda, *J. Phys. Chem.*, **58**, 541 (1954).
12) K. Shinoda, *J. Phys. Chem.*, **59**, No. 5 (1955).
13) H. Lange, a private communication.
14) E. J. W. Verwey and J. Th. G. Overbeek, "Theory of the Stability of Lyophobic Colloids" Elsevier Publishing Co. Inc. 1948.

Equation (4) gives the electrical potential, $\phi_0$, at the charged surface of the micelle.

If the micelle forming ion is anion, $\phi$ will be negative and $-z_i e\phi_0$ will be positive for cations, and negative for anions. As pointed out later the condition $\exp(-z_i e\phi_0/kT) \gg 1$ is satisfied[15], and the contribution of the anions and 1 in the right hand side of equation (4) can be neglected. It is apparent from (4) that the valencies or kinds of ions of the same sign as that of the long chain ions have no effect and only the valencies of ions of the opposite sign are important.

Then equation (4) gives electrical potentials in each of the following cases:

**(1) for long chain salts of uni-univalent type,**

1) with no added salt,

$$\phi_0 = \frac{kT}{e} \log \frac{2000\pi\sigma^2}{C_1 DNkT}, \tag{5.1}$$

where

$$C_1 = \mathrm{CMC} = 1000\, n_1/N,$$

2) with added uni-valent cation salt,

$$\phi_0 = \frac{kT}{e} \log \frac{2000\pi\sigma^2}{C_1 DNkT}, \tag{5.2}$$

where

$$C_1 = \mathrm{CMC} + C_1',$$

3) with added bi-valent cation salt,

$$\frac{2000\pi\sigma^2}{DNkT} = C_1 \exp(e\phi_0/kT) + C_2 \exp(2e\phi_0/kT), \tag{5.3}$$

where

$$C_1 = \mathrm{CMC},$$

4) with added tri-valent cation salt,

$$\frac{2000\pi\sigma^2}{DNkT} = C_1 \exp(e\phi_0/kT) + C_3 \exp(3e\phi_0/kT), \tag{5.4}$$

where

$$C_1 = \mathrm{CMC},$$

**(2) for long chain salts of uni-bivalent type,**

1) with no added salt,

$$\phi_0 = \frac{kT}{2e} \log \frac{2000\pi\sigma^2}{C_2 DNkT}, \tag{5.5}$$

where

$$C_2 = \mathrm{CMC}/2.$$

2) with added uni-valent cation salt,

$$\frac{2000\pi\sigma^2}{DNkT} = C_1 \exp(e\phi_0/kT) + C_2 \exp(2e\phi_0/kT), \tag{5.6}$$

where

$$C_2 = \mathrm{CMC}/2,$$

3) with added bi-valent cation salt,

$$\phi_0 = \frac{kT}{2e} \log \frac{2000\pi\sigma^2}{C_2 DNkT}, \tag{5.7}$$

where

$$C_2 = \mathrm{CMC}/2 + C_2',$$

## Comparison with Experimental Observations

For a given chain length the cohesive energy contribution will be constant; however, it is clear that in the presence of added electrolytes the ions of charge opposite to that of the long chain ions have a marked influence on micelle formation by reducing the electrical repulsive forces between the head groups of the long chain ions; or, in other words, by reducing the electrical potential on the micelle surface.

Formulae (5.1)–(5.7) can be tested by the experimental data for the CMC as a function of the concentration and valency of added salts[7,13]. The CMC of long chain salts is given as[1]

$$\log \mathrm{CMC} = \log \frac{1000}{N\nu} - \frac{m\omega}{kT} + \frac{E_{el.}}{kT} - 1, \tag{6}$$

where $\nu$ is the free volume per molecule in the micellar state, $m$ the number of carbon atoms in hydrocarbon chain, $\omega$ the surface energy change per methylene radical, passing from the bulk of the solution into the micelle, $E_{el.}$ the electrical energy change per micelle forming ion, and would be given as $Ke\phi_0$.

A reasonable alternative is to assume that the dissociation degree of the micelle forming ion is not 1 but $K$.

Considering this alternative and combining equations (5.2), (5.7) and (6), we obtain,

$$\log \mathrm{CMC} = \log \frac{1000}{N\nu} - \frac{m\omega}{kT} + \frac{K}{Z_i} \log \frac{2000\pi K^2\sigma^2}{C_i DNkT} - 1, \tag{7}$$

where $Z_i$ is the valencies of respective counterions and $C_i$ the concentrations of counterions in moles per liter.

It is expected from equation (7) that the log CMC is a linear function of log $C_i$ and the slope of this line is K for sodium dodecyl sulfate and $K/2$ for calcium dodecyl sulfate. Comparing the experimental data measured by Lange[13] with the theoretical equation, it has been found that the slope of the plot

15) A. B. D. Cassie and R. C. Palmer, *Trans. Faraday Soc.*, **37**, 156 (1941).

of log CMC versus log $C_i$ is a linear function and the slope is $0.503(=K)$ for sodium dodecyl sulfate and $0.286(=K/2)$ for Calcium dodecyl sulfate, showing good agreement with the theory*.

Introducing the CMC values of sodium and calcium dodecyl sulfates into equation (7) and substituting $K=0.54$, we obtain at $T=343°K$,

$$\frac{2000\pi K^2\sigma^2}{DNkT}=0.654\,.$$

This value is somewhat smaller than that expected from the values of $\sigma$**, $K$, $D$, $N$, $k$, and $T$, but this will be attributed to the fact that each ion contribute less charge than e to the micelle because of the accompanying counterion with the introduction of another charge.

Introducing these values into equations (5.1)−(5.7) and (6), the comparison between the theory and the experimental CMC values as a function of the concentration and valency of added salts was attained. The results are shown in Table I.

TABLE I

COMPARISON BETWEEN THE OBSERVED (BY LANGE) AND CALCULATED CMC VALUES AS A FUNCTION OF THE CONCENTRATION AND VALENCY OF ADDED SALTS AT 70°C.

| Concn. of added salt in equivalent/liter | obs. CMC | calc. CMC (moles/1.) |
|---|---|---|
| KCl or NaCl | Sodium Dodecyl Sulfate | |
| 0 | 0.0066 | 0.0067 |
| 0.01 | 0.0045 | 0.0045 |
| 0.02 | 0.00315 | 0.0030 |
| 0.05 | 0.00235 | 0.0023 |
| 0.1 | 0.0016 | 0.0016 |
| 0.2 | 0.0012 | 0.00115 |
| 0.5 | 0.00075 | 0.00065 |
| $MgCl_2$ or $CaCl_2$ | | |
| 0.0001 | 0.0060 | 0.0057 |
| 0.0003 | 0.0051 | 0.0048 |
| 0.0005 | 0.0043 | 0.0043 |
| 0.001 | 0.0039 | 0.0038 |
| 0.002 | 0.0030 | 0.0032 |
| 0.005 | 0.0022 | 0.0026 |
| 0.012 | 0.0018 | 0.0020 |
| 0.025 | 0.0015 | 0.0017 |
| 0.05 | 0.0012 | 0.0014 |
| 0.1 | 0.0010 | 0.0011 |
| 0.3 | 0.00077 | 0.0009 |
| $AlCl_3$ | | |
| 0.0007 | 0.0038 | 0.0024 |
| 0.001 | 0.0022 | 0.0022 |
| 0.002 | 0.0016 | 0.0014 |
| NaCl | Calcium Dodecyl Sulfate | |
| 0 | 0.0029 | 0.0029 |
| 0.001 | 0.00285 | 0.00285 |
| 0.004 | 0.0028 | 0.0028 |
| 0.01 | 0.0027 | 0.0027 |
| 0.02 | 0.0026 | 0.0026 |
| 0.03 | 0.0026 | 0.0024 |
| 0.05 | 0.0024 | 0.0021 |
| 0.1 | 0.0017 | 0.0015 |
| 0.2 | 0.00125 | 0.0011 |
| 0.5 | 0.00073 | 0.0006 |
| $CaCl_2$ | | |
| 0.001 | 0.0026 | 0.0028 |
| 0.005 | 0.00215 | 0.0023 |
| 0.025 | 0.00145 | 0.0016 |
| 0.1 | 0.00102 | 0.0011 |
| 0.3 | 0.00077 | 0.0008 |

* The value of K in the case of fatty acid soap is 0.56.

** $\delta$ is equal to the elementary charge divided by the cross sectional area of micelle forming ions.

It is apparent from Table I that the CMC values calculated using relations (5.1)−(5.7) show good agreement with the experimental ones. In the case of the large ionic radius of counterions or of the more concentrated system of counterions, the agreement between the theory and experiments is not so satisfactory.

### The CMC of the Mixture of Sodium and Calcium Dodecyl Sulfates

The CMC of the mixture of sodium and calcium dodecyl sulfates can also be tested with the equation (5.3) or (5.6). In this case, however, the sum of the equivalent concentration of sodium and calcium ions is equal to the CMC, i.e., $C_1+2C_2=$CMC. The comparison between the experimental and the calculated CMC values are given in Table II.

TABLE II

COMPARISON BETWEEN THE OBSERVED (BY LANGE) AND CALCULATED CMC VALUES OF MIXTURES OF SODIUM AND CALCIUM DODECYL SULFATES AT 70°C.

| mole fraction of the calcium dodecyl sulfate | obs. CMC (moles/1.) | calc. CMC (moles/1.) |
|---|---|---|
| 0 | 0.0066 | 0.0067 |
| 0.02 | 0.0057 | 0.0056 |
| 0.05 | 0.0053 | 0.0050 |
| 0.1 | 0.0049 | 0.0046 |
| 0.25 | 0.0040 | 0.0037 |
| 0.5 | 0.0034 | 0.0033 |
| 0.75 | 0.0031 | 0.0031 |
| 1 | 0.0029 | 0.0029 |

## Conclusion

Formulas for the electrical potentials of the micelle surface in various conditions are derived. Using these formulas, the comparison between the theory and the experiments was undertaken. From the good agreement between the theory and experiments, the CMC of sodium and calcium dodecyl sulfates as a function of the concentration and valency of added salts was explained quantitatively. The present investigation is applicable not only to the study of the micelle, but to the elucidation of the outstanding colloid chemical fact of the predominating influence of oppositely charged ions upon the electrical double layer.

The author wishes to express his sincere thanks to Dr. H. Lange (Henkel U. Cie, Deutschland) for his kindness in sending the numerical data of CMC to him.

*Department of Physical Chemistry, Faculty of Engineering, Yokohama National University, Minamiku, Yokohama*

---

# *On the Oxidation of Cellulose. II. On Celluronic Acid Prepared by a Simple Method**

By Seishi MACHIDA and Mitsumasa INANO

(Received February 24, 1955)

During the course of chemical research of natural polyuronides[1], it became desirable to obtain celluronic acid[2] for purposes of comparison.

Pigman[3] oxidized cellulose by concentrated nitric acid added with sodium nitrite. The authors[4], using his method, obtained an oxidized cellulose containing one glucuronic residue per five glucose residues. But the mean degree of polymerisation of the oxidized cellulose was about one-fourth of the original cellulose and its copper value was very high.

The present paper presents the results obtained in the oxidation of cellulose by phosphoric acid added with sodium nitrite.

## Experimental Results and Discussion

In 150 cc. of 90% phosphoric acid, 5 g. of pulp cellulose was placed and a definite quantity of solid sodium nitrite was added. The suspension was stirred and kept at constant temperature for a definite time. The suspension was then diluted with 50 cc. of water and filtered. The oxidized cellulose was suspended in 500 cc. of water, stirred, kept at least 12 hrs., and filtered. The washing was repeated in the same manner until the acidity of the filtrate vanished. The oxidized cellulose was then washed several

TABLE I

| Sample Number | Reaction time (hr.) | Reaction temp. (°C) | $NaNo_2$ (g.) | Carboxyl content (%) | Glucuronic content (%) | Glucurono lacton / Glucose |
|---|---|---|---|---|---|---|
| 1 | 1 | 10 | 0 | 0.08 | 0.31 | 1/311 |
| 2 | 1 | 10 | 2 | 2.09 | 8.17 | 1/12 |
| 3 | 1 | 10 | 5 | 2.30 | 9.00 | 1/12 |
| 4 | 1 | 15 | 10 | 7.90 | 30.90 | 1/4 |
| 5 | 1 | 20 | 15 | 16.07 | 62.85 | 3/5 |
| 6 | 1 | 20 | 20 | 18.32 | 71.65 | 2/3 |
| 7 | 1 | 20 | 2 | 4.17 | 16.31 | 1/7 |
| 8 | 1 | 25 | 5 | 11.92 | 46.62 | 1/2 |
| 9 | 1 | 20 | 10 | 9.75 | 38.13 | 1/3 |

* A portion of this paper was presented before the Annual Meeting of the Chemical Society of Japan in April, 1953 at Kyoto.

1) Reviewed in "A Summary of Chemical Studies on Polyuronides", *Bulletin of the Faculty of Textile Fibres, Kyoto University of Industrial Arts and Textile Fibres*, **1**, 116 (1954) (in English).

2) W. O. Kenyon et al., *J. Am. Chem. Soc.*, **64**, 121, 127 (1942); **69**, 342, 349, 355 (1947); **70**, 270 (1948).

3) W. W. Pigman et al., *J. Am. Chem. Soc.*, **71**, 2200 (1949).

4) S. Machida, N. Uchino and M. Inano, *J. Chem. Soc. Japan*, **74**, 204 (1953).

times with acetone and finally with ether and dried in a vacuum desiccator.

The oxidized cellulose thus obtained was a white powder, and the yield was about 90%. Carboxyl group contents determined by the calcium acetate method and the calculated theoretical glucuronic residue contents of the oxidized cellulose obtained in various reaction conditions are shown in Table I.

As is shown in the table, the highest value of the carboxyl content is 18.32%, which means that one uronic residue is present per 1.5 glucose residue in the chain molecule. The presence of the uronic group in the oxidized cellulose was confirmed by the naphthoresorcinol test. Its content was actually determined by heating the sample with 12% hydrochloric acid and estimating the furfural liberated from it. For example, Sample No. 9, was found to contain 36.5% glucurono lactone in this actual determination. The theoretical uronic residue content calculated for the same sample is 38.13%, assuming that the 9.75% value of carboxyl content is wholly due to uronic groups. Therefore, it is found that carboxyl groups of this substance are largely of the glucuronic type and only a few of them are of other types, such as the aldonic.

The mean degree of polymerisation of the oxidized cellulose was determined by the viscosity measurement of acetone solution of its nitric ester. The results obtained are shown in Fig. 1.

The solubilities of the oxidized cellulose in 1% caustic soda solution at 20°C and 100°C were determined, and are shown in Fig. 2.

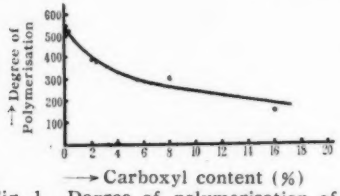


Fig. 1. Degree of polymerisation of the celluronic acids.

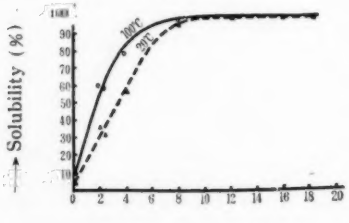


Fig. 2. Solubility of the celluronic acids in 1% caustic soda solution.

As is shown in Fig. 2, the oxidized cellulose, whose carboxyl content was more than 8%, is almost entirely soluble; and, by referring to Fig. 1, it is found that the mean degree of polymerisation of such oxidized cellulose is 322, which is nearly two-thirds that of the untreated cellulose.

These facts indicate that the oxidation of cellulose by concentrated phosphoric acid added with sodium nitrite is much more convenient; that is, the cellulose is not apt to be hydrolyzed heavily and the oxidation proceeds smoothly. The reason, perhaps, is that phosphoric acid as compared with nitric acid has weak acidity and strong ability to make cellulose swell. As the phosphoric acid group was not detected in the oxidized cellulose, it could not be considered that the phosphoric acid group combined chemically with the oxidized cellulose enhanced its solubility.

The alkaline solution of the oxidized cellulose was fluid. Furthermore it was coagulated by adding salts of alkali earth or heavy metal or a large volume of alcohol or acetone. By neutralization with acid, about 85% of the oxidized cellulose was recovered from the alkaline solution. The recovered oxidized cellulose had almost the same carboxyl group content as the original oxidized cellulose and still indicated the color reaction with naphthoresorcinol. However, it can easily be imagined that the molecules must have disintegrated.

## Summary

Cellulose was conveniently oxidized by concentrated phosphoric acid added with sodium nitrite; that is, the cellulose was not apt to be hydrolyzed heavily and the oxidation proceeded smoothly.

It was found that carboxyl groups of the oxidized cellulose were largely of the glucuronic type.

The oxidized cellulose, whose carboxyl content was more than 8%, was almost soluble in dilute caustic soda solution; and the mean degree of polymerisation of such oxidized cellulose was nearly two-thirds of that of the untreated cellulose.

Some properties of the alkaline solution of the oxidized cellulose were investigated.

The expense of this study was defrayed in part by a grant from the Hattori Hokokai, to which the authors' thanks are due.

*Chemical Laboratory of Textile Fibres, Kyoto University of Industrial Art and Textile Fibres, Kyoto*

# *Three Prototypes for the Cathodo-luminescence Spectra of Praseodymium in Various Forms of Alumina*

By Eiichi IWASE, Seijiro NISHIYAMA and Toshiaki ISONO

(Received February 23, 1955)

## Introduction

The structures of aluminas and alumina-hydrates have recently been the subject of extensive researches, the X-ray diffraction method being, as is well known, almost always employed for this purpose. The present authors have tried, in the course of the studies on the similar problems, to apply a spectrographic method of the cathodo-luminescence brought about by a certain rare earth, either praseodymium or samarium, which was imbedded in the various specimens of alumina, and have found this method fairly effective in solving such yet indistinct problems. This paper presents the finding of the three prototypes for the cathodo-luminescence spectra given by the praseodymium-bearing alumina, and at the same time the structural interpretations as well as the preparations for the samples of alumina corresponding to the yielding of these three luminescence prototypes.

## Materials and Experimental Procedures

Three samples of alumina containing praseodymium were prepared as follows.

**Sample 1.**—The hydrous alumina gel was precipitated with ammonia from the solution of aluminium sulphate, washed by decantation, filtered, and dried at about 110°C. This dried gel was soaked with a solution of praseodymium nitrate and then ignited at about 900°C for 1 hr.

**Sample 2.**—Crystals of aluminium nitrate ennea-hydrate were partially calcined at about 180°C until they became fine powders, which were then soaked with a solution of praseodymium nitrate and ignited at 1200–1300°C.

**Sample 3.**—Crystals of alumina-trihydrate produced by Bayer process, namely hydrargillite were previously calcined at about 800°C for 1 hr. The thermally decomposed product was soaked with a solution of praseodymium nitrate and then ignited at about 900°C for 1 hr.

The amount of praseodymium to be introduced was always made about 1% as oxide to the resulting sample of alumina.

The three samples mentioned above were submitted to the cathode-ray bombardment in a small Urbain tube and their luminescences thus yielded were spectrographically investigated by employing a glass-prism spectrograph of Feuss.

## Experimental Results

Fig. 1, (a), (b) and (c) shows schematically the results of the investigations on the cathodo-luminescence spectra given by the samples 1, 2 and 3 respectively. The relative intensities of the luminescence bands were estimated visually, and indicated by the heights in the figures.

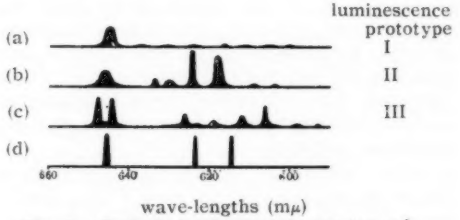


Fig. 1. Cathodo-luminescence spectra of praseodymium-bearing aluminas.

These three luminescence spectra have quite different and readily distinguishable appearances, and may be regarded as the three prototypes for the cathodo-luminescence spectra due to the praseodymium ions exisiting in various kinds of alumina.

The luminescence spectra given by the samples 1, 2 and 3 are, for convenience, called the luminescence prototypes I, II and III respectively.

## Discussions

It has generally been considered that a certain rare earth element imbedded in a colorless inorganic ground-material of definite chemical composition, will give rise to a fixed luminescence spectrum. A few exceptions have, however, been reported: When the europium or samarium is present in either magnesia or calcium sulfide, the luminescence spectrum given by one of these rare earths differs in its details rather widely, depending on the manner of preparations for the luminescent materials, although the ground-materials have the same chemical composition[1].

1) P. Pringsheim; "Fluorescence and Phosphorescence", Interscience publishers, Inc., New York, (1949), p. 470.

The luminescence of praseodymium mentioned here may provide a further noteworthy example of these interesting exceptional cases.

Rohden[2] described a definite luminescence spectrum for the praseodymium-bearing alumina as shown in Fig. 1, (d). It is concluded, from the comparison of Rohden's data with the three luminescence prototypes found by the present authors, that Rohden's spectrum seems to correspond to the prototype II.

The feature of the luminescence bands yielded by a rare earth, which has been introduced in a crystalline ground-material, is mainly determined by the transitions between electronic levels of the rare earth ion. The individual luminescence bands corresponding to these transitions may be influenced by the Stark effect owing to the electric field of the surrounding ions, and also to some extent by the lattice vibrations of the ground-material[3]. Thus the crystal structure of the ground-material would be expected to produce, in some cases, rather remarkable effects upon the feature of luminescence spectrum.

X-ray diffraction photographs have been taken of the samples 1, 2 and 3 in a Debye-Scherrer powder camera using copper $K_\alpha$ filtered radiation, and the results obtained are schematically illustrated in Fig. 2.

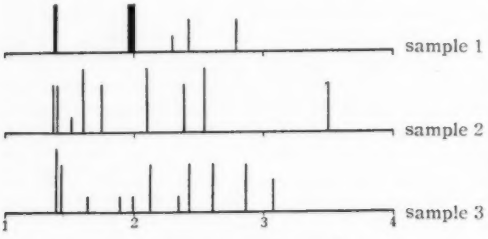


Fig. 2. Graphical representations of X-ray diffraction data for aluminas.

It will be seen that the X-ray diffraction patterns for the samples of alumina 1, 2 and 3 coincide almost entirely with those of $\gamma$-[4], $\alpha$-[5] and $\kappa$-[6] modifications of alumina respectively.

The oxygen arrangement in alumina is hexagonal close-packed for $\alpha$-modification, while it is cubic close-packed for the $\gamma$- and $\kappa$-modifications.

The aluminium ions of the $\alpha$-modification are situated in the octahedral interstices of the oxygen networks, and this configuration of alumina yields decisively the luminescence prototype II of the praseodymium.

In the case of $\gamma$-modification the aluminium ions are said to be situated statistically in the octahedral and tetrahedral interstices of the cubic close-packed oxygen networks evenly, and it may therefore be assumed that the praseodymium ions introduced in this modification of alumina will also be distributed at random through these two kinds of interstices. The luminescence prototype I of the praseodymium given by the $\gamma$-modification of alumina may accordingly be considered as the luminescence spectrum of the praseodymium in solution.

It is also found that the praseodymium contained in an optically isotropic substance, namely ordinary glass emits the cathodoluminescence spectrum almost similar to that of the prototype I. This fact seems to support the above reasoning.

Ervin[7] has recently postulated the position occupied by aluminium ions in the oxygen networks of cubic close-packing, by taking the intensity of the line at 1.985–2.03 Å observed in X-ray diffraction patterns into considerations. This line is caused by the reflection from (400) planes of the spinel lattice, which include all the oxygen positions and the octahedral aluminium positions, but not the tetrahedral aluminium positions. It is to be remarked that this line is found to be weak in the $\kappa$-modification of alumina as compared with the $\gamma$-modification. Provided the postulation described above is valid for the $\kappa$- and $\gamma$- modifications of alumina, the conclusion may then be drawn that the aluminium ions in the $\kappa$-modification should be situated much more predominantly in the tetrahedral rather than the octahedral interstices of oxygen networks.

The praseodymium-luminescence of the prototype III can be seen distinctly only in the case of the praseodymium-bearing alumina, which has been derived from the hydrargillite through the special previous heat treatment.

The practical thermal decomposition of hydrargillite is, at the present, considered to proceed simultaneously through dual routes[8], the one through boehmite followed by a

2) A. de Rohden, *Ann. chim.*, [9] **3**, 361 (1915).
3) R. Tomaschek, *Acta Phys. Polonica*, **6**, 401 (1936).
4) H. C. Stumpf, A. S. Russell, J. W. Newsome, and C. M. Tucker, *Ind. Eng. Chem.*, **42**, 1402 (1950).
5) H. Thibon, J. Charrier and R. Tertian, *Bull. soc. chim. de Fr.*, [5] **18**, 387 (1951).
6) J. F. Brown, D. Clark and W. W. Elliott, *J. Chem. Soc.*, **1953**, 86.
7) G. Ervin, *Acta Cryst.*, **6**, 106 (1953).
8) J. F. Brown, D. Clark and W. W. Elliott, *J. Chem. Soc.*, **1953**, 85; M. R. B. Day and V. J. Hill, *Nature*, **170**, 539 (1952); *J. Phys. Chem.*, **57**, 946 (1953).

series of virtually anhydrous alumina, namely $\gamma$-, $\delta$- and $\theta$-modifications, and the other directly through a sequence of other virtually anhydrous alumina, namely $\chi$- and $\kappa$-modifications, both of these routes leading eventually to a common product, the $\alpha$-modification. Irrespective of whether the formation of boehmite is of primary[9] or of secondary origin[10], it seems to be almost certain that the thermal decomposition of hydrargillite forks off in practice into two branches on the way of the transformation to the $\alpha$-modification of alumina. In the route of conversion directly via the anhydrous aluminas, for example the $\kappa$-alumina, the aluminium ions tend to be arranged in the tetrahedral interstices of the cubic close-packed oxygen networks. This arrangement seems to be characteristic of the thermal transformation sequence derived from the hydrargillite and responsible for giving rise to the luminescence prototype III of praseodymium.

## Conclusion

Almost all the cathodo-luminescence spectra given by the various preparations of the praseodymium-bearing alumina can be regarded as belonging to either one of the three prototypes (I, II and III) or their combinations.

The occurrence of these three fundamental spectral types for the praseodymium-luminescence may closely be related with the three ways for the reciprocal arrangements of oxygen and aluminium in the configuration of alumina.

The prototype II of the praseodymium-luminescence spectrum is obtained for the alumina with the oxygen network of hexagonal close-packing, namely the $\alpha$-modification.

The alumina with the oxygen network of cubic close-packing, shows either the luminescence prototype I or III, depending upon the location of aluminium ions. The prototype I is seen in the $\gamma$-modification of alumina, where the aluminium ions are statistically distributed evenly throughout the two sorts of interstices of the oxygen network, namely octahedral and tetrahedral interstices, while the luminescence prototype III is yielded with the $\kappa$-modification of alumina, in which the aluminium ions take their seats in the tetrahedral rather than in the octahedral interstices.

In connection with the X-ray investigations here included thanks are due to Dr. M. Nakahira. The authors are also grateful to the Ministry of Education for the Scientific Research Encouragement Grant in aid of this work.

*The Institute of Scientific Researches, Komagome, Bunkyo-ku, Tokyo*

9) J. E. Brown, D. Clark and W. W. Elliott, *J. Chem. Soc.*, **1953**, 85.
10) M. K. B. Day and V. J. Hill, *Nature*, **170**, 539 (1952); *J. Phys. Chem.*, **57**, 946 (1953).

---

# *Cathodo-luminescence as Applied to the Detection of Rare Earths Contained in Some Natural Calcareous Substances*

By Eiichi IWASE

(Received February 23, 1955)

## Introduction

Crookes detected minute amounts of yttrium and samarium in calcareous portions of some marine organisms. It has been said that this fact led him to a confirmation of the presence of rare earths in sea water.[1] Goldschmidt found rare earths also in the calcium carbonate, which constitutes reef corals.[2] As is well known, some of the rare earths contained in calcium oxide behave as activators in giving the characteristic luminescence under the cathode-ray bombardment, the spectra of which consist of fairly sharp line-like bands. This phenomenon proved already to be an efficacious aid in making some geochemical researches: Rare earths sparingly present in anorthite and

1) Cited in V. M. Goldschmidt, *J. Chem. Soc.*, **1937**, 667.
2) V. M. Goldschmidt, *J. Chem. Soc.*, **1937**, 667.

TABLE I

CATHODO-LUMINESCENCE SPECTRA DUE TO RARE EARTHS CONTAINED IN CONVERTED CALCIUM-OXIDE SAMPLES

| Wave-length | Miyako Main Isle | | Akiyoshi | Hiroshima |
|---|---|---|---|---|
| (mμ) | *Acropora* | *Pocillopora* | Stalactite | *Licina* |
| 648.0 | w | — | wwb | — |
| 639.5 | w | — | wwb | — |
| 633.4 | m | w | m | — |
| 626.0 | s | w | s | — |
| 620.0 | ww | — | w | — |
| 616.0 | w | ww | w | — |
| 613.2 | w | — | w | — |
| 606.6 | ss | m | ss | w |
| 604.6 | m | — | s | — |
| 596.5<br>594.0 | ww | — | w | — |
| 590.3 | ww | — | — | — |
| 588.0 | w | w | w | — |
| 585.2 | ss | m | s | w |
| 583.4 | w | — | w | — |
| 580.5 | w | — | ww | — |
| 578.5 | w | — | ww | — |
| 575.9 | w | w | w | — |
| 571.3 | w | — | w | — |
| 568.3 | — | — | ww | — |
| 558.6 | — | — | ww | — |
| 555.0<br>552.1 | ww | — | ww<br>w | — |
| 549.2 | — | — | w | — |
| 546.3 | w | — | ww | — |
| 543.3 | — | — | w | — |
| 537.0 | — | — | w | — |
| 517.0 | — | — | ww | — |
| 500.0<br>499.0 | ww | — | ww | — |
| 494.6 | ww | — | ww | — |
| 489.8 | w | — | ww | — |
| 486.9 | ww | — | w | — |
| 483.8 | ww | — | ww | — |
| 481.7 | ww | — | ww | — |
| 479.9 | w | w | ww | — |
| 477.0 | ww | ww | — | — |
| 460.5 | — | — | ww | — |
| 457.2 | — | — | w | — |
| 454.3 | — | — | ww | — |
| 448.5 | — | — | ww | — |
| 439.0 | — | — | ww | — |
| 436.9 | — | — | w | — |
| 421.8 | — | — | ww | — |
| 421.0 | — | — | ww | — |
| 419.5 | — | — | ww | — |
| 418.0 | — | — | ww | — |
| 416.0 | — | — | ww | — |
| 415.0 | — | — | ww | — |
| 413.5 | — | — | ww | — |
| 411.8 | — | — | ww | — |

ordinary augite from Taga volcanoes in Shizuoka Pref. were investigated by means of the cathodo-luminescence spectra, which appeared in one paper[3] entitled "A short note relating to the evolution of magma", and the detection of rare earths was also made by the inspection of cathodo-luminescence spectra, which is seen in another paper[4] entitled "On the crystallisation of fluorites," regarding two kinds of samples of fluorite from Tateiwa village, Fukushima Pref. one is a green octahedral crystal crystallised at an earlier stage and the other a violet cubic one at a later stage.

In the present paper the applicability of the cathodo-luminescence method to the detection of rare earths is revealed on such natural calcareous substances as reef coral, stalactite, molluscan fossil and calc-sinter.

### Materials and Experimental Procedures

Seven specimens were used in the experiments; two reef corals, one stalactite, one molluscan fossil, and three calc-sinters. Two kinds of reef corals from Miyako Main Isle, *Pocillopora Sp.* and *Acropora variabilis Verrill* are reproduced in Figs. 1 and 2 respectively. The former is of amber white antler form and the latter has an appearance closely resembling a group of small flower clusters, like those of a cauliflower. It is to be mentioned that the *Acropora* is soluble in hydrochloric acid without any perceptible residues, while the *Pocillopora* leaves a thin transparent yellow cuticular sack after the same treatment.

Fig. 1. *Pocillopora sp.*

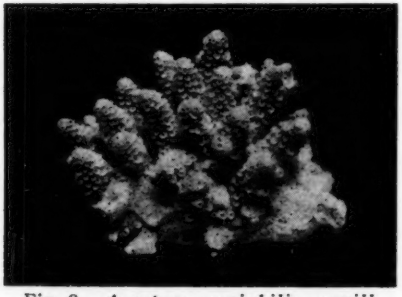

Fig. 2. *Acropora variabilis verrill.*

An ochrey stalactite from Akiyoshi in Yamaguchi Pref. shows, when cut crosswise, onyx-like banding near the periphery and radiated structures in the center portion.

A molluscan fossil, *Licina (Anodontia) Sp.*, which was found at Hiroshima city, is greasy, translucent and stained with reddish brown tint.

Calc-sinters occurring at Senami springs in Niigata Pref., Miné springs is Shizuoka Pref. and Shirahone springs in Nagano Pref. were also delivered to the author.

About 10 g. of each specimen were dissolved in hydrochloric acid, the solution thus produced was made slightly acidic by the controlled addition of ammonia, and then 2 g. of oxalic acid were added. Rare earths, if present in the original specimen, would have been coprecipitated with calcium as oxalates, which would then be converted to the oxide-form by the calcination. The same procedure is repeated once more, the only difference being the application of a much smaller amount of oxalic acid (0.5 g.). In this way the concentration of rare earths in calcium oxide is increased about fifty times, compared with that in the original specimen. The converted calcium oxide thus obtained is subjected to the cathode-ray bombardment in a small Urbain tube and the luminescence brought about is spectrographically investigated by employing a glass-prism spectrograph of Feuss.

### Experimental Results and Discussions

The results of cathodo-luminescence spectra given by the converted calcium-oxide samples from reef corals, stalactite and molluscan fossil are summarised in Table I. Relative intensities are estimated visually and indicated by the following symbols: ss(very strong), s(strong), m(medium), w(weak), ww(very weak) and b(broad).

TABLE II

RARE EARTHS DETECTED BY CATHODO-LUMINESCENCE BANDS

| Localites | Specimens | Rare earths identified |
|---|---|---|
| Miyako Main Isle | *Acropora* | Dy, Pr, (Sm), (Tb) |
| | *Pocillopora* | Dy, Pr, (Sm) |
| Akiyoshi | stalactite | Dy, Pr, Sm, Tb |
| Hiroshima | *Licina* | Dy, Pr |

The presence of dysprosium and praseodymium in these four specimens is confirmed, as illustrated in Table II, by comparing the wave-lengths of the observed luminescence bands with Fagerberg's data[5], which give the precise numerical figures for the wave-lengths of the cathodo-luminescence bands yielded by the calcium oxide containing each individual rare earth element. Furthermore,

3) E. Iwase, *J. Chem. Soc. Japan*, **63**, 633 (1941).
4) E. Iwase, *Bull. Inst. Phys. Chem. Researches* (Tokyo), **21**, 61 (1942).
5) S. Fagerberg, *Nova Acta Regiae Societatis Scientiarum Upsaliensis*, Ser. IV, Vol. 7, No. 6 (1931).

samarium and terbium are distinctly detected in the stalactite and also perceptible in the *Acropora*, whereas not at all in the molluscan fossil. Under the conditions of the present experimental work, none of the calc-sinters investigated here revealed the presence of rare earths.

To be precise, the concentration of rare earths in the samples of converted calcium oxide has been increased 45 and 67 times for the *Acropora* and the *Pocillopora* respectively. It is a remarkable fact that the luminescence bands due to dysprosium, samarium and terbium have been all distinctly visible in the case of *Acropora variabilis Verrill*, but have been, in the case of *Pocillopora Sp.*, found much weaker in intensity with the complete disappearance of the terbium bands, although the latter specimen has been subjected to a considerably higher concentrating treatment than the former one. These observations may possibly be interpreted by a distinction found between the surface conditions of the two reef corals; *Acropora variabilis Verrill* seems to be naked, while the surface of *Pocillopora Sp.* is covered by a thin superfacial membrane of organic nature, which would be expected to exercise various restricting influences on the assimilation of rare earths from sea water during the natural growing process of the reef corals.

**Summary**

Specimens of reef corals, stalactite, molluscan fossil and calc-sinters were converted to the form of oxide, in which rare earths, if present in the original specimens, would be concentrated by chemical means. Luminescence spectra given by these samples of calcium oxide were investigated under the cathode-ray bombardment and the presence of minute amounts of rare earths could be confirmed; dysprosium, praseodymium, samarium and terbium in a stalactite from Akiyoshi, dysprosium, praseodymium and presumably samarium in reef corals from Miyako Main Isle, and dysprosium and praseodymium in a molluscan fossil from Hiroshima. Not even slight traces of rare earths were perceived in calc-sinters from several springs, so far as this detecting method was concerned. Two kinds of specimens of reef corals from the same locality gave a remarkable difference in the rare-earth content and this observation may be explained by the different conditions of the surfaces found in these reef corals, during the growth of which the assimilation of the rare earth ions from sea water were possibly much more disturbed by the existence of an organic membrane covering the surface of one specimen as compared with another lacking such a membrane.

*The Institute of Scientific Researches, Komagome, Bunkyo-ku, Tokyo*

---

# *A Relation between Bond-orders and Bond-lengths of C-Cl Bonds in Conjugated Systems: An Example of the Order-length Relation for Bonds other than C-C Bonds*

By Tosinobu ANNO and Akira SADÔ

(Received January 20, 1955)

## Introduction

By the method of molecular orbital, Coulson[1] has found a relation between bond-order and bond-length in C-C bonds in conjugated systems and derived the relation theoretically. If the order of a bond is known, this relation can be used to predict the bond distance except in special cases. However, as is mentioned by Coulson[2], such a theoretical order-length relation has not yet been derived for other bonds than C-C bonds.

It is the purpose of this paper to show that a relation similar to that for C-C bonds does exist also for C-Cl bonds. The theoretical relation which we present here is similar in form to that given by Coulson and predicts the bond-length from the bond-

1) C.A. Coulson, *Proc. Roy. Soc.* (London), A169, 413 (1939).

2) C.A. Coulson, *J. Phys. Chem.*, 56, 311 (1952).

order which agrees very well with the observed length.

## Theoretical

We shall use the simple LCAO molecular orbital method. The total energy $E$ of $\pi$-electrons is shown to be

$$E=\sum_{r=1}^{k} q_r\alpha_r+2\sum_{i<j}\sum p_{ij}\beta_{ij},$$

where $\alpha_r$ and $\beta_{ij}$ are usual coulomb and resonance integrals and $q_r$ and $p_{ij}$ denote the formal charge and the mobile bond order, respectively.

Consider a hypothetical state where all $\pi$-electrons are localized at "original" atoms giving those $\pi$-electrons, i.e. where $\pi$-bonds are not formed. Then the total $\pi$-electron energy would be

$$E_0=\sum_{r=1}^{k} q_r^{\circ}\alpha_r,$$

where $q_r^{\circ}$ denotes the number of $\pi$-electrons localized at atom $r$. The binding energy of $\pi$-electrons is the energy difference between the actual and the hypothetical state. Allowing for the compression of the $\sigma$-bond, minimization of the total energy (including both the $\sigma$- and $\pi$-energies) with respect to the internuclear distance at constant $p_{ij}$'s and $q_r$'s gives,[1),3)]

$$\sigma_{ij}(x_{ij}-s_{ij})+2p_{ij}(\partial\beta_{ij}/\partial x_{ij})=0, \qquad (1)$$

where $x_{ij}$ is the bond-length of bond $i$-$j$, $\sigma_{ij}$ is its single bond force constant and $s_{ij}$ is the single bond distance.

For the C-Cl bond, we cannot use as standards the single and double bonds to obtain the functional variation of $\beta$ with $x$, since there is no double bond between carbon and chlorine atoms. Instead of the double bond, however, we can take up a C-Cl bond whose mobile order is as near to unity as possible. For this purpose we take the C-Cl bond in chloroacetylene, whose mobile order $p_a$ is calculated at 0.661 (see below). Let us consider a C-Cl bond whose mobile order and bond-length are $p_a$ and $x$, respectively. The $\pi$-electron energy of this bond can be expressed by $2p_a\beta_{C\text{-}Cl}$ where $\beta_{C\text{-}Cl}$ is the resonance integral in this C-Cl bond. On the other hand, taking the methyl chloride and chloroacetylene molecules as standards, considerations similar to the case of C-C bonds[1),3)] show that this $\pi$-electron energy is

$$E_a^0-E_s^0+(1/2)\kappa_a(x-d_a)^2-(1/2)\sigma(x-s)^2,$$

where $E_a^0$, $E_s^0$; $\kappa_a$, $\sigma$ and $d_a$, $s$ are the bond energies, force constants and the internuclear distances in C-Cl bonds in the chloroacetylene and methylchloride molecules, respectively. Equating this to $2p_a\beta_{C\text{-}Cl}$, differentiation with respect to $x$ gives

$$2p_a(\partial\beta_{C\text{-}Cl}/\partial x)\fallingdotseq\kappa_a(x-d_a)-\sigma(x-s). \qquad (2)$$

Combining Eqs. (1) and (2) it follows that

$$x=s-\frac{s-d_a}{1+\dfrac{\sigma}{\kappa_a}\left(\dfrac{1-p'}{p'}\right)}, \qquad (3)$$

where $p'=p/p_a$.

## Test of the Theory

We have calculated the bond-order for the C-Cl bond in some molecules and the result is shown in Table I. In calculating the bond-order the following assumptions were made.

TABLE I

CALCULATED BOND-ORDERS AND OBSERVED BOND-LENGTHS OF SOME C-Cl BONDS

| Molecule | Bond-length*(Å) | Bond-order** |
|---|---|---|
| Chloromethane | 1.77 | (1.00) |
| *trans*-Dichloroethylene | 1.69 | 1.29 |
| 1,3,5-Trichlorobenzene | 1.69 | 1.32 |
| Dichloroacetylene | 1.64 | 1.55 |
| Chloroacetylene | 1.63 | 1.66 |

* These values are taken from reference 9 in text. All values are determined by electron diffraction except for chloroacetylene. The value for chloroacetylene is determined by microwave spectroscopy.

** It should be noted that the figures given here are for total bond orders defined by $(1+p_{ij})$, where $p_{ij}$'s are mobile orders.

(i) The coulomb integral at an atom is proportional to its electronegativity scale[4)] given by Pauling[5)].

(ii) The resonance integral $\beta_{ij}$ is zero when $i$ and $j$ refer to non-neighboring atoms. When $i$ and $j$ refer to neighboring atoms $\beta_{ij}$ is proportional to the overlap integral $S_{ij}$ between these two atoms[6)]. The overlap integral is available in the table by Mulliken et al.[7)].

(iii) The ratio of the coulomb integral $\alpha_C$ at the carbon atom in benzene to the resonance integral $\beta_{CC}$ for the C-C bond in the same molecule is

$$\alpha_C/\beta_{CC}=3.9^{8)}.$$

3) J. E. Lennard-Jones, *Proc. Roy. Soc.* (London), A158, 280 (1937).

4) C. Sandorfy, *Bull. soc. chim. France*, **1949**, 615.

5) L. Pauling, "The Nature of the Chemical Bond", Cornell University Press, Ithaca, New York, (1940).

6) G.W. Wheland, *J. Am. Chem. Soc.*, **64**, 900 (1942).

7) R.S. Mulliken, C.A. Rieke, D. Orloff and H. Orloff, *J. Chem. Phys.*, **17**, 1248 (1949).

8) S. Nagakura, This Bulletin, **25**, 164 (1952).

(iv) The overlap integral is negligible throughout. The empirical internuclear distances are also given in Table I.

If internuclear distances and bond-orders are plotted in a diagram we can expect a simple relation between them. In Fig. 1 the

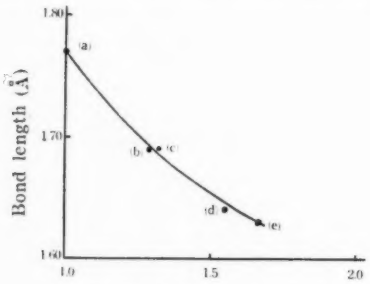


Fig. 1. Relation between bond-order and bond-length in C-Cl bonds. Points represent observed bond-lengths versus calculated bond-orders. Curve is the graphical representation of Eq. (3) (see text).

*a*, Chloromethane;
*b*, *trans*-Dichloroethylene;
*c*, 1,3,5,-Trichlorobenzene;
*d*, Dichloroacetylene;
*e*, Chloroacetylene.

curve of Eq. (3) is drawn, accepting the following numerical values.

$$s=1.77\ \text{Å}^{9)} \qquad d_a=1.63\ \text{Å}^{9)}$$
$$\sigma=3.64\times10^5\ \text{dynes/cm.}^{10)}$$
$$\kappa_a=5.52\times10^5\ \text{dynes/cm.}^{11)}$$

Points in the figure represent the calculated bond-orders and the observed bond-lengths. Fig. 1 shows that these points lie on the theoretical curve within experimental error. Therefore a similar equation as the one for the C-C bond can be seen to be available also for the other bond if the suitable reference molecule is chosen (for example, for C-Cl bonds the chloroacetylene molecule).

However, the effects of hybridization, charge distribution and the repulsion of non-bonding electrons must be taken into consideration.

Hybridization effect can be considered in the same way as in the case of the C-C bond. For various C-Cl bonds, the hybridization ratio of the $\sigma$-atomic orbital of the chlorine atom can be considered as approximately constant in all cases. Only the variation in the hybridization ratio of the carbon atomic orbital needs to be considered. Accepting Coulson's result (see Fig. 2 of reference 12) which shows carbon atomic radius as the function of the hybridization ratio, a separate order-length curve should apply according to the hybridization of the carbon $\sigma$-atomic orbital. However, our insufficient knowledge concerning the geometrical structure of polyatomic molecules will invalidate such a treatment. It is to be noted that Coulson's result shows that the difference between carbon atomic radii corresponding to $sp$ and $sp^3$ hybridizations is 0.035 Å.

It is true that the effect of the charge distribution must be taken into account in cases where the migration of the charge is large, but for C-Cl bonds in molecules whose bond-orders are calculated here, the effect of the charge distribution considered as described by Coulson[12] amounts only to a few thousandths of an angstrom which may be immaterial.

The effect due to the repulsion of non-bonding electrons would have to be considered in the absolute calculation of bond length. For bonds between a particular pair of atoms this type of effect can be considered as constant. Therefore in the relative calculation using the order-length curve, this effect may cancel out.

Thanks are due to Prof. S. Imanishi who read this manuscript.

*Department of Chemistry, Faculty of Science, Kyushu University, Fukuoka*

9) Landolt-Börnstein, "Zahlenwerte und Funktionen", Springer, Berlin, (1951).
10) G. Herzberg, "Infrared and Raman Spectra of Polyatomic Molecules," D. Van Nostrand Co. Inc., New York (1945), p. 193.
11) W. S. Richardson and J.H. Goldstein, *J. Chem. Phys.*, **18**, 1314 (1950).
12) C. A. Coulson, Contribution à l'étude de la structure moléculaire, Desoer, Liège (1948), p. 15.

# *Infrared and Raman Spectra of Pyridine N-Oxide*

By Mitsuo Ito and Norisuke Hata*

(Received January 13, 1955)

In a previous work[1], we have observed the ultra-violet absorption spectrum of pyridine N-oxide vapor with a complex vibrational structure. In order to carry out the vibrational analysis of this spectrum, assignments of the fundamental frequencies of pyridine N-oxide molecule are required, but we had no datum available for this.

In the present paper, infrared and Raman spectra of pyridine N-oxide have been measured under various conditions, and assignments based on these data are presented.

## Experimental

The sample of pyridine N-oxide was prepared according to the procedure of Ochiai[2] and was purified by repeated vacuum distillations. All precautions were taken to eliminate the absorption of atmospheric moisture by the sample.

The Raman spectrograph used in this investigation was a spectrograph with two dense flint glass prisms constructed in our laboratory, having a linear dispersion of 24 A/mm. at 4500 Å. Raman spectrum of pyridine N-oxide was obtained for both the liquid and the solution. For the liquid, hot water was circulated through the outer jacket of Wood's tube during the exposure in order to prevent the formation of crystal (the melting point of pyridine N-oxide is 59°C). For the solutions, chloroform, ethyl alcohol and water were used as solvents and concentration of each solution was about 20 g. pyridine N-oxide/20 cc. solvent. The Raman data for these conditions are listed in Table I, together with relative intensities based upon an arbitrary value of 5 for the strongest Raman line on the spectrogram. Although very broad Raman lines are also observed near 3000 $cm^{-1}$, they are not included in the table on account of their doubtful values.

Table I

Infrared and Raman frequencies of pyridine N-oxide ($cm^{-1}$)

| Infrared | | | Raman | | | | Average | Assignment |
|---|---|---|---|---|---|---|---|---|
| Solid | Chloroform solution | Ethyl alcohol solution | Liquid | Chloroform solution | Ethyl alcohol solution | Water solution | | |
| | | | 281 (1) | | 286 (1) | | 283 | $\nu_1$ non-planar O bending vib. |
| | | | 375 (1) | 371 (0) | | | 373 | $\nu_2$, ($B_2$), ring vib. |
| | | | | | 402 (1) | | 402 | $\nu_3$, ($A_2$), ring vib. |
| 482 w | | | 477 (0) | | 480 (1) | | 478 | $\nu_4$, planar O bending vib. |
| 512 w | | | | | | | 512 | |
| 546 w | | | | 548 (0) | 550 (1) | | 549 | $\nu_5$, ($A_1$), ring vib. |
| | | | 635 (1) | | 638 (3) | 641 (1) | 638 | $\nu_6$, ($B_1$), ring vib. |
| 679 s | | | 687 (1) | 660 (3) | | | 674 | $\nu_7$, ($B_2$), non-planer H bending vib. |
| | 803 m | | | | | | 803 | 2×402 |
| | 835 s | 835 s | 833 (4) | 832 (4) | 835 (4) | 829 (3) | 832 | $\nu_8$, ($A_1$), O stretching vib. |
| | 880 w | | | | | | 880 | 402+478 |
| | 902 m | 910 w | | | | | 906 | |
| | 1015 s | 1011 m | 1015 (5) | 1015 (5) | 1015 (5) | 1015 (5) | 1015 | $\nu_9$, ($A_1$), ring vib. |
| | 1044 w | | | | | | 1044 | 402+638 |
| | 1055 w | | | | | | 1055 | 512+549 |
| | 1096 w | | | | | | 1096 | 2×549 |
| | 1180 s | 1185 s | 1143 (2) | 1158 (3) | 1177 (3) | 1177 (3) | 1170 | $\nu_{10}$, ($A_1$), planar H bending vib. |
| | | 1240 s | 1239 (3) | 1250 (1) | 1240 (2) | | 1243 | $\nu_{11}$, ($B_1$), planar H bending vib. |
| | 1285 s | | | | | | 1285 | 2×638 |
| | | | 1312 (4) | 1318 (3) | 1329 (4) | 1327 (4) | 1321 | $\nu_{12}$, ($B_1$), planar H bending vib. |
| | 1386 w | | | | | | 1386 | 549+832, 373+1015 |
| | 1402 w | | | | | | 1402 | |

* Present address, Department of Pharmacy, Nagasaki University, Nagasaki.

1) M. Ito and N. Hata, This Bulletin, 28, 260 (1955).
2) E. Ochiai, *J. Org. Chem.*, 18, 534 (1953).

| Infrared | | Raman | | | | | |
|---|---|---|---|---|---|---|---|
| Solid | Choro-from solu-tion | Ethyl alcohol solu-tion | Liquid | Choro-from solu-tion | Ethyl alcohol solu-tion | Water solution | Average | Assignment |
| | 1473 s | 1466 m | 1469 (2) | 1466 (2) | 1466 (2) | | 1467 | $\nu_{13}$, ($A_1$), ring vib. |
| | 1608 s | 1608 m | 1599 (5) | 1604 (5) | 1608 (5) | 1606 (5) | 1605 | $\nu_{14}$, ($A_1$), ring vib. |
| | 1720 m | 1680 m | | | | | 1700 | |
| | 1864 w | | | | | | 1864 | 832+1015 |
| | 1968 w | | | | | | 1968 | 638+1321 |
| | 2050 w | 2015 w | | | | | 2032 | 2×1015 |
| | 2100 w | | | | | | 2100 | |
| | 2472 m | 2435 w | | | | | 2452 | |
| | 2926 s | | | | | | 2926 | $\nu_{15}$, H stretching vib. |
| | | 2990 w | | | | | 2990 | |
| | 3084 m | | | | | | 3084 | 1467+1605 |
| | 3223 w | | | | | | 3223 | 2×1605 |

$\nu$ represents fundamental vibration.

An infrared spectrum was obtained with a Perkin-Elmer model 112 spectrometer with NaCl and KBr prisms. Measurements were made in the region of KBr for the solid sample and in the region of NaCl for the chloroform and alcohol solutions.* The frequencies of infrared absorption maxima are given in Table I, together with the Raman data. The abbreviated notations for absorption intensity, w, m and s represent weak, medium and strong, respectively.

## Discussion

If the oxygen atom of pyridine N-oxide lies on a straight line connecting the nitrogen atom with the opposite carbon atom in the pyridine ring, symmetry of this molecule belongs to a point group $C_{2v}$, like that of the parent molecule pyridine. This structure is the most possible one and the other structures (point group $C_2$ and $C_s$) are difficult to consider. Here, assignments of the fundamental frequencies are carried out on the basis of the $C_{2v}$ symmetry.

**Ring Vibration.**—As the heterocyclic ring of pyridine N-oxide is similar to that of pyridine, the ring vibration frequencies and their normal modes of the two molecules must also be similar to each other. On the other hand, the chemical similarity between benzene and pyridine is well known and electron diffraction[3], infrared and Raman data[4] show that the ring structures of benzene and pyridine are almost the same. Therefore, it is expected that the ring vibration frequencies of pyridine N-oxide should nearly coincide with those of benzene or its derivatives. That this is actually the case for the fundamental frequencies, 373($\nu_2$), 402($\nu_3$), 1015($\nu_9$), 1467($\nu_{13}$) and 1605 $cm^{-1}$($\nu_{14}$), can be recognized in Table II, where numbers in the first column denote the normal modes for the vibrations of monodeuterobenzene shown in Fig. 1[5]. Accordingly, it is evident that these vibrations belong to the ring vibrations with almost the same normal

Table II

Ring vibrations of benzene, monodeuterobenzene, pyridine and pyridine N-oxide

| Normal mode[a] for monodeutero-benzene (Fig. 1) | Benzene[a] | Monodeutero-[a] benzene | Pyridine[b] | Pyridine N-oxide | Symmetry class ($C_{2v}$) |
|---|---|---|---|---|---|
| I | 405 | 380 | 374 | 373 ($\nu_2$) | $B_2$ |
| II | 405 | 405 | 404 | 402 ($\nu_3$) | $A_2$ |
| III | 605.6 | 601 | 604 | 549 ($\nu_5$) | $A_1$ |
| IV | 605.6 | 603 | 604 | 638 ($\nu_6$) | $B_1$ |
| V | 1010 | 1006.8 | 1028 | 1015 ($\nu_9$) | $A_1$ |
| VI | 1485 | 1480 | 1485 | 1467 ($\nu_{13}$) | $A_1$ |
| VII | 1596 | 1591.1 | 1580 | 1605 ($\nu_{14}$) | $A_1$ |

a) Reference 5) b) Reference 4)

* The authors are indebted to Prof. S. Akiyoshi and Mr. T. Matsuda of Engineering Department of Kyushu University for tracing the infrared spectra.

3) Schomaker and Pauling, *J. Am Chem Soc.*, **61**, 1769 (1939).

4) C.H. Kline and J. Turkevich, *J. Chem. Phys.*, **12**, 300 (1944).

5) C.K. Ingold and his coworkers, *J. Chem Soc.*, 1946 299 and 316.

TABLE III

HYDROGEN BENDING VIBRATIONS OF BENZENE, MONODEUTEROBENZENE, PYRIDINE AND PYRIDINE N-OXIDE

| Normal mode[a] for monodeutero-benzene (Fig. 1) | Benzene[a] | Monodeutero-benzene[a] | Pyridine[b] | Pyridine N-oxide | Symmetry class ($C_{2v}$) |
|---|---|---|---|---|---|
| VIII | 671 | 698 | 652 | 674 ($\nu_7$) | $B_2$ |
| IX | 1110 | 1158.2 | 1139 | 1243 ($\nu_{11}$) | $B_1$ |
| X | 1178 | 1175.6 | 1139 | 1170 ($\nu_{10}$) | $A_1$ |
| XI | 1326 | 1292 | 1290 | 1321 ($\nu_{12}$) | $B_1$ |

a) Reference 5). b) Reference 4).

modes as those of the corresponding vibrations of monodeuterobenzene.

In addition to these, the vibrations of 549 $cm^{-1}$($\nu_5$) and 638 $cm^{-1}$($\nu_6$) are also the ring vibrations and can be interpreted as the $A_1$ and $B_1$ component vibrations deriving from the doubly degenerate $E_g^+$ vibration of benzene (605.6 $cm^{-1}$). This assignment seems to be reasonable from the fact that in monohalogenated benzenes, for example, $A_1$ component vibration shifts to lower frequency than 605.6 $cm^{-1}$ and $B_1$ component vibration to higher frequency[6].

**Hydrogen and Oxygen Bending Vibrations.**—The frequency 674 $cm^{-1}$($\nu_7$) is assigned to the non-planar hydrogen bending vibration (mode VIII in Fig. 1) on the basis of its frequency value and on analogy with the frequencies of the corresponding vibrations in other molecules (Table III). In the cases of benzene and pyridine derivatives, planar hydrogen bending vibrations generally possess their characteristic frequencies in the region of 1100~1300 $cm^{-1}$ [6]. Pyridine N-oxide have three fundamental frequencies, 1170 $cm^{-1}$ ($\nu_{10}$), 1243 $cm^{-1}$($\nu_{11}$), and 1321 $cm^{-1}$($\nu_{12}$), in this region. As seen from Fig. 1, the planar hydrogen bending vibrations with X and XI normal modes might be expected to be almost unchanged in their frequencies on passing from benzene to pyridine N-oxide, but the vibration frequency with IX normal mode should be greatly changed in pyridine N-oxide as the result of a considerable contribution of planar oxygen bending vibration. Therefore, as shown in Table III, 1170 $cm^{-1}$($\nu_{10}$) and 1321 $cm^{-1}$($\nu_{12}$) are assigned to X and XI normal modes ($A_1$ and $B_1$ classes) respectively, and 1243 $cm^{-1}$($\nu_{11}$) is assigned to IX normal mode ($B_1$ class).

For 283 $cm^{-1}$($\nu_1$) and 478 $cm^{-1}$($\nu_4$), there are no comparable frequencies in the other molecules, so that these vibrations can be taken as oxygen vibration frequencies. Their frequency values suggest that 283 $cm^{-1}$($\nu_1$) is non-planar oxygen bending vibration and 478 $cm^{-1}$($\nu_4$) planar oxygen bending vibration.

**Oxygen Stretching Vibration.**—As 832 $cm^{-1}$ ($\nu_8$), which occur strongly in both infrared and Raman, has no corresponding frequency in benzene and pyridine, this vibration is also an oxygen vibration. In general, N-O stretching vibration in oxime compounds appears strongly in both infrared and Raman spectra in the region from 790 $cm^{-1}$ to 850 $cm^{-1}$.[6] For example, acetoxime have this vibration at 813 $cm^{-1}$ [7]. Therefore, 832 $cm^{-1}$($\nu_8$) can be assigned to a characteristic N-O stretching vibration, ($A_1$).

The authors wish to express their sincere thanks to Prof. S. Imanishi for his kind guidance and helpful suggestions. They are also indebted to Prof. S. Akiyoshi and Mr. T. Matsuda of the Engineering Department of this University for the free use of the Perkin-Elmer infrared spectrometer.

*Department of Chemistry,*
*Faculty of Science,*
*Kyushu University,*
*Fukuoka, Japan*

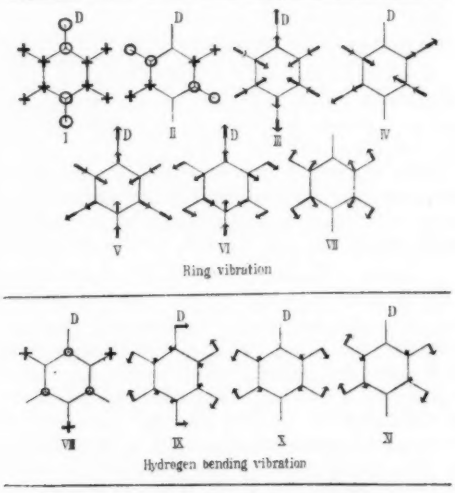


Fig. 1. Normal modes of vibrations of monodeuterobenzene (after C. K. Ingold, ref. 5).

Notes: (1) Vectors perpendicular to the plane of the ring are represented by + and ○.
(2) For each point-set ○ : ○ = ↑ : ↑ = 2 : 1.

6) See, for example, Landolt-Börnstein, "Atom u Molekularphysik," 2 Teil, Molekeln 1.

7) L. Kahovec and K.W.F. Kohlrausch, *Ber.*, 75, 627 and 1541 (1942).

# *Note on the Polymer-Mixed Solvent System. IV. Deviation from the Single Liquid Approximation in Osmotic, Viscometric and Swelling Measurements*

By Tōru KAWAI

(Received February 1, 1955)

## Introduction

In discussing the problems encountered in the treatment of the interaction of a polymer with a mixed solvent, the single liquid approximation is often used, assuming that the mixture of the two liquids behaves as a homogeneous liquid to the polymer. For the sake of its simplicity, the experimental results of osmotic pressure, viscosity, swelling ratio and other measurements for mixed solvents have been interpreted with considerable confidence by the terms usually employed in the binary system of a polymer and a liquid. In some polymer-mixed solvent systems, however, the deviation from the single liquid approximation cannot be ignored, due to selective adsorption. In the preceding paper[1], the relation between the liquid compositions in the two phases has been derived for the equilibrium between a mixed solvent and an isolated polymer molecule in solution. In this paper we shall apply this treatment to the equilibrium between a mixed solvent and a cross-linked polymer, or between a polymer-mixed solvent solution and a mixed solvent through a semi-permeable membrane, and shall investgate how the influence of the selective adsorption must be considered in osmotic, viscometric, and swelling measurements.

## Theoretical

In the two-phase systems, the thermodynamical condition for equilibrium requires that the partial molar free energy of each component (liquid 1 or liquid 2) be the same in both phases:

$$\Delta\bar{F}_1=\Delta\bar{F}_1' \tag{1a}$$

$$\Delta\bar{F}_2=\Delta\bar{F}_2' \tag{1b}$$

The partial molar free energies of the components in the binary phase of the two liquids may be written as[2]

$$\Delta F_1=\ln\theta_1+\theta_2\{1-(V_1/V_2)\}+(V_1/RT)A_{12}\theta_2^2 \tag{2a}$$

$$\Delta F_2=\ln\theta_2+\theta_1\{1-(V_2/V_1)\}+(V_2/RT)A_{12}\theta_1^2 \tag{2b}$$

where $\theta_1$ and $\theta_2$ are compositions (volume fractions), $V_1$ and $V_2$ molar volumes of the two liquids, and $A_{12}$ is a constant related to the heat interaction between the liquids 1 and 2.

For the ternary phase which consists of a cross-liked gel and the two liquids, Flory's expression for entropy change in swelling of a cross-linked gel in a single liquid may be applied to the present system in somewhat modified form. We may represent the entropy change associated with the swelling of a network of functionality $f$ formed from $\nu$ chains in a single liquid as the sum of two terms, the osmotic and elastic contributions, and according to Flory[3], may write,

$$\Delta S_{sw}=\Delta S_{osm}+\Delta S_{el} \tag{3a}$$

$$\Delta S_{osm}=-R\{n\ln(1-v_3)\} \tag{3b}$$

$$\Delta S_{el}=-R\{(3/2)\nu(v_3^{-2/3}-1)+(\nu/2)\ln v_3\} \tag{3c}$$

where $n$ is the number of solvent molecules and $v_3$, volume fraction of the polymer in the gel phase.

Since the effect of the segment size must be considered for the calculation of the entropy of dilution as in our previous treatments[1),4),5)], Eq. (3b) should be rewritten as

$$S_{osm}=-R[\{(n_1V_1+n_2V_2)/V_3\}\{\ln(1-v_3)+\mu_s' v_3\}] \tag{3b'}$$

for the present three component system, where $n_1$ and $n_2$ are the numbers of molecules of liquid 1 and liquid 2 respectively, $V_3$, molar volume of a polymer segment and $\mu_s'$ may be assumed to involve all the complicated factors except the effect of the segment size in the calculation of the entropy of dilution[5),6)]. Replacing $v_3$ in Eqs. (3b') and (3c)

1) T. Kawai, This Bulletin, 26, 6 (1953).

2) J. H. Hildebrand and R. L. Scott, "Solubility of Non-electrolytes", 3rd Ed. Reinfold Publishing Corp., New York (1950).

3) P. J. Flory, *J. Chem. Phys.*, 18, 108 (1950).

4) T. Kawai, This Bulletin, 25, 336 (1952); 25, 342 (1952).

5) T. Kawai, This Bulletin, 26, 409 (1953).

6) The parameter $\mu_s'$ differs from the entropy contribution $\mu_s$ in the customarily used parameter $\mu$, since the effect of segment size is not considered in the usual treatment of polymer solutions ($\mu_s'$ is the same with $f$ in reference 5).

by $Z\nu V_3/(n_1V_1+n_2V_2+Z\nu V_3)$ ($Z$ is the number of segments between the cross links) and differentiating the resultant expressions of Eqs. (3b′) and (3c) with respect to $n_1$ and $n_2$, the following equations are obtained,

$$\Delta\bar{S}_1=-R(V_1/V_3)[\ln(1-v_3)+\{1-(2/Zf)\}v_3+\mu_s'v_3^2+(1/Z)v_3^{1/3}] \quad (4a)$$

$$\Delta\bar{S}_2=-R(V_2/V_3)[\ln(1-v_3)+\{1-(2/Zf)\}v_3+\mu_s'v_3^2+(1/Z)v_3^{1/3}] \quad (4b)$$

Adding the terms for the mixing of the two liquids[4], and employing the expressions already given in the preceding paper [Eqs. (2a) and (2b) in the reference (4)] for the partial molar heat of mixing, the right hand sides of Eq. (1a) and (1b) are obtained, and then, combining them with Eqs. (2a) and (2b), Eqs. (1a) and (1b) may be written as follows,

$$\ln\theta_1+\{1-(V_1/V_2)\}\theta_2+(V_1/RT)A_{12}\theta_2^2=(V_1/V_3)[\ln(1-v_3')+\{1-(2/Zf)\}v_3'+\mu_s'v_3'^2+(1/Z)v_3'^{1/3}]+\ln\theta_1'+\{1-(V_1/V_2)\}\theta_2'+(V_1/RT)\{A_{12}v_2'^2+A_{13}v_3'^2+(A_{12}+A_{13}-A_{23})v_2'v_3'\} \quad (5a)$$

$$\ln\theta_2+\{1-(V_2/V_1)\}\theta_1+(V_2/RT)A_{12}\theta_1^2=(V_2/V_3)[\ln(1-v_3')+\{1-(2/Zf)\}v_3'+\mu_s'v_3'^2+(1/Z)v_3'^{1/3}]+\ln\theta_2'+\{1-(V_2/V_1)\}\theta_1'+(V_2RT)\{A_{12}v_1'^2+A_{23}v_3'^2+(A_{12}+A_{23}-A_{13})v_1'v_3'\} \quad (5b)$$

where the A's are the constants characteristic to each pair of the components (the gel phase being designated by a prime).

From Eqs. (5a) and (5b), there is easily obtained,

$$\ln(\theta_1/\theta_1')-(V_1/V_2)\ln(\theta_2/\theta_2')=(V_1/RT)[\{A_{13}-A_{23}-A_{12}(\theta_2'-\theta_1')\}v_3'+A_{12}\{(\theta_2'-\theta_1')-(\theta_2-\theta_1)\}] \quad (6)$$

If we write $\theta_1=\theta$, $\theta_1'=\theta+\Delta\theta$, $\theta_2=(1-\theta)$, and $\theta_2'=(1-\theta)-\Delta\theta$[7], Eq. (6) may be converted to the form,

$$(V_1/V_2)\ln\{1-(\Delta\theta/(1-\theta)\}-\ln\{1+(\Delta\theta/\theta)\}=-(V_1/V_2)\{\Delta\theta/(1-\theta)\}-(\Delta\theta/\theta)-(1/2)(V_1/V_2)\{\Delta\theta/(1-\theta)\}^2+(1/2)(\Delta\theta/\theta)^2-\cdots\fallingdotseq(V_1/RT)[\{A_{13}-A_{23}-A_{12}(1-2\theta-\Delta\theta)\}v_3'-2A_{12}(\Delta\theta)] \quad (7)$$

Hence, to a satisfactory approximation[8],

$$\Delta\theta\fallingdotseq-(1/RT)\{A_{13}-A_{23}-A_{12}(1-2\theta)\}v_3'/[\{(1/V_1\theta)+\{1/V_2(1-\theta)\}]-(A_{12}/RT)(2-v_3')\} \quad (8a)$$

And when

$$(1/V_1\theta)+\{1/V_2(1-\theta)\}\gg(A_{12}/RT)(2-v_3'),$$

$$\Delta\theta\fallingdotseq\{-\theta(1-\theta)/[(\theta/V_2)+\{(1-\theta)/V_1\}]\}(1/RT)\{A_{13}-A_{23}-A_{12}(1-2\theta)\}v_3' \quad (8b)$$

Since $\Delta\theta/\theta$ is assumed to be a measure of the magnitude of selective adsorption, Eq. (8) shows the relation between its magnitude and the compositions, molar volumes of the two liquids or the interaction parameters. The magnitude of the selective adsorption for various types of the polymer-mixed solvent systems was discussed in details in the preceding paper[1]. It must be noted, however, that the effect of molar volumes of the two liquids should be considered also. The smaller the values of both $V_1$ and $V_2$, the smaller the magnitude of the selective adsorption. As seen from Eq. (8), however, the smaller $V_2$ values of nonsolvents would be effective in solvent-rich compositions to make the above magnitude smaller, and vice versa.

Now, the $\mu^*$ values, which are customarily used to express the polymer-solvent interaction, are often calculated from the experiments of swelling of cross-linked polymers, even in mixed solvents, by the equation,

$$-\mu^*v_3'^2=\ln v_0'+v_3'+(V_0/ZV_3)v_3'^{1/3} \quad (9)$$

which Flory presented for the cross-linked polymer-single liquid (designated by 0) system[9]. (For mixed solvents, the "single liquid approximation", assuming that the mixture of the two solvents behaves as a homogeneous liquid, is widely used. Then, $v_0=v_1+v_2$, and $V_0=x_1V_1+x_2V_2$, where the $x$'s are mole fractions of the two liquids). Let us consider how the calculation of the $\mu^*$ values from this equation must be corrected for the cross-linked polymer-mixed solvent system, owing to the effect of the selective adsorption.

Since the terms involving the $\theta$'s in Eqs. (5a) and (5b) can be expressed as $(\Delta\theta/\theta)-1/2(\Delta\theta/\theta)^2+\cdots$ and $-(\Delta\theta/1-\theta)-1/2(\Delta\theta/1-\theta)^2\cdots$ respectively, multiplying Eq. (5a) by $\theta V_0/V_1$ and Eq. (5b) by $(1-\theta)V_0/V_2$, and adding the resultant two equations, there is obtained,

7) It must be noted that the ratio of volume fractions of the two liquids was expressed by $\theta$ in reference 1.

8) Since $\Delta\theta$ is supposed to be far smaller than $\theta$ or $(1-\theta)$ in usual cases, and the second terms in the expanded equations of the logarithmic terms in Eq. (7) are inclined to be canceled with each other, Eq. (8a) may afford a satisfactory approximation, unless $\theta$ or $(1-\theta)$ is extremely small. Further more, the last terms $(A_{12}/RT)(2-v_3')$ in Eq. (8a) can be ignored so long as $|(V_1/V_2)\theta_1+\theta_2|/\theta_1\theta_2>2A_{12}V_1/RT$. (this condition is usually satisfied except in the systems having extremely large values of $A_{12}$) as mentioned also in reference 1.

9) P.J. Flory, J. Rehner, Jr., *J. Chem. Phys.*, **11**, 512 (1943).

$$(V_0/V_3)[\ln(1-v_3')+\{1-(2/Zf)\}v_3'+\mu_s'v_3'^2+(1/Z)v_3'^{1/3}]=-(V_0/V_1)\theta\ln\{1+(\Delta\theta/\theta)\}-(V_0/V_2)(1-\theta)\ln\{1-(\Delta\theta/1-\theta)\}+\{(V_0/V_1)-(V_0/V_2)\}\Delta\theta-(A_{12}V_0/RT)(\Delta\theta)^2-(V_0/RT)\{A_{13}(\theta+\Delta\theta)+A_{23}(1-\theta-\Delta\theta)-A_{12}(\theta+\Delta\theta)(1-\theta-\Delta\theta)\}v_3'^2-(V_0/RT)\{\theta(1-\theta-\Delta\theta)-(1-\theta)(\theta+\Delta\theta)\}[A_{13}-A_{23}-A_{12}\{1-2(\theta+\Delta\theta)\}]v_3'$$
$$\fallingdotseq(V_0/2)[(1/V_1\theta)+\{1/V_2(1-\theta)\}](\Delta\theta)^2-(A_{12}V_0/RT)(1-2v_3'+v_3'^2)(\Delta\theta)^2-(V_0/RT)\{A_{13}\theta+A_{23}(1-\theta)-A_{12}\theta(1-\theta)\}v_3'^2+(V_0/RT)\{A_{13}-A_{23}-A_{12}(1-2\theta)\}v_3'(1-v_3')\Delta\theta \quad (10)^{10)}$$

Substituting the expression of Eq. (8a) for $\Delta\theta$ in Eq. (10), and combining Eq. (9) with (10),

$$\mu^*v_3'^2\fallingdotseq[1/2-(V_0/V_3)(1/2-\mu_s'+(V_0/RT)\{A_{13}\theta+A_{23}(1-\theta)-A_{12}\theta(1-\theta)\}]v_3'^2+[\{1-(V_0/V_3)\}\{(1/3)v_3'^3+(1/4)v_3'^4+\cdots\}-(2V_0/V_3Zf)v_3']+[\{1/(RT)^2\}\{A_{13}-A_{23}-A_{12}(1-2\theta)^2\theta(1-\theta)/\{(\theta/V_2)+(1-\theta)/V_1\}\{(\theta/V_1)+(1-\theta)/V_2\}]\times[1/2-v_3'+B\{1-4v_3'+(5/4)v_3'^2+\cdots\}+B^2\{2-12v_3'+(17/2v_3'^2)+\cdots\}+\cdots]v_3'^2 \quad (11)^{10)}$$

where, $B=(A_{12}/RT)/[(1/V_1\theta)+\{1/V_2(1-\theta)\}]$ ($B$ is very small in usual cases[8]). The last bracketed terms are due to the selective adsorption, and the first and second bracketed terms correspond to the expresion for a single liquid, which usually may be written,

$$\mu=\mu_s+(V_0RT)A_{30} \quad (12)$$

where $\mu_s$ is a correction factor, mentioned in reference (6). It is easily seen from Eq. (11) that Eq. (12) must be replaced by

$$\mu=1/2-(V_0/V_3)(1/2-\mu_s')+(V_0/RT)A_{30}-(2V_0/V_3Zf)v_3'^{-1}+\{1-(V_0/V_3)\}\{(1/3)v_3'+(1/4)v_3'^2+\cdots\}. \quad (13)$$

On this point, strictly speaking, lies an important source of inaccuracy in the customary calculation of the $\mu$ values from swelling measurements, which will be discussed in detail elsewhere (In extremely poor solvents, the dependency of $\mu$ upon $v_3'$ can not be ignored).

Actually, even for single liquids, the $\mu$ values determined from swelling measurements are often larger than those obtained from osmotic pressure measurements[11),12)], and the influence of the molar volume of the solvent must be considered when the solvent power of the solvent is estimated from the $\mu$ value thus obtained[5)].

For the present three-component system, however, we shall confine ourselves to the investigation of the effect of the selective adsorption, and assuming that all the complicated factors, such as those seen from Eq. (13), are involved in the term $\mu_s$ in Eq. (12), may write for the "single liquid approximation"[4),13)],

$$\mu^{**}=\mu_{13}\theta+\mu_{23}(1-\theta)-\mu_{12}\theta(1-\theta) \quad (14)$$

where $\mu_{13}=\mu_s+(V_0/RT)A_{13}$, $\mu_{23}=\mu_s+(V_0/RT)A_{23}$, and $\mu_{12}=(V_0/RT)A_{12}$[14)] (Eq. (14) corresponds to the expression in Part II[4)], which is a somewhat improved form of Scott's[13)]). Thus, Eq. (11) reduces to

$$\mu^*=\mu^{**}+[\{(1/RT)^2\}\{A_{13}-A_{23}-A_{12}(1-2\theta)\}^2\theta(1-\theta)/\{(\theta/V_2)+(1-\theta)/V_1\}\{(\theta/V_1)+(1-\theta)/V_2\}]\times[1/2-v_3'+B\{1-4v_3'+(5/4)v_3'^2+\cdots\}+B^2\{2-12v_3'+(17/2)v_3'^2+\cdots\}+\cdots] \quad (15).$$

It may be notable that, as seen in Eq. (15), $\mu^*$ always gives a larger value than that expected for its original meaning due to the selective adsorption ($1/2>v_3'$, except in the case of swelling in an extremely poor solvent i.e. in the nonsolvent-rich region). Moreover, its deviation increases, of course, with the magnitude of the selective adsorption (accordingly, with the content of the nonsolvent), but, decreases rapidly in the neighbourhood of pure nonsolvent.

Several attempts[15),16)] have been made to correlate intrinsic viscosities with the thermodynamic properties of the solution. The writer[4)] has developed the procedure of Flory[15)], who treated the interaction of an isolated polymer molecule with solvent as a

10) For the same reason as mentioned in reference (8), Eqs. (10) and (11) would give a satisfactory approximation.

11) T. Kawai, This Bulletin, 24, 69 (1951).

12) P. Doty, M. Brownstein, W. Schlener, *J. Phys. Colloid Chem.*, 53, 213 (1949).

13) R.S. Scott, *J. Chem. Phys.*, 17, 268 (1949).

14) Eq. (14) is merely a convenient representation of $\mu^{**}$ by employing $\mu_s$. And, strictly speaking, the parameter $\mu_{13}$, or $\mu_{23}$ employed here differs from that calculated from experiments in the polymer 3–single liquid 1 (or 2) system, also because $V_0$ is a function of $\theta$ (cf. Eqs. (16) and (17)).

15) P.J. Flory, *J. Chem. Phys.*, 17, 303 (1949).

16) T.G. Fox, Jr., P.J. Flory, *J. Am. Chem. Soc.*, 73, 1904; 1909; 1915 (1951)

swelling phenomenon, to the polymer-mixed solvent system, and formulated the relation between intrinsic viscosity and the parameter $\mu$ for the single liquid approximation. Now, we can apply the treatment developed in the preceding pages for the swelling of a cross-linked polymer in a mixed solvent to discuss the effect of the selective adsorption on intrinsic viscosities. In another treatment[5], which is developed in consideration of the effect of segment size, the writer pointed out a more satisfactory correspondence of the volume swelling ratio of polymer gels, or intrinsic viscosities of polymer solutions with the values of $(1/2-\mu)/V_0$ rather than with the $\mu$ values themselves. There[5], the parameter $\mu$ which has been usually interpreted in terms of Flory-Rehner's theory, was expresed by

$$\mu=1/2-(V_0/V_3)(1/2-\mu_s')+(V_0/RT)A_{30} \quad (16)$$

instead of Eq. (13)[17]. The last bracketed terms in the right hand side of Eq. (13) were ignored in Eq. (16), since this can afford a satisfactory approximation when the values of $v_3'$ is sufficiently small[18]. The similar approximation may be applied to the present problem on intrinsic viscosity, and we may write for the single liquid approximation,

$$\begin{aligned}\mu^{**}&=1/2-(V_0/V_3)(1/2-\mu_s')\\&+(V_0/RT)\{A_{13}\theta+A_{23}(1-\theta)\\&-A_{12}\theta(1-\theta)\}\end{aligned} \quad (17)$$

Considering the effect of the selective adsorption, the values of intrinsic viscosity in mixed solvents are expected to vary with

$$\begin{aligned}(1/2-\mu^*)/V_0&=(1/V_3)(1/2-\mu_s')\\&-(1/RT)\{A_{13}\theta+A_{23}(1-\theta)-A_{12}\theta(1-\theta)\}\\&-\{1/(RT)^2\}[\{A_{13}-A_{23}\\&-A_{12}(1-2\theta)\}^2\theta(1-\theta)/\{(\theta/V_2)\\&+(1-\theta)/V_1\}]\times[1/2-v_3'\\&+B\{1-4v_3'+(5/4)v_3'^2+\cdots\}\\&+B^2\{2-12v_3'+(17/2)v_3'^2+\cdots\}+\cdots]\end{aligned} \quad (18)$$

Finally, the treatment developed above will be applied to the interpretation of osmotic pressure in mixed solvents. The expressions for osmotic pressure $\pi$ in the present system were already derived by Gee[19], Scott[13] and Scatchard[20]. Here, the errors introduced by employing the "single liquid approximation" in the customary calculations of the $\mu$ values will be discussed. The condition for equilibrium between both sides of the membrane in an osmometer may be expressed thus:

$$\begin{aligned}&\ln\theta_1+\{1-(V_1/V_2)\}\theta_2+(V_1/RT)A_{12}\theta_2^2\\&=(V_1/V_3)[\ln(1-v_3')+\{1-(1/x)\}v_3'\\&+\mu_s'v_3'^2]+\ln\theta_1'+\{1-(V_1/V_2)\}\theta_2'\\&+(V_1/RT)\{A_{12}v_2'^2+A_{13}v_3'^2\\&+(A_{12}+A_{13}-A_{23})v_2'v_3'\}+(\pi V_1/RT),\end{aligned} \quad (19a)$$

$$\begin{aligned}&\ln\theta_2+\{1-(V_2/V_1)\}\theta_1+(V_2/RT)A_{12}\theta_1^2\\&=(V_2/V_3)[\ln(1-v_3')+\{1-(1/x)\}v_3'\\&+\mu_s'v_3'^2]+\ln\theta_2'+\{1-(V_2/V_1)\}\theta_1'\\&+(V_2/RT)\{A_{12}v_1'^2+A_{23}v_3'^2\\&+(A_{12}+A_{23}-A_{13})v_1'v_3'\}+(\pi V_2/RT),\end{aligned} \quad (19b)$$

where $x$ is the number of segments (number average) in a polymer molecule. Meanwhile, the $\mu$ values for mixed solvents have been usually calculated by

$$\begin{aligned}-\pi V_0&=RT[\ln(1-v_3')+\{1-(V_0/xV_3)\}v_3'\\&+\mu^*v_3'^2]\end{aligned} \quad (20)$$

Combining Eqs. (19a, b) and (20), an entirely analogous evaluation to the derivation of Eq. (11) leads to

$$\begin{aligned}\mu^*&=1/2-(V_0/V_3)(1/2-\mu_s')\\&+(V_0/RT)\{A_{12}\theta+A_{23}(1-\theta)-A_{12}\theta(1-\theta)\}\\&+[\{1/(RT)^2\}\{A_{13}-A_{23}\\&-A_{12}(1-2\theta)\}^2\theta(1-\theta)/\{(\theta/V_2)\\&+(1-\theta)/V_1\}\{(\theta/V_1)+(1-\theta)/V_2\}]\\&\times[1/2-v_3'+B\{1-4v_3'+(5/4)v_3'^2+\cdots\}\\&+B^2\{2-12v_3'+(17/2)v_3'^2+\cdots\}+\cdots]\end{aligned} \quad (21)$$

The last bracketed terms in Eq. (21) give the contribution of the selective adsorption and the other terms are equivalent to those obtained for the binary system of a polymer and a solvent in consideration of the effect of the segment size.

Applications of the above treatment will be given in the next paper to the osmotic, viscometric, and swelling data in a few polymer-mixed solvent systems.

After this paper had been read at the Special Meeting on High polymers, held by the Chemical Society of Japan, and the Society of High Polymer, Japan, at Tokyo University, on 31st Oct., 1953, Dr. Krigbaum sent me a copy of the manuscript of his paper, which was due to appear on J. Polymer Sci., He dealt with the composition

17) The complications, which arise from the last bracketed terms in Eq. (13) and from Flory's modification of his own original equation (cf. Eqs. (3c) and (9)), are avoided in Eq. (16), and this approximation is equivalent to assuming an equal $\mu$ value for both osmotic and swelling measurements.

18) When the $v_3'$ values are considerably large (i.e. $v_3'\rightarrow 0.1$), it may be suitable to express $\mu$ by Eq. (13) instead of Eq. (16). Actually, the validity of the approximate treatment (Eq. (16)) in reference 5 fails when it is applied to the swelling in extremely poor solvents.

19) G. Gee, *Trans. Faraday Soc.*, **40**, 463 (1944).

20) G. Scatchard, *J. Am. Chem. Soc.*, **68**, 2315 (1946).

relationship of the two phases in equilibrium between a polymer and a mixed solvent, and drew the conclusion similar to that of my preceding paper[1], except for the effect of the difference in molar volumes of the two liquids. Also this effect of molar volumes of the liquids had been involved in this treatment, although somewhat different results had been obtained because the effect of the segment size was considered in this treatment. A few points of difference between my treatment and Krigbaum's will be explained elsewhere, after an exchange of views with him.

*Laboratory of Textile Chemistry,*
*Tokyo Institute of Technology,*
*Tokyo*

---

# *Alkylalkoxypolysiloxanes. III.*[1] *Lower Members of Ethylmethoxypolysiloxanes with One to Six Silicon Atoms*

By Rokuro ŌKAWARA

(Received February 16, 1955)

In the preceding papers, ethylethoxypolysiloxanes[2] and ethylisopropoxypolysiloxanes[1] have been prepared and characterized. This paper will describe a series of lower members of linear ethylmethoxypolysiloxanes as indicated by formula (I).

$$L_n;\quad CH_3O\left[\begin{array}{c}C_2H_5\\|\\SiO\\|\\OCH_3\end{array}\right]_n CH_3,\quad n=1\sim6 \qquad (I)$$

As already described, the partially alcoholyzed ethyltrichlorosilane was easily polymerized by refluxing, liberating ethylalkoxypolysiloxanes. Thus ethylethoxy- and ethylisopropoxy- polysiloxanes have been prepared.

On the other hand, however, when the mixture of ethyltrichlorosilane and methanol in various mole ratios (1.6-2.5) was refluxed, the thermal reaction occurred with difficulty on prolonged refluxing. It was found that by the addition of sodium bicarbonate the condensation reaction occurred easily by evolving hydrogen chloride and carbon dioxide to the formation of polysiloxanes of the various polymer sizes.

$$C_2H_5Si(OCH_3)_xCl_{3-x}+\frac{(3-x)}{2}NaHCO_3$$
$$=C_2H_5Si(OCH_3)_xO_{\frac{3-x}{2}}+\frac{(3-x)}{2}NaCl$$
$$+\frac{(3-x)}{2}HCl+\frac{(3-x)}{2}CO_2 \qquad (1)$$

This reaction takes place even at room temperature until the mixture becomes chlorine-free and a slight excess of sodium bicarbonate calculated from the above formula has been required to produce chlorine-free polysiloxanes. Furthermore, the chlorine-free product, such as ethyltrimethoxysilane, does not easily react with sodium bicarbonate in a short period of time even at the refluxing temperature.

On fractional distillation, a small amount of methanol and the lower members of the series (I) ($L_n$) were obtained. The amounts of these polymers were varied with the chlorine content of the mixture. The distribution of the lower members of series (I) was plotted against the mole ratios $x$ of methanol to ethyltrichlorosilane, and the results are shown in Fig. 1. By redistilling these polymers, the presence of a small amount of cyclocompounds of the series (II) ($C_n$) was also found between the succeeding plateaus of the linear polymers ($L_n$),

$$C_n;\quad \left[\begin{array}{c}C_2H_5\\|\\SiO\\|\\OCH_3\end{array}\right]_n \qquad n=3\sim6 \qquad (II)$$

but they could not be accurately characterized. Analysis and physical properties of the linear polymers are given in Table II.

## Experimental

**Starting Materials.**—The ethyltrichlorosilane used in this experiment was prepared by the reaction of ethylchloride with copper-silicon and was purified by fractionation through a helices-

1) Part II of this series, R. Ōkawara and I. Ishimaru, This Bulletin, 27, 582 (1954).
2) R. Ōkawara, This Bulletin, 27, 428 (1954).

packed column of about 20 plates. The redistilled fraction having the boiling point 98°–99°C/760 mm Hg was taken as a starting material. Analysis of hydrolyzable chlorine was carried out by hydrolysis in water and titrating the liberated acid.

Anal. Calcd. for $C_2H_5SiCl_3$: Cl, 65.0 Found: Cl, 64.0.

**Preparation of Ethylmethoxypolysiloxanes**

**(a) Partial Methanolysis.** — Ethyltrichlorosilane was placed in a 300 cc. three-necked flask equipped with an efficient stirrer, a dropping funnel and a reflux condenser and was cooled with an ice bath. Methanol was added drop by drop with vigorous stirring. After the addition the temperature of the mixture was gradually raised to 40°–50°C. Then the mixture was replaced in a 100 cc. flask equipped with a reflux condenser and heated gradually to its boiling point. The constant refluxing mixture was obtained. The refluxing temperature and the weight of the mixture scarcely changed even after refluxing 30 hours. In this experiment, the constant refluxing mixture was heated on its refluxing temperature for a few additional hours in order to completely remove any trace of free hydrogen chloride which resulted in the methanolysis. The yield and the refluxing temperature were slightly different according to its composition as shown in Table I.

**(b) Reaction of the Partial Methanolysis Product with Sodium Bicarbonate.**—To this mixture sodium bicarbonate was added. Hydrogen chloride may also be produced by the reaction, so it is desirable that sodium bicarbonate is added differentially to partially methanolyzed product and the free hydrogen chloride formed is removed successively from the reaction system. Since sodium bicarbonate powder causes a violent reaction even at room temperature, 1–2 g. of sodium bicarbonate powder, or more conveniently tabletted powder, was added differentially to the ethylmethoxychlorosilane at room temperature and the mixture was gradually heated to its refluxing temperature in order to expel the free hydrogen chloride after carbon dioxide had ceased to evolve. Then the mixture was cooled to room temperature and the same treatment was repeated until the fuming chlorine compound could not be detected in the mixture. The sodium chloride formed was filtered off and the filtrate was again tested with the Beilstein test to assure that no trace of chlorine compound was present in the mixture.

The amounts of bicarbonate required to produce chlorine-free mixture are given in Table I. It was found that the yields of the polymer based on the amount of the starting materials were 75–85%.

To test whether the ethylmethoxypolysiloxanes react with sodium bicarbonate or not, redistilled ethyltrimethoxysilane (21 g.) mixed with powdered sodium bicarbonate (5 g.) was refluxed for 10 hours. The filtrate (16 g.) was composed of methanol (1 g.), unreacted ethyltrimethoxysilane (12 g.) and the residue (3 g.). This reaction did not proceed smoothly, but with violent bumping.

**Distillation of the Polymer.**—The polymer thus formed was rigorously fractionated through a semi-micro Stedman column of about 20 theoretical plates. Methanol which may be formed

TABLE I

RESULTS OF THE SODIUM BICARBONATE TREATMENT

| Exp. | Starting Materials A $C_2H_5SiCl_3$ g. (mole) | B $CH_3OH$ g. (mole) | $x$=B/A (mole ratio) | Ethylmethoxychlorosilane Refluxing Temp. °C | Yield g. | Yield %theory | Sodium Bicarbonate Added g. | Calcd. g. | Ethylmethoxypolysiloxane Yield g. | Yield %theory* |
|---|---|---|---|---|---|---|---|---|---|---|
| 1 | 54.5 (0.333) | 27 (0.85) | 2.54 | 123 | 47 | 92 | 7.3 | 6.0 | 39.5 | 85 |
| 2 | 54.5 (0.333) | 24 (0.75) | 2.25 | 119 | 47 | 92 | 12.3 | 9.7 | 34.0 | 77 |
| 3 | 81.7 (0.5) | 30.5 (0.95) | 1.9 | 118 | 73 | 94 | 27.0 | 21.8 | 48.5 | 78 |
| 4 | 81.7 (0.5) | 29 (0.9) | 1.82 | 116 | 75 | 96 | 26.5 | 24.0 | 48.0 | 78 |
| 5 | 81.7 (0.5) | 25.6 (0.8) | 1.6 | 115 | 74 | 95 | 30.1 | 27.8 | 44.0 | 75 |

* Based on the amount of the starting materials.

When an incompletely dehydrochlorinated mixture was used, the free hydrogen chloride which remained in the methanolysis product reacted with sodium bicarbonate added in the following step to liberate water, and the condensation reaction resulted in the formation of the highly polymerized product.

by the fission of Si-$OCH_3$ in the bicarbonate treatment, distilled out at first; and then monomer, dimer, trimer and tetramer fractions were obtained as the succeeding plateaus. The relation between the percentage composition of these fractions and the composition of the starting materials are shown in Fig. 1.

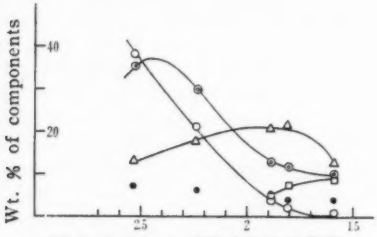


Mole ratio $x = CH_3OH/C_2H_5SiCl_3$

Fig. 1. Composition of the chlorine-free products obtained from sodium bicarbonate treatment.
● Methanol, ○ Monomer,
◎ Dimer, △ Trimer,
□ Tetramer.

Monomer, dimer and trimer fractions were redistilled through the same column and the refractive index was observed throughout the distillation. The middle portion of the plateau having the constant refractive index was taken for the sample. Data on these polymers are given in Table II.

Between the plateaus of dimer and linear trimer, at the boiling point of 69°C/0.5 mm Hg, a knick point on the distillation curve was found and the higher refractive index ($n_D^{20}$ 1.4100) at this point than the other portions was also found. From analogy with the preceding papers, the presence of the cyclotrimer may be supposed at this point, but as the amount of this portion was very small, the rigorous separation could not be attained.

As the amount of the tetramer fraction was small in each experiment, the residues of each experiment of Table I and the similar several runs (120 g.) were simply distilled and the fraction distilled out under 200°C/0.3 mm Hg was collected (80 g.). Since the still temperature was not over 240°C it may be supposed that the thermal rearrangement of the polysiloxane[3], which has been reported to begin at above 350°C, did not occur. This distillate was rigorously fractionated through the same semi-micro Stedman column. It was found from the silicon content that the separation of cyclotetramer and linear tetramer was fairly good, but with the polymer higher than this, the rigorous separation could not be attained.

To attain the rigorous separation, the distillation was again carried out through a high efficient semi-micro Stedman column (packed length 54 cm., inner diameter 1.1 cm., 60 theoretical plates, hold-up 3 cc. and pressure drop 2 mm Hg at the total reflux rate of 80 cc./hour). The results with regard to the polymers except monomer and dimer are shown in Fig. 2.

Comparing the distillation curve and the refrac-

3) W. Patnode and D.F. Wilcock, *J. Am. Chem. Soc.*, **68**, 358 (1946).

TABLE II

ETHYLMETHOXYPOLYSILOXANES: $CH_3O\left[\begin{matrix}C_2H_5\\|\\SiO\\|\\OCH_3\end{matrix}\right]_n CH_3$

| Polymer Size | Boiling Point °C/mm Hg | Density $d_4^{20}$ | Refractive Index $n_D^{20}$ | Molar Refraction Found (Calcd.)** | Molecular Weight Found*** (Calcd.) | % Si Found (Calcd.) |
|---|---|---|---|---|---|---|
| Series I: $L_n$ | | | | | | |
| Monomer* ($n$=1) | 124.3/760 | 0.9488 | 1.3838 | 37.02 (37.19) | — (150.3) | 18.66 (18.69) |
| Dimer ($n$=2) | 97/20 | 1.0071 | 1.3979 | 60.95 (61.22) | 252 (254.4) | 22.05 (22.08) |
| Trimer ($n$=3) | 90/0.5 | 1.0335 | 1.4045 | 84.93 (85.25) | 359 (358.6) | 23.48 (23.50) |
| Tetramer ($n$=4) | 125/0.3 | 1.0499 | 1.4094 | 109.07 (109.28) | 462 (462.8) | 24.29 (24.28) |
| Pentamer ($n$=5) | 150/0.3 | 1.0621 | 1.4140 | 133.40 (133.31) | 554 (567.0) | 24.79 (24.77) |
| Hexamer ($n$=6) | 170/0.3 | 1.0744 | 1.4180 | 157.43 (157.34) | — (671,2) | 25.29 (25.11) |

* A. Ladenburg, *Ann.*, **173**, 143 (1874): Ber., **5**, 1081 (1872) b.p. 126/760, $d^0$ 0.9747. J. Emeleus and S. R. Robinson, *J. Chem. Soc.*, **1947** 1592 b.p. 123.
** Calculated from bond refractivities by E. L. Warrick, *J. Am. Chem. Soc.*, **68**, 2455 (1946).
*** Cryoscopic measurements in benzene.

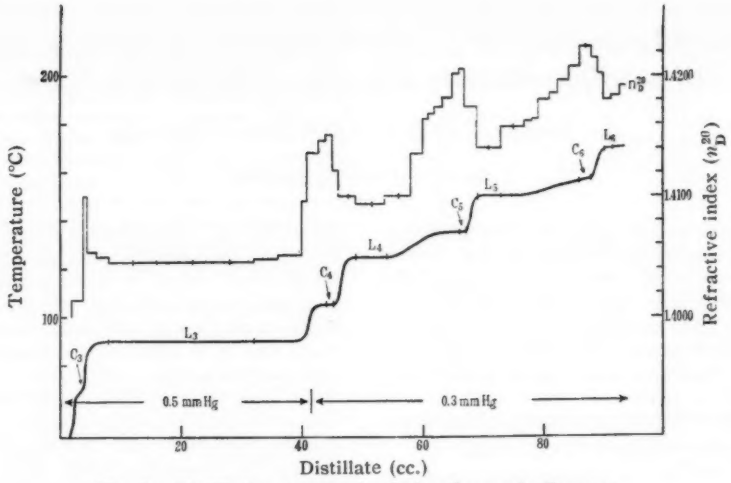


Fig. 2. Distillation curve of ethylmethoxypolysiloxanes.
$L_n$: Linear $n$-mer, $C_n$: Cyclo-$n$-mer

tive index of the distillate in Fig. 2, the plateaus of $L_3$, $C_4$, $L_4$, $C_5$, $L_5$, $C_6$ and $L_6$ were taken for the sample.

From the analytical data of $C_4$* and $C_5$* and from the analogy of a preceding paper[1], it was supposed that $C_n$ is the cyclocompound as indicated by formula (II), but the amount of these cyclocompounds is not enough to separate them from the neighbouring linear compounds. It was found in Fig. 2, that between the plateaus of linear trimer ($L_3$) and linear tetramer ($L_4$) there had appeared a plateau of cyclotetramer ($C_4$), having a higher refractive index than $L_3$ and $L_4$ and having a boiling point closer to $L_3$ than $L_4$. The similar relations may be seen with the other cyclocompounds.

**Analysis of Silicon.**—Monomer was weighed in gelatine capsule, the higher polymer were weighed in a platinum crucible and decomposed by concentrated sulfuric acid.

* Anal. Calcd. for $C_4$: Si, 26.96%. Found: Si, 25.31%.
Anal. Calcd. for $C_5$ (mol. wt. 521): Si, 26.96%.
Found: Si, 25.92% (mol. wt. 490, in benzene).


## Summary

(1) Ethylmethoxypolysiloxanes have been prepared by the reaction of sodium bicarbonate with partially methanolyzed ethyltrichlorosilane.

(2) Distribution of the lower polymers was determined with regard to the composition of the partially methanolyzed product.

(3) Linear ethylmethoxypolysiloxanes containing from one to six silicon atoms have been prepared and characterized.

(4) Ethylmethoxycyclopolysiloxanes containing from three to six silicon atoms have been found, but they could not be accurately characterized.


The author wishes to express his hearty thanks to Mr. H. Osawa for his assistance in this investigation.

*Department of Applied Chemistry,*
*Faculty of Engineering, Osaka*
*University, Osaka*

# *Alkylalkoxypolysiloxanes. IV.*[1] *Lower Members of Methoxy End-blocked Dimethylpolysiloxanes with One to Six Silicon Atoms*

By Toshio TANAKA and Rokuro ŌKAWARA

(Received February 16, 1955)

In the preceding paper[1] ethylmethoxypolysiloxanes were synthesized by the condensation reaction of partially methanolyzed ethyltrichlorosilane using sodium bicarbonate. Here, the condensation reaction with sodium bicarbonate has been applied to partially methanolyzed dimethyldichlorosilane, and a series of lower members of methoxy end-blocked dimethylpolysiloxanes has been prepared as indicated below:

$$CH_3O\left[\begin{array}{c}CH_3\\|\\SiO\\|\\CH_3\end{array}\right]_n CH_3, \quad n=1\sim6.$$

Of these compounds the first member, dimethyldimethoxysilane ($n=1$), was previously obtained by Simpson[2] and by Kantor[3], but the boiling point only was reported.

Condensation reaction by the use of sodium bicarbonate is shown stoichiometrically in the following expression:

$$(CH_3)_2Si(OCH_3)_xCl_{2-x}+\frac{2-x}{2}NaHCO_3$$

$$\rightarrow (CH_3)_2Si(OCH_3)_xO_{\frac{2-x}{2}}+\frac{2-x}{2}NaCl$$

$$+\frac{2-x}{2}HCl+\frac{2-x}{2}CO_2$$

Just like the ethylmethoxychlorosilane described in the preceding paper[1] this reaction takes place even at room temperature and a slight excess of the amount of sodium bicarbonate calculated from the above formula has been required to produce chlorine-free polysiloxanes.

On fractional distillation of the condensation product, azeotropic mixture of dimethyldimethoxysilane and methanol, a small amount of methanol, and then the lower members of this series were obtained. The distribution of these distillates, varying with the mole ratio (0.9~1.7) of methanol to dimethyldichlosilane, was plotted against the mole ratios, and the results are shown in Fig. 1. By redistilling these polymers, the presence of a small amount of cyclo-compounds, $[(CH_3)_2SiO]_n$, was found between the succeeding plateaus of the linear compounds from the measurements of refractive index, but the cyclo-compounds have been too small in quantity to be characterized. Physical constants on these linear compounds were determined, and are shown in Table II together with the analytical data.

## Experimental

**Starting materials.** — Dimethyldichlorosilane used in these experiments were supplied from

TABLE I

| Exp. No. | Starting Material A $(CH_3)_2SiCl_2$ g. (mole) | Starting Material B $CH_3OH$ g. (mole) | $x$=B/A (mole ratio) | Dimethylmethoxychlorosilane Yield g. | Dimethylmethoxychlorosilane Yield % theory | Sodium Bicarbonate Calcd. g. | Sodium Bicarbonate Added g. | Methoxy End-blocked dimethylpolysiloxane Yield g. | Methoxy End-blocked dimethylpolysiloxane Yield % theory* |
|---|---|---|---|---|---|---|---|---|---|
| 1 | 64.5 (0.5) | 27.0 (0.84) | 1.68 | 52 | 87 | 5.6 | 7.0 | 40 | 73 |
| 2 | 64.5 (0.5) | 24.0 (0.75) | 1.50 | 53 | 87 | 9.1 | 10.5 | 39 | 74 |
| 3 | 65 (0.5) | 21.0 (0.66) | 1.31 | 51 | 83 | 12.0 | 13.0 | 38 | 74 |
| 4 | 129 (1.0) | 38.5 (1.20) | 1.20 | 105 | 85 | 28.6 | 31.0 | 73 | 74 |
| 5 | 65 (0.5) | 17.5 (0.55) | 1.10 | 54 | 86 | 16.8 | 20.5 | 37 | 76 |
| 6 | 65 (0.5) | 14.5 (0.45) | 0.90 | 56 | 88 | 20.5 | 22.5 | 34 | 72 |

* Based on the amounts of the starting materials.

1) Part III of this series, R. Ōkawara, This Bulletin, 28, 360 (1955).

2) P.W. Simpson, Brit. Patent, 635, 726 (April 12, 1950).

3) S.W. Kantor, *J. Am. Chem. Soc.*, 75, 2712 (1953).

the Shin-etsu Chem. Ind. Co. Analysis of hydrolizable chlorine was carried out by hydrolysis in water and titrating the liberated acid. Calcd. for $(CH_3)_2SiCl_2$: Cl, 54.9%. Found: Cl, 54.9%.

**Preparation of Methoxy End-blocked Dimethylpolysiloxanes.**—Partial methanolysis of dimethyldichlorosilane and the treatment by sodium bicarbonate were carried out as described in the preceding paper[1]. Before the treatment by sodium bicarbonate, the partially methanolyzed product was heated on its refluxing temperature (60°~65°C) for six to eight hours in order to remove free hydrogen chloride which resulted in the methanolysis.

The amounts of sodium bicarbonate required to obtain the chlorine-free product are given in Table I.

It was found that the yields of the products based on the amount of starting materials were 72~76%.

**Distillation of the Product.**—The products obtained in this manner were rigorously fractionated through a semi-micro Stedman column of about 20 theoretical plates. The azeotropic mixture of monomer and methanol was distilled out at first, and methanol which may be formed by the fission of Si-$OCH_3$, then monomer and dimer fractions, etc., were obtained as the succeeding plateaus. This azeotrope (b.p. 62°C, $n_D^{20}$ 1.3532) was broken with *n*-hexane to give the methanol-*n*-hexane azeotrope (b.p. 49°C). The composition was determined to be 53% dimethyldimethoxysilane and 47% methanol from the above distillation with *n*-hexane and the measurements of refractive index of the mixture of dimethyldimethoxysilane[4] and methanol in various ratios.

The relation between the percentage of each fraction and the mole ratio of the starting materials is shown in Fig. 1.

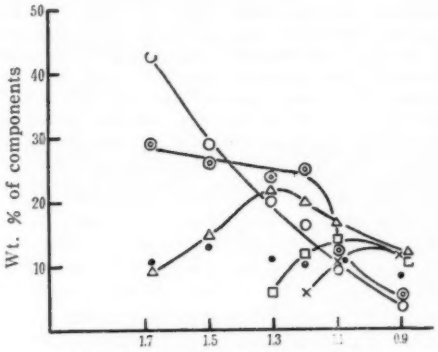


Mole ratio $x = CH_3OH/(CH_3)_2SiCl_2$

Fig. 1. Composition of the chlorine-free products obtained from sodium bicarbonate treatment.

● Methanol ○ Monomer
◎ Dimer △ Trimer
□ Tetramer × Pentamer

Here, the amounts of azeotrope were assigned to each component, and the middle fractions between two plateaus were also assigned to both side fractions.

Monomer[5], dimer and trimer fractions in each run were collected, respectively, and redistilled through the same column. The portions of each plateau having the constant refractive index were

4) This sample was obtained by the redistillation of monomer fraction, and the data are given in Table II.

5) Monomer fraction was found in the case of mole ratios 1.2~1.7.

TABLE II

METHOXY END-BLOCKED DIMETHYLPOLYSILOXANES: $CH_3O\left[\begin{matrix}CH_3\\|\\SiO\\|\\CH_3\end{matrix}\right]_n CH_3$

| Polymer Size | Boiling Point °C/mmHg | Density $d_4^{20}$ | Refractive Index $n_D^{20}$ | Molecular Weight Found[b] (Calcd.) | Molar Refraction Found (Calcd.)[c] | % Si Found (Calcd.) |
|---|---|---|---|---|---|---|
| Monomer ($n$=1) | 82/760[a] | 0.8646 | 1.3708 | — (120.2) | 31.51 (31.80) | 23.34 (23.36) |
| Dimer ($n$=2) | 139/760 | 0.9048 | 1.3835 | 195 (194.4) | 50.17 (50.44) | 28.83 (28.90) |
| Trimer ($n$=3) | 83/24 | 0.9241 | 1.3892 | 271 (268.5) | 68.67 (69.08) | 31.42 (31.38) |
| Tetramer ($n$=4) | 90/5 | 0.9346 | 1.3923 | 345 (342.7) | 87.37 (87.72) | 32.83 (32.79) |
| Pentamer ($n$=5) | 89/0.5 | 0.9424 | 1.3950 | 415 (416.9) | 106.06 (106.36) | 33.64 (33.69) |
| Hexamer ($n$=6) | 104/0.5 | 0.9470 | 1.3972 | 484 (491.0) | 124.91 (125.00) | 34.34 (34.32) |
| Heptamer ($n$=7) | 116/0.5 | 0.9492 | 1.4007 | — (565.2) | 144.57 (143.64) | — — |

a) b.p., 81.7°~82.2°C[2]; 80°~80.5°C[3].
b) Cryoscopic measurements in benzene.
c) Calculated from bond refractivities by E. W. Warrick, *J. Am. Chem. Soc.*, **68**, 2455 (1946).

used for the measurements of the physical constants and analysis. Data on these materials are given in Table II.

As the amounts of higher members than tetramer fraction were small in each run, the rigorous separation may not have been attained by the above distillation. Accordingly all of these fractions were collected together, then the distillation was again carried out through a high efficient semi-micro Stedman column (about 60 theoretical plates) as described in the preceding paper[1] and the refractive index was observed throughout the distillation. The results are shown in Fig. 2.

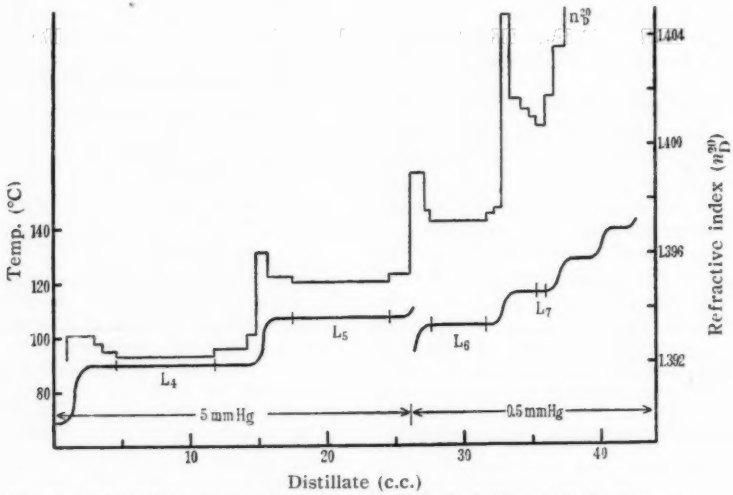


Fig. 2. Distillation curve of methoxy end-blocked dimethylpolysiloxanes.
$L_n$: Linear $n$-mer

Between the neighbouring plateaus, refractive index higher than that of the both side plateaus was found. From analogy with the preceding paper[1], the presence of the cyclo-compounds may be supposed. Comparing the distillation curve and the refractive index of the distillate in Fig. 2, the plateaus of $L_4$, $L_5$ and $L_6$ were taken as samples. Data on these polymers are also given in Table II. Judging from the refractive index, the members higher than heptamer may not have been separated from cyclo-compounds in this experiment. This fact has been ascertained by comparing the observed and calculated values of the molar refraction for the heptamer as shown in Table II.

**Analysis of Silicon.**—Silicon in these samples could not be determined by the usual digestion method with concentrated sulfuric acid, so the method using a gelatine capsule with concentrated sulfuric acid was developed. The analytical procedure, which will be soon published in detail, is as follows: 0.2 to 0.5 g. of sample weighed in a size 0 or 1 gelatine capsule was placed in a platinum crucible and the full amount of concentrated sulfuric acid to cover the capsule was added. At this time, the capsule floating on the sulfuric acid was pushed to the bottom of the platinum crucible by pressing it down with a glass rod, and it was left alone there at the room temperature. After two or three hours, the sulfuric acid decomposed the gelatine capsule and was mixed with the sample. This mixture in the covered crucible was heated with a small flame until a brown color appeared, then the acid was evaporated and the carbon was burned off using a low flame. The white residue was then ignited and weighed as silica.

**Summary**

(1) Methoxy end-blocked dimethylpolysiloxanes have been prepared by the reaction of sodium bicarbonate with partially methanolyzed dimethyldichlorosilane.

(2) Distribution of the lower polymers was determined in regard to the composition of the partially methanolyzed dimethyldichlorosilane.

(3) Methoxy end-blocked dimethylpolysiloxanes from monomer (dimethyldimethoxysilane) to hexamer have been characterized.

*Department of Applied Chemistry,*
*Faculty of Engineering,*
*Osaka University,*
*Osaka*

# *Alkylalkoxypolysiloxanes. V.*[1] *Lower Members of Vinylmethoxypolysiloxanes with One to Five Silicon Atoms*

By Rokuro Ōkawara and Minoru Sakiyama

(Received February 16, 1955)

Recently, some data on vinylalkoxy-silanes and -disiloxanes[2] were presented, but no data on higher vinylalkoxypolysiloxanes have been reported. We wish now to report on the preparation and properties of vinylmethoxypolysiloxanes indicated by formula (I).

$$L_n;\ CH_3O\left[\begin{array}{c} HC=CH_2 \\ | \\ SiO \\ | \\ OCH_3 \end{array}\right]_n CH_3,\ (n=1\sim5)\quad (I)$$

For the preparation of the polymers, the method was used which is similar to that in the case of preparing ethylmethoxypolysiloxanes[3] and methoxy end-blocked dimethylpolysiloxanes.[1] Sodium bicarbonate was added to the partially methanolyzed vinyltrichlorosilane, which was prepared by mixing 1 mole of vinyltrichlorosilane and $x$ moles ($x$=1.6–2.6) of methanol. The liberated chlorine-free product was fractionated at as low a temperature as possible under reduced pressure to avoid the thermal polymerization of vinyl radical. A small amount of methanol was distilled out at first; then the lower members of the series (I) were obtained. The percentage composition of the lower members were plotted against the mole ratios $x$, and the results are shown in Fig. 1.

Monomer and dimer fractions were redistilled, respectively. The higher polymers were obtained from the residue of each experiment. To avoid the polymerization, the residue was rapidly distilled out at a pressure of 1 mm Hg until the stil-pot temperature reaches 220°C. The distillate thus obtained was rigorously fractionated through a high efficient column. Properties of the linear polymer are given in Table II. During the course of this fractionation, a long peroid of heating at high temperature (until 200°C/1 mm Hg) were required, but any polymeric changes such as gellation were not observed. The appearance of cyclo-compounds as indicated by formula (II) were also observed between the plateaus of the linear compounds, as in the case of preceding papers [1,3] but they could not be accurately characterized.

$$C_n;\quad \left[\begin{array}{c} HC=CH_2 \\ | \\ SiO \\ | \\ OCH_3 \end{array}\right]_n \quad (n=4 \text{ and } 5)\quad (II)$$

## Experimental

**Starting Material.**—Vinyltrichlorosilane was presented from Linde Air Products Company.

### Preparation of Vinylmethoxypolysiloxanes

**(a) Partial Methanolysis and Polymerization with Sodium Bicarbonate.**—In this experiment, a procedure similar to that already described[1),3)] was used. To complete the reaction,

1) Part IV of this series, T. Tanaka and R. Ōkawara, This Bulletin, 28, 364 (1955).
2) R. Nagel and H.W. Post, *J. Org. Chem.*, 17, 1382 (1952); R. Nagel, C. Tamborski and H.W. Post, ibid., 16, 1768 (1951).
3) R. Ōkawara, This Bulletin, 28, 360 (1955).

TABLE I

| | Starting Material | | | Vinylmethoxychlorosilane | | | | Sodium Bicarbonate | | Vinylmethoxypolysiloxane | |
|---|---|---|---|---|---|---|---|---|---|---|---|
| | A $CH_2=CHSiCl_3$ | B $CH_3OH$ | $x$=B/A | Refluxing Temp. | Cl | Yield | | Added | Calcd*. | Yield | |
| | g. | g. | mole ratio | °C | % | Found g. | %theory % | g. | g. | Found g. | %theory** % |
| 1 | 40.4 | 20.9 | 2.6 | 122 | 4.5 | 35.5 | 94.7 | 2.7 | 2.5 | 28.5 | 82 |
| 2 | 40.4 | 18.4 | 2.3 | 122 | 12.3 | 35.0 | 92.5 | 5.5 | 5.0 | 27.0 | 82 |
| 3 | 80.8 | 32.0 | 2.0 | 122 | 20.0 | 70.0 | 91.7 | 17.8 | 17.5 | 45.0 | 73 |
| 4 | 40.4 | 15.2 | 1.9 | 123 | 16.0 | 34.0 | 88.8 | 7.9 | 7.4 | 21.0 | 68 |
| 5 | 80.8 | 28.8 | 1.8 | 121 | 23.5 | 71.0 | 92.4 | 20.0 | 19.5 | 43.0 | 71 |
| 6 | 40.4 | 12.8 | 1.6 | 120 | 22.0 | 34.0 | 88.1 | 10.5 | 10.0 | 12.0 | 42 |

* 1 Mol. of sodium bicarbonate was assumed to be equivalent to 2 g.-atoms of Cl contained in the chlorosilane mixture.

** Based on the amount of the starting materials.

TABLE II

VINYLMETHOXYPOLYSILOXANES: $CH_3O\left(\begin{array}{l}CH=CH_2\\|\\SiO\\|\\OCH_3\end{array}\right)_n CH_3$

| Polymer Size | Boiling Point °C/mm Hg | Density $d_4^{20}$ | Refractive Index $n_D^{20}$ | Molecular Weiget Found* (Calcd.) | Molar Refraction Found (Calcd.)** | % Si Found (Calcd.) |
|---|---|---|---|---|---|---|
| Monomer ($n=1$)a) | 122/760 | 0.9700 | 1.3930 | — (148.24) | 36.48 (36.72) | 18.85 (18.95) |
| Dimer ($n=2$)b) | 86/11 | 1.0361 | 1.4107 | 248 (250.40) | 59.97 (60.28) | 22.55 (22.44) |
| Trimer ($n=3$) | 81/0.8 | 1.0636 | 1.4192 | 354 (352.57) | 83.74 (83.84) | 23.94 (23.90) |
| Tetramer ($n=4$) | 109/0.3 | 1.0784 | 1.4230 | 448 (454.73) | 107.36 (107.40) | 24.67 (24.71) |
| Pentamer ($n=5$) | 135/0.3 | — | 1.4284 | — (556.91) | — (130.96) | 24.94 (25.22) |

a) R. Nagel, C. Tamborski and H. W. Post, loc. cit b.p. 52.9/46, 59.5/62, $d_4^{25}$ 0.9669, $n_D^{25}$ 1.3910 and $MR_D$ 36.42.

b) R. Nagel, C. Tamborski and H. W. Post, ibid. b.p. 120–20.6/46, $d_4^{25}$ 1.0627, $n_D^{25}$ 1.4172 and $MR_D$ 59.28.

* Cryoscopic measurements in benzene.

** Calculated from bond refractivities by E. L. Warrick, *J. Am. Chem. Soc.*, **68**, 2455 (1946).

the partially methanolyzed product was refluxed for 8–10 hours. The results are summarized in Table I.

The distribution of the lower polymers in the product was determined by fractionation through a semi-micro Stedman column of about 30 theoretical plates. The results are shown in Fig. 1.

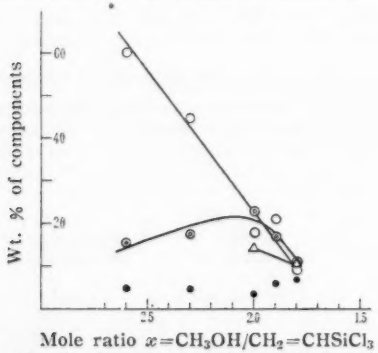


Mole ratio $x=CH_3OH/CH_2=CHSiCl_3$

Fig. 1. Composition of the chlorine-free products obtained from sodium bicarbonate treatment.

● Methanol, ○ Monomer,
◎ Dimer, △ Trimer.

The product of Exp. 6 was a slightly viscous liquid and the composition could not be determined by fractionation, because the gellation occurred at 180°C/15 mm Hg in the stil-pot.

**(b) Redistillation of the Polysiloxanes.**— Monomer and dimer fractions were redistilled through the same column and the portions having the constant boiling point and refractive index were analyzed. The residues of Exp. 1–5 were simply distilled by a Claisen flask under 1 mm Hg until the stil-pot temperature reaches 220°C. The product distilled out below 170°C (40 g.) was fractionated rigorously through a high efficient semi-micro Stedman column of about 60 theoretical plates. The refractive index and the silicon content of the distillate are shown in Fig. 2.

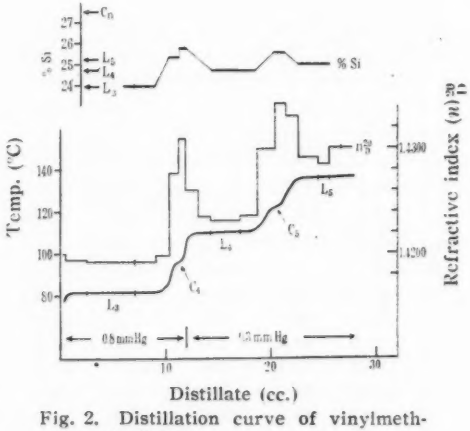


Fig. 2. Distillation curve of vinylmethoxypolysiloxanes.

$L_n$: Linear $n$-mer,
$C_n$: Cyclo-$n$-mer

The plateaus $L_3$, $L_4$ and $L_5$ were those of linear trimer, tetramer and pentamer, respectively. Between these plateaus the portions, $C_4$ and $C_5$, having a higher refractive index and a higher silicon content than the neighbouring portions were found.

From the silicon content and from the analogy of the preceding papers, $C_4$ and $C_5$ may be seen to be impure cyclotetramer and cyclopentamer respectively, indicated by formula (II). A slightly higher value of refractive index in front of the plateau of linear trimer was found in this experiment, but it may not be enough to suppose the presence of cyclotrimer.

**Analysis of Silicon.**—Monomer and dimer were weighed in gelatine capsule[1]; the higher polymers were weighed in a platinum crucible and decomposed by concentrated sulfuric acid.

## Summary

(1) Vinylmethoxypolysiloxanes have been prepared by the reaction of sodium bicarbonate with partially methanolyzed vinyltrichlorosilane.

(2) Distribution of the lower members was determined with regard to the composition of the partially methanolyzed product.

(3) Linear vinylmethoxypolysiloxanes containing from one to five silicon atoms have been prepared and characterized.

(4) Vinylmethoxycyclopolysiloxanes were found between the plateaus of linear polymer but they could not be accurately characterized.

The authors wish to express their hearty thanks to Mr. C. O. Strother of Linde Air Products Company for presenting them with vinyltrichlorosilane.

*Department of Applied Chemistry, Faculty of Engineering. Osaka University, Osaka*

---

# *Hyperconjugation. I. General Theory and Its Applications to Simple LCAO MO Calculations*

By Yasumasa I'HAYA

(Received March 16, 1955)

## I. Introduction[#]

It has been noticed by several writers that the alkyl group may have the power to conjugate with other resonating systems. In 1935, Baker and Nathan[1] introduced the concept later called hyperconjugation in order to explain the abnormal reaction rates of alkyl-substituted compounds. After that, the large increases in dipole moments of alkyl-substituted compounds were attributed by several authors[2-6] to a charge migration from the alkyl radical to the attached resonating systems. On the other hand, it has been found[7-9] that the length of the C-Me bond in such systems is less than the normal C-C bond length of 1.54Å. In 1939, Mulliken[10] has given a theoretical explanation on the basis of hyperconjugation to the red shifts of spectra and increases in the exaltation of molecular refractivity in alkylsubstituted resonating systems. Concerning the heats of hydrogenation of hyperconjugated systems, several investigations[11,13] have been published; for instance, Cullis, Hinshelwood and Mulcahy[12] state that the phenomenon of hyperconjugation seems to be significant in the oxidation of hydrocarbons.

[#] For reviews on experimental aspects, see C.L. Deasy, *Chem. Revs.*, **36**, 145 (1945), and more recently, V.A. Crawford, *Quart. Revs.*, **3**, 226 (1949).

1) J.W. Baker and W.S. Nathan, *J. Chem. Soc.*, 1840, 1844 (1935).
2) J.W. Baker and L.G. Groves, *J. Chem. Soc.*, 1144 (1939).
3) J.W. Baker, *J. Chem. Soc.*, 1150 (1939).
4) Mariott, Hobbs and Gross, *J. Am. Chem. Soc.*, **63**, 659 (1941).
5) H.C. Hurdis and C.P. Smyth, *J. Am. Chem. Soc.*, **64**, 2829 (1942).
6) H.C. Hurdis and C.P. Smyth, *J. Am. Chem. Soc.*, **65**, 89 (1943).
7) G. Herzberg, F. Patat and H. Verleger, *J. Phys. Chem.*, **41**, 123 (1937).
8) L. Pauling, H.D. Springall and K.J. Palmer, *J. Am. Chem. Soc.*, **61**, 927 (1939).
9) D.P. Stevenson, H.D. Burham and V. Schomaker, *J. Am. Chem. Soc.*, **61**, 2922 (1939).
10) R.S. Mulliken, *J. Chem. Phys.*, **7**, 121, 339, 356 (1939).
11) J.B. Conant and G.B. Kistiakowsky, *Chem. Revs.*, **20**, 181 (1937).
12) C. F. Cullis, C. N. Hinshelwood and M. F. R. Mulcahy, *Proc. Roy. Soc.* (London), **A196**, 160 (1949).

Mulliken, Rieke and Brown[13] give a description of an application of the molecular orbital method to the computation of hyperconjugation energies and bond orders in methylated hydrocarbon molecules. Explanations were given for the observed shortening of C-Me bonds and decrease in heats of hydrogenation in hyperconjugated molecules. They estimated an empirical exchange integral for C-$H_3$ bond, but assumed a coulomb integral for $H_3$ to be the same as for carbon atoms in a conjugated hydrocarbon. Thus, their new interpretations involve some bold assumptions, nevertheless their work seems to be very successful. Sklar[14] has computed the extent of migration of an electron from the methyl radical into the benzene ring by the method of antisymmetrized molecular orbitals, and obtained results which were in agreement with the experimental data. Roberts and Skinner[15] discussed the dissociation energies of carbon bonds in hydrocarbon radicals in terms of hyperconjugation

Herzfeld[16] and Matsen[17] independently discussed the effect of the migration of an electron from the substituent in the ring on the red shift and intensity of spectra; however they treat the methyl radical not as $-C\equiv H_3$ but as one group. More recently, Coulson and Crawford[18,19] have computed the hyperconjugation energies, charge distributions and red shifts in the spectra in methyl-substituted ethylenes and benzenes using the MO method.

Thus, although considerable work has been done in recent years in discussing hyperconjugation[20], no attempt has been made to compute the electronic structures of either methyl- or ethyl-substituted molecules with the common parameters. In this series, the effect of hyperconjugation is discussed in ethyl-substituted $\pi$-electron systems as well as in methyl-substituted ones using the LCAO MO method with common numerical parameters determined from the experimental aspects.

13) R.S. Mulliken, C.A. Rieke and W.G. Brown, *J. Am. Chem. Soc.*, 63, 41 (1941).

14) A.L. Sklar, *J. Chem. Phys.*, 7, 184 (1939).

15) J.S. Roberts and H.A. Skinner, *Trans. Faraday Soc.*, 45, 339 (1949).

16) K.F. Herzfeld, *Chem. Revs.*, 41, 233 (1947).

17) F.A. Matsen, *J. Am. Chem. Soc.*, 72, 5243 (1950).

18) C.A. Coulson and V.A. Crawford, *J. Chem. Soc.*, 2052 (1953).

19) V.A. Crawford, *J. Chem. Soc.*, 2058, 2061 (1953).

20) More interesting calculations concerning aromatic carbonium ions have recently been made; (a) E. Heilbronner and M. Simonetta, *Helv. Chim. Acta*, 35, 1049 (1952), (b) N. Muller, L.W. Pickett and R.S. Mulliken, *J. Am. Chem. Soc.*, 76, 4770 (1954).

## II. General Theory of Hyperconjugation*

From the MO view point, the methyl group should have orbitals of $\pi$-character in order to conjugate with the $\pi$-orbitals of the resonating systems; namely it should have a structure of $-C\equiv H_3$. Now if the hydrogen atoms with 1s AO's $\psi_a$, $\psi_b$, $\psi_c$, ($\psi_a$ in yz plane) are called $H_a$, $H_b$, $H_c$, respectively, then we may form the following group orbitals with approximate contours (z-axis perpendicular to the paper) shown in Fig. 1‡.

$$\begin{aligned} \phi_s &= (\psi_a+\psi_b+\psi_c)/(3+6S)^{1/2} && \sigma\text{-type} \\ \phi_y &= (2\psi_a-\psi_b-\psi_c)/(6-6S)^{1/2} && \pi_y\text{-type} \\ \phi_x &= (\psi_b-\psi_c)/(2-2S)^{1/2} && \pi_x\text{-type} \end{aligned} \qquad (1)$$

where $S$ is the overlap integral between hydrogen atoms. The MO's such as $\phi_x$ and $\phi_y$ of Eq. (1), which may be called quasi-x and quasi-y MO's following Mulliken, are strictly equal in energy. Thus, in general, hyperconjugation is a two dimensional affair, namely in methylacetylene we have both x- and y- hyperconjugations, but in toluene we may have only one species of hyperconjugation for the reason that the other type of hyperconjugation perpendicular to the above one may be assumed to make no more contribution to the resonance energy for double bond than is present for simple unsaturated molecules like methylacetylene itself.

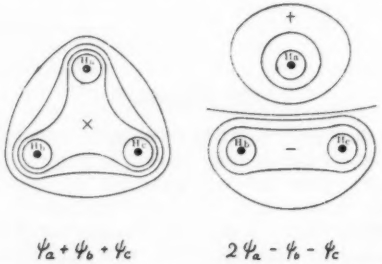


Fig. 1. $\sigma$ and $\pi_y$ group orbitals in methyl group.

Besides the $\pi$-character of the $-C\equiv H_3$ group, in ethylacetylene and ethylbenzene the quasi double bond between C and $H_2$ involves one $\sigma$-bond and one $\pi$-bond with the following quasi MO's:

* The interpretation of hyperconjugation is a little different according to molecular orbital or valence bond descriptions. See, C. A. Coulson, "Valence", Oxford Univ. Press (1951), p. 310.

‡ This figure is reproduced from Professor Coulson's "Valence" with his kind permission.

21) The hyperconjugative effect may be accompanied with the inductive effect, as the former always causes polarities in various bonds to some extent. In this paper, however, the inductive effect except for next neighboring carbon atom is ignored because the hyperconjugative effect is to be chiefly dealt with.

$$\phi_\sigma=(\psi_a+\psi_b)/(2+2S)^{1/2}$$
$$\phi_\pi=(\psi_a-\psi_b)/(2-2S)^{1/2} \quad (2)$$

Here $\psi_a$ and $\psi_b$ refer to the two hydrogen atoms on opposite sides of the yz plane. If the orientation of the ethyl radical is assumed to be,

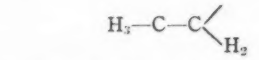

we have another type of hyperconjugation perpendicular to the above one. The proper quasi y-orbital would be

$$\phi_y=N\{2\times 2te\sigma-(\psi_a+\psi_b)/(2+2S)^{1/2}\} \quad (3)$$

where $2te\sigma$ is the tetrahedral orbital of the carbon atom of the methyl group which extends toward the other carbon atom of the ethyl group to make the C-C single bond within the ethyl group, and N is the normalization factor. This quasi y-orbital is to be hyperconjugated with the y-orbital of the carbon atoms of the attached conjugated systems, namely of the triple bond of acetylene. Thus in ethylacetylene we have two-dimensional hyperconjugation, but in ethylbenzene the treatment of x-hyperconjugation only is probably satisfactory just as it is in toluene.

After all, in the present study, it is assumed that the hyperconjugation of the substituted ethyl group is essentially the same as of the methyl group itself.

## III. Outline of Method and Empirical Parameters

It is convenient to express the molecular orbitals of the electrons as linear combinations of atomic orbitals (LCAO). If each MO is constructed out of n definite AO's $\phi_r(r=1,2,\ldots\ldots,n)$, we may write it down in the form,

$$\chi_j=\sum_{r=1}^{n}C_{jr}\phi_r \quad (4)$$

We have then following equations:

$$(\alpha_r-\varepsilon)C_r+\sum_{s\neq r}(\gamma_{rs}-S_{rs}\varepsilon)C_s=0 \qquad (r=1,2,\ldots\ldots,n) \quad (5)$$

where

$$a_r=\int\phi_r H\phi_r d\tau, \qquad \gamma_{rs}=\int\phi_r H\phi_s d\tau,$$
$$S_{rs}=\int\phi_r\phi_s d\tau \quad (6)$$

and $\varepsilon$'s are the energies of LCAO MO's. We write $\gamma_{rs}=\beta_{rs}+\frac{1}{2}S_{rs}(\alpha_r+\alpha_s)$ and assume that the Coulomb integral $\alpha_r$ has the same value $\alpha$ for all the carbon atoms in the system, and is $\alpha+\lambda_1\beta$ and $\alpha+\lambda_2\beta$ for pseudo atom $H_3$ or $H_2$ and next neighboring carbon atom respectively. Here $\beta$ corresponds to the benzene C-C, and $\lambda_1$ and $\lambda_2$ are empirical parameters to be determined from experimental aspects; particularly $\lambda_2$ is a measure of the inductive effect[21]. We also assume that $\beta_{rs}$ is proportional to the overlap integral between atoms r and s if r and s are bonded, otherwise zero[22,23]. That is

$$\beta_{rs}=(S_{rs}/S)\beta\equiv\gamma_{rs}\cdot\beta \quad (7)$$

where S is the overlap integral between adjacent carbon atoms in benzene (C-C distance is 1.39Å).

With these assumptions and neglecting the overlap integrals, the equations (5) take the following forms,

$$(\alpha_r-\varepsilon)C_r+\sum_{s\neq r}\rho_{rs}\beta C_s=0 \quad (r=1,2,\ldots\ldots,n) \quad (8)$$

where the summation is carried out over all $s$ bonded to $r$. Then we get the sets of coefficients $C_{jr}$ corresponding to each eigenvalue $\varepsilon_j$. According to the definitions[24,25], the total $\pi$-electron density of atom $r$ is given by

$$q_r=2\sum_j C_{jr}^2 \quad (9)$$

and the bond order of a bond $r$-$s$ by

$$p_{rs}=2\sum_j C_{jr}C_{js} \quad (10)$$

where $q_r$ and $p_{rs}$ are given as a sum over all occupied MO's.

The overlap integrals needed to evaluate the $\rho$ values are computable from the table given by Mulliken et al[26], using the experimental data for internuclear distances, and are shown in Table I. Although the overlap integral of the group orbitals such as C-$H_3$ and C-$H_2$ is also computable by the method of Mulliken et al. ($S=0.541$)[27], the parameter $\rho$ which was derived from the above overlap integral value was found to be not suitable for the present calculations probably because of neglecting all overlap integrals. If the

22) G.W. Wheland, *J. Am. Chem. Soc.*, **64**, 900 (1942).
23) R.S. Mulliken and C.A. Rieke, *J. Am. Chem. Soc.*, **63**, 1770 (1941).
24) G.W. Wheland and L. Pauling, *J. Am. Chem. Soc.*, **57**, 2086 (1935).
25) C.A. Coulson, *Proc. Roy. Soc.* (London), **A169**, 413 (1939).
26) R.S. Mulliken, C.A. Rieke, O. Orloff and H. Orloff, *J. Chem. Phys.*, **17**, 1248 (1949).
27) The overlap integral of the group orbital C-$H_3$ is computed as follows:

$$S(C,H_3)=\sqrt{\frac{2}{3}}\sin\alpha\,[1-S(1s,1s;H-H)]^{-\frac{1}{2}}$$
$$\times S(1s,2te\sigma;C-H)$$

where $2\alpha$ is the tetrahedral valence angle 109.5°. See ref. 26), Section Vd.
28) See references 7) and 8).

overlap integral between C and $H_3$ or $H_2$ is estimated as the one between carbon $sp_3$ tetrahedral hybrid-AO and hydrogen 1s AO using the C-H internuclear distance 1.09Å[28], then we get $S(1s, 2te\sigma)=0.685$ and $\rho_{CH_3}$ or $\rho_{CH_2}=2.77$. The more suitable value was found to be chosen as 2.92[29] through calculations.

TABLE I

C($\pi$)-C($\pi$) OVERLAP INTEGRALS AND $\rho$ VALUES

| r(C-C), Å | S(2p$\pi$,2p$\pi$) | $\rho_r$* |
|---|---|---|
| 1.53 | 0.196 | 0.794 |
| 1.51 | 0.203 | 0.822 |
| 1.50 | 0.206 | 0.834 |
| 1.47 | 0.217 | 0.879 |
| 1.42 | 0.236 | 0.955 |
| 1.39 | 0.247 | 1.000 |
| 1.205 | 0.335 | 1.356 |

* $\rho_r=S(r)/S(1.39)$.

The overlap integral between the quasi $\pi_y$-orbital (3) and the tetrahedral orbitals of the attached carbon atom of the ethyl group is computed as 0.435[30] by the method of Mulliken et al., but the $\rho$ value derived from this was not adequate as mentioned above, $\rho_{CH_2-C}$ value is therefore taken as 2.35 in proportion to $\rho_{CH_3}$ or $\rho_{CH_2}$ (2.92).

As for another parameter $\lambda_1$, it seems certainly to be negative according to a theoretical explanation which was recently given by Muller, Pickett and Mulliken[20], and probably in the neighborhood of $-0.5$. In this paper $-0.5$[31] was most suitable for reproducing experimental data, particularly dipole moments of hyperconjugated systems. Since the trigonal and digonal carbon atoms of the double and triple bonds are more electronegative than the tetrahedral carbon of the methyl group, parameter $\lambda_2$ will be also negative and is chosen as $-0.1$ taking account of the inductive effect from the adjacent $H_3$ group.

Since no precise method gives the numerical values of these quantities, the above assumed values involve considerable uncertainties. Therefore, as far as the reliability of these parameters is concerned, we should be contented with the agreement between predicted and observed values when these parameters are used in computations.

## IV. Application to Methyl and Ethylacetylenes

Following the ideas of Sec. II, methylacetylene has eight delocalized $\pi$-electrons and ethylacetylene ten delocalized ones. Therefore, the secular determinants are

$$\begin{vmatrix} z+\lambda_1 & \rho_{12} & 0 & 0 \\ \rho_{12} & z+\lambda_2 & \rho_{23} & 0 \\ 0 & \rho_{23} & z & \rho_{34} \\ 0 & 0 & \rho_{34} & z \end{vmatrix} = 0 \quad \text{twice} \qquad (11)$$

for methylacetylene, and

$$\begin{vmatrix} z+\lambda_1 & \rho_{12} & 0 & 0 & 0 & 0 \\ \rho_{12} & z+\lambda_2 & 0 & \rho_{24} & 0 & 0 \\ 0 & 0 & z+\lambda_1 & \rho_{34} & 0 & 0 \\ 0 & \rho_{24} & \rho_{34} & z+\lambda_2 & \rho_{45} & 0 \\ 0 & 0 & 0 & \rho_{45} & z & \rho_{56} \\ 0 & 0 & 0 & 0 & \rho_{56} & z \end{vmatrix} = 0,$$

$$\begin{vmatrix} z+\lambda_1 & \rho^* & 0 & 0 \\ \rho^* & z+\lambda_2 & \rho_{45} & 0 \\ 0 & \rho_{45} & z & \rho_{56} \\ 0 & 0 & \rho_{56} & z \end{vmatrix} = 0 \qquad (12)$$

for ethylacetylene. In Eqs. (11) and (12), $z=(\alpha-\varepsilon)/\beta$ and the numberings of atoms are shown in Fig. 2.

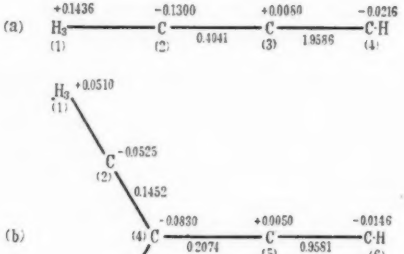


Fig. 2. The numberings of the atoms and the $\pi$-electron charge distribution and mobile bond order diagrams in methylacetylene (a) with both x and y-hyperconjugations and ethylacetylene (b) with x-hyperconjugation only and (c) with y-hyperconjugation only (taking the x-axis to be perpendicular to the plane of the paper and omitting bond orders between C and quasi-$\pi$ group orbitals).

29) In ref. 13), the $\rho_{CH_3}$ value was taken as 4; Pullman and Metzger took it as 2.5; *Bull. Soc. Chim.*, 57, 1021 (1948). The same value 2.5 was chosen by Coulson and Crawford in ref. 18) in calculations including overlap. Mulliken and Rieke found that if the overlap integral is included in the computations, the magnitude of the parameter $\rho_{CH_3}$ is reduced from 4 to about 2; see ref. 23) or R.S. Mulliken, *Rev. Modern Phys.*, 14, 265 (1942). The author has checked this evaluation, and obtained the value 2.19. The self-consistent computation including overlap integrals using such a parameter is in course of computation.

30) This value is obtained as follows:

$$S(CH_2,C)=N_1[\sin\alpha\times S(2te\sigma,2te\sigma;\ C-C) + 2N_2\cos^2\alpha\times S(1s,2te\sigma;C-H)],$$

where $N_1$ and $N_2$ are the normalization factors.

31) In ref. 18), Coulson and Crawford also took as $\lambda_1=-0.5$ and $\lambda_2=-0.1$ from the dipole moment evidence.

Using the following values of empirical parameters: for methylacetylene, $\lambda_1=-0.5$, $\lambda_2=-0.1$, $\rho_{12}=2.92$, $\rho_{23}=0.879$ (as 1.469 Å)[32], $\rho_{34}=1.356$ (as 1.205 Å)[32], and for ethylacetylene, $\lambda_1=-0.5$, $\lambda_2=-0.1$, $\rho_{12}=2.92$, $\rho_{24}=0.834$ (as 1.50 Å)[33], $\rho_{45}=0.879$ (as 1.47 Å)[33], $\rho_{56}=1.356$, $\rho^*=2.35$, computational results are given in Table II, and final charge distribution diagrams in Fig. 2.

TABLE II

THE OCCUPIED ENERGY LEVELS AND DIPOLE MOMENTS OF METHYL AND ETHYLACETYLENES

| | Occupied energy levels | μ (D) | |
|---|---|---|---|
| | z[a] | calcd. | obsd. |
| Methyl-acetylene | +1.260226[b] | 0.727 | 0.72[d] |
| | +2.915310[b,c] | | 0.77[e] |
| Ethyl-acetylene | +1.195202 | 0.783 | 0.80[e] |
| | +1.243628 | | |
| | +2.280381[c] | | |
| | +2.391106[c] | | |
| | +3.251446[c] | | |

a. Note $z=(\varepsilon-\alpha)/\beta$, where $\varepsilon$'s are the energies of MO's.

b. In methylacetylene, the occupied energy levels are doubly degenerate.

c. These are attributable to the hyperconjugated quasi-$\pi$ orbitals.

d. H. E. Watson and K. L. Ramaswamy, Proc. Roy. Soc. (London), **A156**, 130 (1936).

e. F. J. Krieger and H. H. Wenzke, J. Am. Chem. Soc., **60**, 2115 (1938).

**Bond Order and Bond Length.**—Using the bond order and bond length curve[34], we can estimate the approximate bond lengths from the calculated bond orders shown in Fig. 2. Thus we obtained $C_2$-$C_3$(1.47 Å), $C_3$-$C_4$(1.20 Å) in methylacetylene and $C_2$-$C_4$(1.52 Å), $C_4$-$C_5$ (1.47 Å), $C_5$-$C_6$(1.20 Å) in ethylacetylene. The experimental values of internuclear distance are given only for methylacetylene, and the agreements between the calculated and observed values are complete. Consequently, we may consider that the values of parameters assumed before are certainly adequate. In ethylacetylene, no appropriate experimental data for C-C length have been given, but the calculated values shown above might be very suggestive if experimental data could be available on the bond length of the carbon-carbon bond adjacent to the triple bond in ethylacetylene.

32) Spectroscopic data; G. Herzberg, "Infrared and Raman Spectra of Polyatomic Molecules" (D. Van Nostrand, New York, 1945).

33) These are estimated values.

34) C. A. Coulson, *Proc. Roy. Soc.*, A169, 413 (1939), A207, 91 (1951).

**Resonance Moment.**—The dipole moment due to the migration of electrons from alkyl group to carbon atoms of acetylene, assuming it to be a resonance moment only, may be calculated from the charge distribution diagrams. In Table II, the calculated values are compared with the observed ones and agreements are very satisfactory in both cases. Attention should be called to the neglect of dipole moment which may arise from the $\sigma$-electrons (mainly C-H moment).

The comparison of the computed and the empirical conjugation energies will be investigated in the subsequent paper including overlap integrals[35].

## V. Application to Methyl and Ethylbenzenes

When making computations by the MO method, the total effective number of $\pi$-electrons is taken to be eight and ten respectively for toluene and ethylbenzene each numbered as in Fig. 3. In these cases, the treatment of $\pi$-hyperconjugation only is probably satisfactory as mentioned in Sec. II.

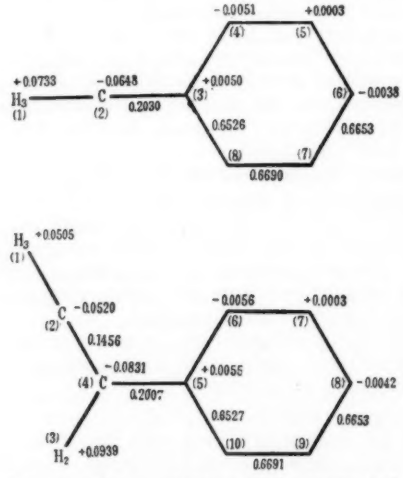


Fig. 3. The numberings of the atoms and the $\pi$-electron charge distribution and mobile bond order diagrams in toluene and ethylbenzene (omitting bond orders between C and quasi-$\pi$ group orbitals).

Using the same empirical parameters in secular equations as those for substituted acetylenes (cf. Sec. IV.), the energy levels of molecular orbitals (in Table III), charge distributions (in Fig. 3) and resonance moments (in Table IV) are obtained.

35) In ref. 13) and 18), Mulliken et al. and Coulson and Crawford computed the empirical conjugation energies from heats of combustion and compared with the theoretical values corrected for extension and compression of the $\sigma$-bonds. See Series II of this article.

TABLE III

THE CALCULATED ENERGY LEVELS OF TOLUENE AND ETHYLBENZENE

| Toluene | Ethylbenzene |
|---|---|
| z[a] | z[a] |
| −1.000000 | −1.000000 |
| −0.986142[b] | −0.994367[b] |
| +0.952463 | +0.950784 |
| +1.000000 | +1.000000 |
| +1.936516 | +1.914324 |
| +2.823428[c] | +2.324890[c] |
| | +3.156861[c] |

a. See foot-note (a) of Table II.

b. These correspond to the lowest unoccupied levels.

c. These are attributable to the hyperconjugated quasi—orbitals.

**The Red Shifts of the Near Ultraviolet Absorption Spectra.**—The above computed migration of electrons from alkyl group to the ring causes wave-length shift and the variation of intensity of 0–0 band in the absorption spectra of alkylsubstituted benzene. In order to compute the extent of these shifts, we must estimate the nature of the transition in alkylbenzene. In benzene, the excitation of the electron from the highest occupied orbitals in the ground state to the lowest unoccupied orbitals produced singlet and triplet states. Excitation energies computed without electron repulsion may be thought to give the average values of the actual levels[36]. In alkyl-substituted benzenes, the original orbital degeneracy is removed by the perturbation of the attached alkyl group. Therefore, in this case, we may assume that the average values of the theoretical excitation energies will give the approximate transition energy of alkylbenzene.

Thus for toluene, we assume a set of hypothetical states with the electron configurations as follows[37]:

$$\begin{array}{ll} \mathrm{Y}: & (\chi_0)^2\ (\chi_1)^2\ (\chi_2)\ \ (\chi_3)^2\ (\chi_5) \\ \mathrm{Y}': & (\chi_0)^2\ (\chi_1)^2\ (\chi_2)^2\ (\chi_3)\ \ (\chi_4) \\ \mathrm{Z}: & (\chi_0)^2\ (\chi_1)^2\ (\chi_2)\ \ (\chi_3)^2\ (\chi_4) \\ \mathrm{Z}': & (\chi_0)^2\ (\chi_1)^2\ (\chi_2)^2\ (\chi_3)\ \ (\chi_5) \end{array} \qquad (13)$$

For instance, a transition from the ground state N to the upper hypothetical state Y would involve transition of an electron from $\chi_2$ to $\chi_5$, leaving a second electron in $\chi_2$ and all other electrons in closed shells. Therefore,

$$\Delta\varepsilon_{\mathrm{av.}} = (1/2)(\varepsilon_5+\varepsilon_4-\varepsilon_3-\varepsilon_2) = h\nu \qquad (14)$$

where $\varepsilon_j$ is the $j$'th MO energy, and $\nu$ is the frequency of a transition from the ground state to an averaged hypothetical state which corresponds to the average height of the actual state.

Now we show that the relative shift in frequency between the $\nu$ of Eq. (14) and the corresponding mean frequency of benzene, $\nu' = -2\beta/h$, is given by

$$(\nu'-\nu)/\nu' = 1+(\varepsilon_5+\varepsilon_4-\varepsilon_3-\varepsilon_2)/4\beta \qquad (15)$$

These quantities are computed for toluene and ethylbenzene from the energy levels in Table III, and are shown in Table IV with the ones calculated from our observed 0–0 bands of the near ultraviolet absorption spectra (see Sec. VI). We find that they are in complete agreement with each other. A prediction for the 0–0 band frequencies in alkylbenzenes is also possible if the corresponding position in benzene is estimated. The calculated frequencies both in vapor and in solution are shown in Table IV, taking the values for benzene as 2625 Å[38] and 2640 Å[39] corresponding to vapor and solution states respectively.

TABLE IV

DIPOLE MOMENTS, ABSORPTION FREQUENCIES AND OSCILLATOR STRENGTHS OF TOLUENE AND ETHYLBENZENE

| | | Toluene | Ethylbenzene |
|---|---|---|---|
| $\mu$ (D) | calcd. | 0.362 | 0.549 |
| | obsd. | 0.37[a] | 0.58[a] |
| $\frac{\nu'-\nu}{\nu'}$ | calcd. | 0.016 | 0.014 |
| | obsd. | 0.019[b], 0.016[c] | 0.015[b] |
| Vapor $\lambda$, (Å) | calcd. | 2666 | 2661 |
| | obsd. | 2668[d] | 2664[d] |
| Solution $\lambda$, (Å) | calcd. | 2681 | 2678 |
| | obsd. | 2692[b] | 2680[b] |
| $f\times10^4$ | calcd. | 20.5 | 14.2 |
| | obsd. | 15[b], 10[e], 30[f] | 9[b] |

a. J. W. Baker and L. G. Groves, J. Chem. Soc., 1144 (1939).

b. Our experimental data. See Sec. VI and Fig. 4.

c. H. Sponer and E. Teller, Rev. Modern Phys., **13**, 75 (1941).

d. F. A. Matsen, W. W. Robertson and R. L. Chuoke, Chem. Revs., **41**, 273 (1947).

e. R. S. Mulliken and C. A. Rieke, "Reports on Progress in Physics", vol. 8, p. 331 (1941).

f. Sponer and Löwe, J. Opt. Soc. Am., **39**. 840 (1949).

36) C.C.J. Roothaan and R.S. Mulliken, *J. Chem. Phys.*, **16**, 118 (1948).

37) R.S. Mulliken, *J. Chem. Phys.*, **7**, 353 (1939).

38) H. Sponer, G. Nordheim, A.L. Sklar and E. Teller, *J. Chem. Phys.*, **7**, 207 (1939).

39) F.A. Matsen, W.W. Robertson and R.L. Chuoke, *Chem. Revs.*, **41**, 273 (1947).

**Oscillator Strength.**—Before calculation of the oscillator strength[40],

$$f=1.085\times10^{11}\nu Q^2 \qquad (16)$$

where $\nu$ is the frequency of the transition in $cm^{-1}$, we need to calculate the dipole strength $Q$ for the transition. In alkylbenzenes, the wave function of the lowest-lying singlet state is approximately given as follows by analogy with the corresponding one ($^1B_{2u}$) of benzene[41].

$$\psi(V)=[\psi(Z)-\psi(Z')]/2^{1/2} \qquad (17)$$

where $\psi(Z)$ and $\psi(Z')$ correspond to the electron configurations of third and forth lines shown in (13) respectively. The $Q$-values of the $N\rightarrow Z$ and $N\rightarrow Z'$ transitions in alkylbenzenes are z-polarized (figure axis is taken to be z), and

$$Q(N\rightarrow V)=[\int\psi_N(z_1+z_2)\psi_z d\tau - \int\psi_N(z_1+z_2)\psi_{z'}d\tau]/2^{1/2} \qquad (18)$$

where $z_1$ and $z_2$ refer to the two electrons occupied initially in the $\chi_2$ or $\chi_3$ orbitals (cf. (13)). The transition moments for the other axis which is perpendicular to $z$-axis in the benzene plane are zero. In the case of toluene, for example, this reduces to

$$Q(N\rightarrow V)=2^{1/2}[\int\chi_2 z\chi_1 d\tau-\int\chi_3 z\chi_5 d\tau] \qquad (19)$$

Using Eq. (4) and calculated coefficients $C_{jr}$, we get

$$Q(N\rightarrow V)=[1-2(C_{23}C_{43}+C_{24}C_{44} -C_{25}C_{45}-C_{27}C_{47})]r/2^{1/2} \qquad (20)$$

where $r$ is the carbon-carbon distance in benzene. Then we can calculate $f$ by Eq. (16). The $f$-value thus obtained theoretically is shown in Table IV with the one for ethylbenzene, in which the procedure of computation is the same as above.

The discussions for the conjugation energy are delayed in the subsequent paper.

## VI. The Near Ultraviolet Absorption Spectra of Alkylbenzenes

On account of the lack in the data of the near ultraviolet absorption spectra of alkylbenzenes, the solution spectra were obtained in normal hexane on a Beckman quartz spectrophotometer DU (see Fig. 4). The 0–0 band of benzene in solution was estimated to be 2640 Å (note the 0–0 band in benzene is forbidden). The oscillator strengths for the transitions were computed from the integrated areas under the extinction curves, by the following equation[42],

$$f=4.32\times10^{-9}\int\varepsilon_\nu d\nu \qquad (21)$$

where $\nu$ is the frequency in $cm^{-1}$. No correction was made for the effect of solution on the $f$-value.

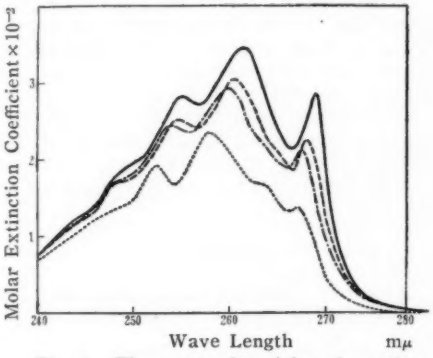


Fig. 4. The near ultraviolet absorption spectra in normal hexane of toluene (——), ethylbenzene (– – – –), iso-propylbenzene (–·–·–·–) and tert-butylbenzene (·····).

## VII. Critical Discussion

From the outset, it was our intention to calculate the electronic states of alkylbenzenes with a view to extending the theory of hyperconjugation. However, the precise computations of the electronic states in such complicated molecules are impossible for the present, so we cannot help making use of the empirical LCAO MO method with empirical parameters. Since no precise computations can be made for the Coulomb integrals of $H_3$ or $H_2$ groups or for the exchange integrals between C and $H_3$ or $H_2$, we meet first of all with a difficulty when we attempt to give reasonable values to these quantities. Consequently, values of these parameters which were chosen from several assumptions, so as to reproduce the observed dipole moments as well as possible were applied not only to alkylbenzenes but to alkyl-substituted acetylenes, and fairly satisfactory results were obtained. Therefore, these empirical parameters seem to be considerably reliable when the overlap integrals are ignored.

The calculations show that the theory of

40) R. S. Mulliken and C. A. Rieke, "Reports on Progress in Physics", Vol. 8, p. 231 (1941).

41) For benzene $\phi(Z)$ and $\phi(Z')$ are degenerated so that the coefficients of $\phi(Z)$ and $\phi(Z')$ should be equal in magnitude, for the alkylbenzenes, however, $\phi(Z)$, $\phi(Z')$ are no longer degenerate and the coefficients should be slightly unequal. This inequality will not affect the center of gravity of the excited states, but it must not give sufficiently correct $Q$-values for the transitions since equal mixing should not be expected. Matsen discussed the resulting errors in an appendix of ref. 17). See also refs. 37) and A. L. Sklar, *J. Chem. Phys.*, 5, 669 (1937), M. Goeppert-Mayer and A. L. Sklar, *J. Chem. Phys.*, 6, 645 (1938).

42) J. R. Platt and H. B. Klevens, *Rev. Modern Phys.*, 16, 182 (1944).

hyperconjugation introduced by Mulliken, Rieke and Brown has a real importance for the study of the electronic structure not only of methylated organic molecules but of other alkyl-substituted ones; namely even when the methyl group is substituted for a hydrogen atom of the methyl group, the hyperconjugation is recognized as being the same as in the case of methyl group only. For such a complicated organic molecule, the usual method consists of computing its electronic structure taking only $\pi$-electrons of carbon atoms involved; however the phenomenon of hyperconjugation suggests that to a large extent the 1s electrons of the hydrogen atoms and even the tetrahedral hybridized orbital of the carbon atoms in the alkyl group take part in $\pi$-conjugation. More accurate calculations are made in the subsequent papers using the LCAO MO and LCAO SCF MO methods including the overlap integrals.

**Summary**

The theory of hyperconjugation has been extended and applied to computations of the electronic structures of methyl and ethyl-substituted acetylenes and benzenes using the empirical LCAO MO method not including the overlap integrals. The common empirical parameters introduced from experimental aspects were used consistently through the calculations. Charge distributions of the $\pi$-electrons, bond orders, resonance moments, relative shifts of near ultraviolet absorption spectra and oscillator strengths were calculated, and fairly satisfactory results, compared with the observed values, were obtained. Because of the lack of appropriate absorption data, the near ultraviolet absorption spectra of alkylbenzenes in normal hexane were obtained. The calculations show that when the methyl group is substituted for a hydrogen atom of the methyl group, the hyperconjugative effect is recognized as same as before.

The author wishes to thank Professor A. Kotera and Dr. S. Nagakura for many helpful discussions.

*Department of Chemistry, Tokyo University of Education, Tokyo*

---

# *Hyperconjugation. II. The Electronic Structures and Conjugation Energies of Alkylbenzenes*

By Yasumasa I'HAYA

(Received March 16, 1955)

## I. Introduction

It was shown in Part I[1] that even in ethyl-substituted acetylene and benzene the ideas of extended hyperconjugation could be also applied. In this paper, the author gives more detailed calculations of the electronic structures and conjugation energies not only in toluene and ethylbenzene but in *tert*-butylbenzene by the empirical LCAO MO method including overlap integrals for neighboring atoms. Since such a computation including overlap has been made only by Coulson and Crawford[2] for a series of methyl-substituted benzenes and ethylenes, it is desirable to investigate the electronic structures of the other alkyl-substituted resonating systems, particulary of alkylbenzenes which have long been a question, using the same method as in the case of toluene.

The models for the methyl and ethyl groups were already established in Sec. II of Part I, but a model for the *tert*-butyl group remains unsettled. In this case, it seems fairly reasonable to consider the three $CH_3$ as one group such as $H_3$ in toluene; that is

$$-C-(CH_3)_3.$$

Therefore, we have two dimensional hyperconjugation to be conjugated with an attached resonating system, but in *tert*-butylbenzene only one type of hyperconjugation is probably effective for just the same reason as in toluene.[3]

* A part of this work was presented at the 7th Annual Meeting of the Chemical Society of Japan, Tokyo University, April 3, 1954.

1) The preceding paper.

2) (a) C.A. Coulson and V.A. Crawford, *J. Chem. Soc.*, 2052 (1953); (b) V. A. Crawford, ibid., 2058, 2061 (1953).

3) See Sec. II of Part I.

## II. Method of Computations

The method of LCAO MO (Linear Combination of Atomic Orbitals Molecular Orbital) with inclusion of the overlap integrals between adjacent atomic orbitals requires certain changes in the forms of the equations and the definitions mentioned in Sec. III of Part I. If we denote different atoms by a Greek suffix $\mu$, $\nu$,..... and molecular orbitals (MO) by a Latin suffix i, j,....., each MO $\psi_j$ is represented by n AO's $\phi_\mu$ in the form

$$\psi_j=\sum_{\mu=1}^{n} x_{j\mu}\phi_\mu \tag{1}$$

where tne coefficients $x_{j\mu}$ are determined by minimizing the total energy. The energy levels of MO's $\psi_j$ are given by the roots of the secular determinant

$$\det|H_{\mu\nu}-\varepsilon S_{\mu\nu}|=0 \tag{2}$$

where

$$H_{\mu\mu}=\int\phi_\mu H\phi_\mu d\tau=\alpha_\mu,$$
$$H_{\mu\nu}=\int\phi_\mu H\phi_\nu\, d\tau=\tau_{\mu\nu},$$
$$S_{\mu\nu}=\int\phi_\mu\phi_\nu\, d\tau.$$

Neglecting interactions of non-neighbor atoms, making replacements $\beta=\tau-\alpha S$, $\xi_\mu=1-\lambda_\mu S$, and $z=(\alpha-\varepsilon)/(\tau-S\varepsilon)$, and assuming $\tau_{\mu\nu}$ is proportional to $S_{\mu\nu}$ [4], the above secular determinant is simplified as a polynomial of $z$. (note $\alpha$, $\beta$, $\tau$ and $S$ correspond to benzene).

Illustration for the case of toluene, the numbering of atoms shown in the diagram, is as follows; this molecule has eight $\pi$-electrons in orbitals made by combining the six $2p\pi$ carbon AO's and the two quasi-$\pi$ orbitals of the methyl group. Because of the $C_{2v}$ symmetry of the molecule[5], the MO's are divided into two groups, one is $a_2$ and the other is $b_1$ symmetries.

$$\Delta(a_2)=\begin{vmatrix} z & 1 \\ 1 & z \end{vmatrix}=0 \tag{3}$$

$$\Delta(b_1)=\begin{vmatrix} \xi_1 z+\lambda_1 & \rho_{12} & 0 & 0 & 0 & 0 \\ \rho_{12} & \xi_2 z+\lambda_2 & \rho_{23} & 0 & 0 & 0 \\ 0 & \rho_{23} & z & 1 & 0 & 0 \\ 0 & 0 & 2 & z & 1 & 0 \\ 0 & 0 & 0 & 1 & z & 2 \\ 0 & 0 & 0 & 0 & 1 & z \end{vmatrix}=0 \tag{4}$$

In these determinants, $\rho$'s are the proportional constants of the exchange integrals to overlap ($\rho_{\mu\nu}=S_{\mu\nu}/S$) and $\lambda$'s are the correction terms for the Coulomb integrals in units of $\beta$. Solution of above determinantal equations (3) and (4) provides us with the orbital energies $\varepsilon_j$ (shown in Table II) using the relation

$$\varepsilon_j=\alpha-\frac{z}{1-Sz}\beta \tag{5}$$

and the corresponding coefficients $x_{j\mu}$'s.

TABLE I
EMPIRICAL PARAMETERS

| | $\lambda_1$ | $\lambda_2$ | $\rho_{12}$ | $\rho_{23}$ |
|---|---|---|---|---|
| Toluene | −0.5 | −0.1 | 2.92 | 0.834 |
| *tert*-Butylbenzene | −1.0 | −0.1 | 3.0 | 0.777 |
| | $\lambda_1,\lambda_3$ | $\lambda_2,\lambda_4$ | $\rho_{12},\rho_{34}$ | $\rho_{24},\rho_{45}$ |
| Ethylbenzene | −0.5 | −0.1 | 2.92 | 0.822 |

TABLE II
ORBITAL ENERGIES $w_i$ OF ALKYLBENZENES*

| | Toluene | Fthylbenzene | *tert*-Butylbenzene |
|---|---|---|---|
| $2a_2$ | −1.328021 | −1.328021 | −1.328021 |
| $4b_1$ | −1.297212 | −1.297330 | −1.320806 |
| $3b_1$ | +0.767269 | +0.768415 | +0.770480 |
| $1a_2$ | +0.801925 | +0.801925 | +0.801925 |
| $2b_1$ | +1.305127 | +1.290928 | +1.298214 |
| $1b_1$ | +1.623852 | +1.439167 | +1.515066 |
| $0b_1$ | | +1.745722 | |

* $w_i=(\varepsilon_i-\alpha)/\beta$, and orbital energies higher than $2a_2$ are not recorded.

The empirical parameters used are the same as that of Part I excepting *tert*-butylbenzene and some refinements made in $\rho_{23}$ both in toluene and ethylbenzene, and are recorded in Table I. Since the choice of parameters for *tert*-butylbenzene are quite arbitrary, considerable uncertainties remain. Judging from a result of calculations, however, they seem not to be very seriously wrong. The author of course wishes that further support will be provided for these numerical values of the empirical parameters.

The influences of the inductive effect to the Coulomb integrals of the ring carbon atoms are ignored.[6]

## III. Conjugation Energies and Hyperconjugation Energies

In order to obtain conjugation and hyperconjugation energies, the total energies $E(L)$ and $E(S)$ of the $\pi$-electrons in localized and semi-localized bond structures must be calculated, in addition to the total energy of the delocalized model $E(D)$. Here what is called the total energy of the semi-localized bond structure $E(S)$ is the total sum of each $\pi$-electron energies in $C-H_3$ group and the delocalized benzene. Now we get the vertical conjugation (or vertical $\pi$-resonance) energy

4) G.W. Wheland, *J. Am. Chem. Soc.*, **63**, 2025 (1941); ibid., **64**, 900 (1942).

5) In this paper, the benzene ring in ethylbenzene is approximately treated to be also $C_{2v}$ symmetry.

6) See foot-note 21) of Part I.

$E(CJ)$[7] and the vertical hyperconjugation energy $E(HCJ)$ as follows:

$$E(CJ)=E(L)-E(D)$$
$$E(HCJ)=E(S)-E(D). \quad (6)$$

These energies computed theoretically for a series of alkylbenzenes are listed in column 3 of Table IV ($E(HCJ)$ is given in bracket).

On the other hand, it has been shown by Mulliken, Rieke and Brown[8] (hereafter called M. R. B.) that the following empirical formula for the heats of combustion fits the available data for saturated hydrocarbons with considerable accuracy:

$$-\Delta H_{298^\circ}=54.625N_{CH}+48.25N_{CC}-1.5N_{Me}+22.18N_{C-C}+56.6N_{C=C} \quad (7)$$

where $N_{CH}$, $N_{CC}$, $N_{Me}$, $N_{C-C}$ and $N_{C=C}$ are the numbers of C–H bonds, C–C bonds (counting each bond in a multiple bond; e.g., nine in benzene), methyl groups, C=C double bonds, and C≡C triple bonds, respectively. Then the difference $\Delta$ between the value empirically predicted by Eq. (7) and observed heat of combustion[9] is 39.46, 40.96 and 40.91 kcals. for benzene, toluene and ethylbenzene respectively. Therefore, the value $\Delta(HCJ)$, which is obtained after subtraction from the $\Delta$ of benzene, is 1.5 kcal. for toluene and 1.45 kcal. for ethylbenzene.

## IV. Third-Order Conjugation

It has been noticed that when comparing empirical and theoretically computed (vertical) conjugation energies, we should make two corrections; the one to the energy of compression and extension of the C–C bond length, the other to the energy of the third-order conjugation. The importance of doing the former correction for the empirically determined conjugation or resonance energies from the formula (7), has been demonstrated by several writers[10,11,12] and more recently Coulson and Crawford[2a] have recalculated the compression and extension energies using Morse functions. In this paper, the value C=35.49 kcal. for benzene which was given by above authors is used without revision.

The latter correction for the theoretically computed conjugation energies which was first stressed by M. R. B., is based upon the fact that ideal single (or double) bond is one which is slightly weaker and longer than that found in ethane (or ethylene), because the single (or double) bond in ethane (or ethylene) is strengthened by third-order conjugation. The corrected total conjugation energy is therefore given by the sum of the ordinary of first-order ($E(CJ)$ in Eq. (6)) and third-order conjugation energies; that is

$$E(CJ)=E_1(CJ)+E_3(CJ)$$

The third-order conjugation energies per bond are readily computed for various bond lengths on the basis of the variation method including overlap integrals between adjacent atomic orbitals:

$$\varepsilon(r)=2\left\{\frac{z_1(D)}{1-Sz_1(D)}+\frac{z_2(D)}{1-Sz_2(D)}-\frac{2z(L)}{1-Sz(L)}\right\} \quad (8)$$

per dimension where $-z_1(D)$ and $-z_2(D)$ are the lower two roots of the secular equation for both delocalized ethane and ethylene and take the following forms;

$$\left.\begin{matrix}z_1(D)\\z_2(D)\end{matrix}\right\}=\frac{1}{2\xi_1\xi_2}[\xi_1\lambda_2+\xi_2\lambda_1\pm\xi_1\rho_{23}+\{(\xi_1\lambda_2+\xi_2\lambda_1\pm\xi_1\rho_{23})^2-4\xi_1\xi_2(\lambda_1\lambda_2-\rho_{12}^2\pm\lambda_1\rho_{23})\}^{1/2}] \quad (9)$$

and $-z(L)$ is a doubly degenerated root of the quadric secular equation for localized two $CH_3$ groups.

$$z(L)=\frac{1}{2\xi_1\xi_2}[\xi_1\lambda_2+\xi_2\lambda_1+\{(\xi_1\lambda_2+\xi_2\lambda_1)^2-4\xi_1\xi_2(\lambda_1\lambda_2-\rho_{12}^2)\}^{1/2}] \quad (10)$$

In Eqs. (9) and (10), $\rho_{12}$ and $\rho_{23}$ refer to the C≡$H_3$ or C=$H_2$ and C–C bonds respectively, and $\lambda$'s and $\xi$'s have the same meaning mentioned in Sec. II.

Taking the C–C overlap integral $S$ in benzene as 0.247, values of $\varepsilon(r)$ are evaluated for various bond lengths and are listed in Table III.

TABLE III
THIRD-ORDER CONJUGATION ENERGIES

| r(C–C), in Å | $\varepsilon(r)$, in units of $\beta$ |
|---|---|
| 1.54 | 0.001267 |
| 1.53 | 0.001308 |
| 1.52 | 0.001350 |
| 1.51 | 0.001396 |
| 1.50 | 0.001445 |
| 1.46 | 0.001659 |
| 1.39 | 0.002115 |
| 1.33 | 0.002595 |

7) This vertical conjugation energy corresponds to a quantum-mechanical resonance energy named by Coulson and Altmann in ref. 12).

8) R.S. Mulliken, C.A. Rieke and W.G. Brown, *J. Am. Chem. Soc.*, 63, 41 (1941).

9) Heat of combustion for benzene, toluene and ethylbenzene is 789.08, 943.58 and 1101.13 kcals., respectively; W.C. Price, *Chem. Revs.*, 41, 257 (1947). No appropriate data is given for *tert*-butylbenzene.

10) J. E. Lennard-Jones, *Proc. Roy. Soc.* (London), A138, 280 (1937).

11) D.F. Hornig, *J. Am. Chem. Soc.*, 72, 5772 (1950).

12) C.A. Coulson and S.L. Altmann, *Trans. Faraday. Soc.*, 48, 293 (1952).

Now it has been shown (M. R. B.)

$$\Delta+C=E_1(\mathrm{CJ})+E_3(\mathrm{CJ})-2\varepsilon(1.54)N_{\mathrm{C-C}}-\varepsilon(1.33)N_{\mathrm{C=C}} \quad (11)$$

where $C$ is the conjugation energy correction due to compression and extension of the bonds, and $\varepsilon$ is the hyperconjugation energy per bond per dimension for bond distance 1.54 and 1.33 Å respectively. The right hand sides of Eq. (11) computed theoretically for three alkylbenzenes are given in Table IV together with the value for benzene, for the purpose of comparison between the theoretical and empirical conjugation energies $\Delta+C$ for benzene and of computing the hyperconjugation energies in three alkylbenzenes.

The value $\beta$ obtained by comparison of both $\Delta+C$ for benzen is $-70.0$ kcal.[13], and is somewhat larger than that of the spectroscopic value $-60$ kcal. Using the value for $\beta$ of $-70.0$ kcal., the corrected hyperconjugation energies for toluene, ethylbenzene and *tert*-butylbenzene are 1.45, 1.24 and 0.79 kcals. respectively, and this is the quite satisfactory order to be expected.

The third-order conjugation energies listed in Table III are appreciably less than the M. R. B., Roberts and Skinner[14] and even than the Coulson and Crawford[2a] values. This might be ascribed to including the corrected Coulomb integrals in Eqs. (9) and (10) but not including in the reference (2a)[15].

## V. Charge Distributions and Bond Orders

It was already mentioned in Sec. II that when overlap is included the definitions for the charge and the bond order must be changed. Following Chirgwin and Coulson[16], the total $\pi$-electron density $q_\mu$ on atom $\mu$ and the mobile bond order $p_{\mu\nu}$ between adjacent atoms $\mu$, $\nu$ are given by

$$q_\mu=\sum_{j=1}^{m} n_j x_{j\mu} y_{j\mu} \quad (12)$$

$$p_{\mu\nu}=\frac{1}{2}\sum_{j=1}^{m} n_j (x_{j\mu} y_{j\nu}+x_{j\nu} y_{j\mu}) \quad (13)$$

where $y_{j\mu}$ is the "covariant" coefficients associated with $\psi_j$ in contrast with the "contravariant" ones $x_{j\mu}$, and defined by the relation

$$y_{j\mu}=\sum_{\nu=1}^{n} S_{\mu\nu} x_{j\nu}$$

with the normalization condition

$$\sum_{\nu=1}^{n} x_{j\nu} y_{j\nu}=1 \quad (j=1, 2, \cdots\cdots n).$$

In Eqs. (12) and (13), the summation is carried over all the occupied molecular orbitals $j$, and $n_j$ is the number of electrons in the $j$'th MO. The computed values of the total $\pi$-electron charge densities and mobile bond orders thus obtained are shown in the following diagram.

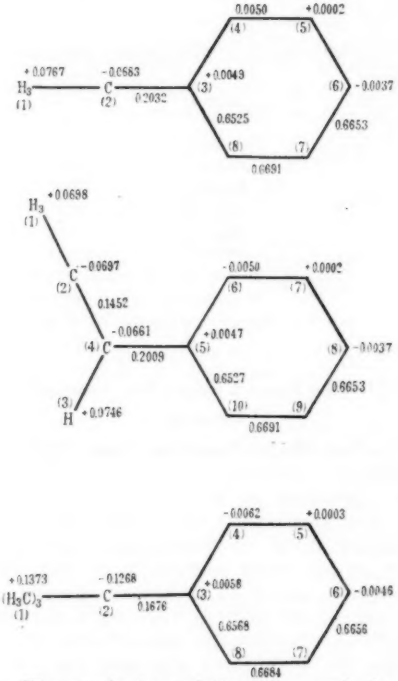


The numberings of the atoms and the $\pi$-electron charge distribution and mobile bond order diagrams in toluene, ethylbenzene, and *tert*-butylbenzene, omitting bond orders between C and $H_2$ or $H_3$ group in toluene and ethylbenzene and between C and $(CH_3)_3$ in *tert*-butylbenzene.

The dipole moment due to the migration of electrons from alkyl group to benzene ring can be evaluated from the calculated charge densities and the bond lengths predicted from the bond orders (see column 2 of Table IV). Assumption of a resonance moment only is taken here as in Sec. IV of Part I. The results recorded in Table V show considerable agreements with the observed values.

13) Coulson and Crawford give the value $-71.6$ kcal. for $\beta$.

14) J. S. Roberts and H. A. Skinner, *Trans. Faraday Soc.*, **45**, 339 (1949).

15) The third-order conjugation energies computed in the present study were somewhat rescrutinized; Y. I'Haya, to be published.

16) B.H. Chirgwin and C.A. Coulson, *Proc. Roy. Soc.* (London), **A201**, 196 (1950).

TABLE IV

CONJUGATION ENERGIES OF ALKYLBENZENES, IN UNITS OF $\beta$

| | r(C-C), Å | $E_1$(CJ) | $E_3$(CJ)* | Deduction** | $\Delta$+C |
|---|---|---|---|---|---|
| Benzene | 1.39 | 1.073526 | 0.012690 | 0.015387 | 1.070829 |
| Toluene | 1.39 | 1.095352 | 0.014086 | 0.017921 | 1.091517 |
| | (2-3) 1.51 | (0.021826) | | | |
| Ethylbenzene | 1.39 | 1.093538 | 0.015394 | 0.020455 | 1.088477 |
| | (2-4) 1.53 | (0.020012) | | | |
| | (4-5) 1.51 | | | | |
| t-Butyl-benzene | 1.39 | 1.086034 | 0.014040 | 0.017921 | 1.082153 |
| | (2-3) 1.52 | (0.012508) | | | |

* $\sum_r \varepsilon(r) N_{C-C}(r)$

** $2\varepsilon(1.54)N_{C-C}+\varepsilon(1.33)N_{C=C}$.

TABLE V

DIPOLE MOMENTS, ABSORPTION FREQUENCIES AND OSCILLATOR STRENGTHS IN ALKYLBENZENES

| | | Benzene | Toluene | Ethylbenzene | t-Butylbenzene |
|---|---|---|---|---|---|
| $\mu$ (D) | calcd. | — | 0.372 | 0.491 | 0.746 |
| | obsd.* | — | 0.37 | 0.58 | 0.70 |
| Vapor $\lambda$, (Å) | calcd. | (2625) | 2666 | 2665 | 2649 |
| | obsd.** | 2625 | 2668 | 2664 | 2655 |
| Solution $\lambda$, (Å) | calcd. | (2640) | 2681 | 2680 | 2664 |
| | obsd.‡ | 2640 | 2692 | 2680 | 2672 |
| $f\times10^{-4}$ | calcd. | — | 16.1 | 11.0 | 8.2 |
| | obsd.‡ | — | 15 | 9 | 5 |

* J. W. Baker and L. G. Groves, *J. Chem. Soc.*, **1939,** 1144.

** F. A. Matsen, W. W. Robertson and R. L. Chuoke, *Chem. Revs.*, **41**, 273 (1947).

‡ Y. I'Haya, the preceding Paper.

## VI. The Near Ultraviolet Absorption Spectra

**The Red Shifts Resulting from Alkyl Substitution.**—The general features have already been explained in Sec. V of Part I and it has been shown that the substitution of the hydrogen atoms of resonating molecules by alkyl groups cause the shift of the whole absorption curve to a longer wave-length (cf. Fig. 4 of Part I). We have also seen that this may result undoubtedly from a raising of the highest occupied level and a lowering of the lowest unoccupied level, and this lowering may be a characteristic feature of hyperconjugation. The simple LCAO MO calculations of $\pi$-electron transitions are also used here as done in Part I, and are compared with the observed values in Table V. In spite of using such a simple method instead of a more accurate method of antisymmetrized molecular orbitals[17], the agreement between them is fairly satisfactory.

**Intensities of Spectra.**—The oscillator strength $f$ is computed for each of a series of alkyl benzens using the same equations as Eqs. (16) and (20) of Part I, and listed in Table V. Also in this case, therefore, the difficulty which was mentioned in foot note 41) of Part I is inevitable. However, the agreement between the computed and observed values shows that the omission of resulting errors from it is probably not too serious.

Although more detailed reasons for these wave-length shifts and intensities of the absorption spectra are not yet clear, a question which has long been unexplained seems to be semi-quantitatively solved; that is the absorption spectra representing $\pi$-electronic transitions allowed by the lower symmetries than benzene due to charge migrations from alkyl groups into benzene ring shift to longer wave-length and become stronger on passing from *tert*-butylbenzene to toluene. This result can also be explained by the computed hyperconjugation energies mentioned in the last paragraph of Sec. IV, for it is ascribed to increasing of hyperconjugation in a series of alkylbenzenes from *tert*-butylbenzene to toluene.

## VII. Critical Discussion

It has long been a question why the absorption spectra of a series of alkylbenzenes should become stronger and shift to longer wavelength but on the other hand the dipole moments should become smaller on passing from *tert*-butylbenzene to toluene. The re-

17) See A.L. Sklar, *J. Chem. Phys.*, 7, 984 (1939).

sults of computations obtained in the present study can explain this difficulty for the first time in spite of taking the simple LCAO MO method including overlap and choosing some unjustified empirical parameters.

However, here remains another difficulty to be settled; that is the inoization potential. That hyperconjugation plays a more important role here than any other alkyl-substituted resonating systems is indicated by the smaller lowering in ionization potentials on passing from *tert*-butylbenzene to toluene compared with the lowering in other systems[18]. In this connection, if more elaborated computations should be made as nonempirically as possible, an improvement would be made concerning this problem.

Attention should also be called to neglecting the inductive effect. The inductive effect has usually been regarded as being one of short range and is therefore unlikely to be of greater importance in large molecules such as alkylbenzenes than small ones[19]. However, Muller, Pickett and Mulliken[20] have recently stressed in the study of the benzenium ion that a joint inductive-hyperconjugative effect gives a considerably greater additional stabilization than the hyperconjugative effect only. This is likely to occur. Computations together with the inductive effect are in progress, and the result of both, including alkylbenzenes, will be presented before long.

18) See ref. 9).

19) Daub and Vandenbelt have concluded that the redshifts of the absorption spectra are chiefly due to a resonance effect and that they are very insensitive to an inductive effect; *J. Am. Chem. Soc.*, **69**, 2714 (1947); ibid., **71**, 2414 (1949), and in ref. 2b) Crawford has obtained very satisfactory agreement with experimental data in computations of methyl-substituted benzenes using the same method without induction.

20) N. Muller, L.W. Pickett and R.S. Mulliken, *J. Am. Chem. Soc.*, **76**, 4770 (1954).

## Summary

The theory of hyperconjugation has been rescrutinized for a series of alkylbenzenes using the empirical LCAO MO method including overlap integrals for neighboring atoms. A detailed comparison of the theoretically computed and empirically determined conjugation energies of benzene gives a value of $-70.0$ kcal. for $\beta$, the reasonance integral for benzene C–C. Using this value, hyperconjugation energies for toluene, ethylbenzene and *tert*-butylbenzene are 1.45, 1.24 and 0.79 kcals. respectively. The third-order conjugation energies are found to be considerably less than any previous evaluations. Comparison of the predicted and observed dipole moments, absorption frequencies and oscillator strengths show fairly satisfactory agreements between them.

The author extends his thanks to Professor A. Kotera for his helpful comments.

*Department of Chemistry, Tokyo University of Education, Tokyo*

## SHORT COMMUNICATION

### *Anion Exchange Separation of Arsenic (V) and Phosphorus (V) from Arsenic (III) and Germanium (IV)**

By Yukichi YOSHINO

(Received May 6, 1955)

Present study on the anion exchange in hydrochloric acid solutions showed the existence of striking difference in adsorbability between As (III) and As (V), i.e., As (III) was found to be considerably adsorbed by Dowex 2 resin in concentrated hydrochloric acid, whereas that of As (V) was negligible at concentrations between 2 and 12 M of the acid. As was expected, P(V) (Phosphate) behaved just in the same way as As (V). On the other hand, Kakihana[1] reported the excellent adsorbability of Ge (IV) in concentrated hydrochloric acid solutions.

In order to clarify the conditions necessary for the separation of these elements, the author determined the distribution coefficients *Kd* (amount per gram resin/amount per ml. solution) of As (III) and Ge (IV) as a function of hydrochloric acid concentration. The results of the equilibrium experiments[2] are shown in Fig. 1 indicating that both elements can be considerably adsorbed in the range more than 6 M HCl with maximum adsorption at ca. 10 M.

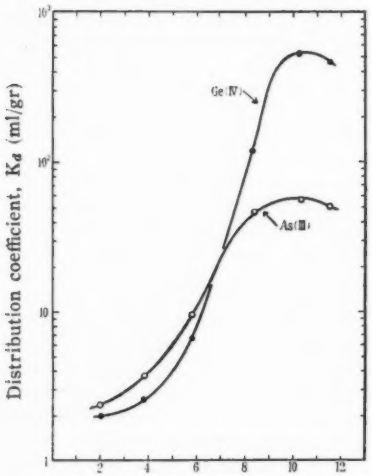


Fig. 1. Anion exchange adsorption of As (III) and Ge (IV). Dowex 2 (8% cross linked), 120-200 mesh, Cl-form. Less than 2% loading[2]. 9±1°C. As and Ge in the liquid phase were determined colorimetrically (molybdenum blue method[3] for As and phenylfluorone method[4] for Ge)

This behavior implies that the ready separation of As (V) and P (V) from As (III) and Ge (IV) should be possible. To demonstrate this, first of all, the separation of As (V) and As (III) was tried using 0.93 cm.²×9.0 cm. column of Dowex 2 and adding to it a 12 ml. of sample containing each 0.1 m mol. of As (V)

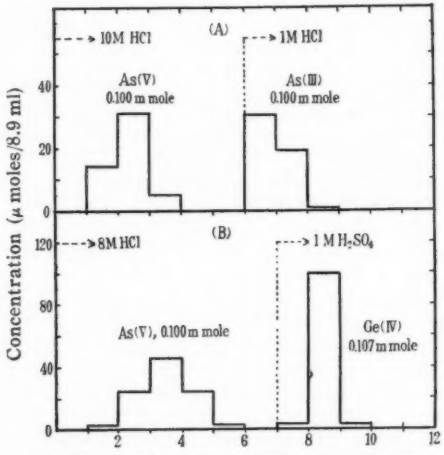


Fig. 2-(A) Separation of As (V) and As (III) Dowex 2-X 8, 80-120 mesh, Cl-form, 0.93 cm²×9.0 cm. Flow rate, 0.7 ml/min. As (V) and As (III) were determined iodometrically[5].

(B) Separation of As (V) and Ge (IV) Dowex 1-X 8, 80-120 mesh, Cl-form, 0.92 cm²×13 cm. Flow rate, 1.0 ml/min. Ge (IV) was determined by iodometry[6].

and As (III) in 10 M HCl. As shown in Fig. 2-(A), As (V) appeared rapidly in the effluent in 10 M HCl and then all the As (III) was removed with 1 M HCl. The same technique was found to be applicable to the separation

of P (V) and As (III) and to As (V) and Ge (IV). However, it was observed that if the HCl-concentration of Ge-containing sample exceeds 9 M, the quantitative removal of the element could not be achieved, which is presumably due to the irreversible precipitation of Ge (IV) in concentrated HCl. Detailed experiments revealed that the use of 8 M HCl sample was effective for the complete elution of Ge (IV) with dilute HCl or $H_2SO_4$. A typical run of the separation of As (V) and Ge (IV) was illustrated in Fig. 2-(B).

The author is indebted to Mr. Y. Sasaki for his valuable suggestion and to Miss M. Asada for her advice on colorimetric determination of germanium.

* Read before the Eighth Annual Meeting of the Chemical Society of Japan, April 3, 1955, Tokyo.

1) H. Kakihana, *Report of Germanium Research Committee of Japan*, No. 15 (1954).
2) See, for example, K.A. Kraus et al., *J. Phys. Chem.*, 58, 11 (1954).
3) Y. Kakida, *Sci. Rep. Research Inst.*, Tohoku Univ., A-1, 399 (1949).
4) H.J. Cluley, *Analyst*, 76, 523 (1951).
5) J.T. Odencrantz and W. Rieman III, *Anal. Chem.*, 22, 1066 (1950); Y. Yoshino, This Bulletin, 24, 39 (1950).
6) B. N. Ivanov-Emin, *Zavod. Lab.*, 13, 161 (1947); *C.A.*, 42, 480 (1948); D. A. Everest, *J. Chem. Soc.*, 1670 (1952), 4117 (1953).

*Department of Chemistry, College of General Education, University of Tokyo, Meguro-ku, Tokyo*